

Pharmacokinetics and Oral Absorption of Various Creatine Supplements

**By
Eman Alraddadi**

**A thesis submitted to
the Faculty of Graduate Studies
in partial fulfillment
of the requirements for the degree of
DOCTOR OF PHILOSOPHY**

**Department of Pharmacology and Therapeutics
Max Rady College of Medicine, Rady Faculty of Health Sciences
University of Manitoba**

Copyright © 2021 by Eman Alraddadi

Abstract

Creatine is a dietary supplement with an extensive history of use in athletes and more recently in various neurological and muscular pathologies. For both indications, large doses (>30 g/day) of creatine monohydrate (CM) are required for beneficial effects to manifest. Based on the doses required and the physicochemical characteristics of creatine, oral absorption of CM is likely incomplete. The research objectives of this dissertation were to determine the absolute oral bioavailability and pharmacokinetic (PK) profile of CM and to identify through *in-silico* simulations, alternative dosing strategies and formulations resulting in improved oral bioavailability and/or tissue distribution. The absolute oral bioavailability of CM was determined in rats at two different doses (10 mg/kg and 70 mg/kg) and found to be 53% and 16% for low and high dose CM, respectively. Using GastroplusTM software, a physiology-based PK (PBPK) model for CM was constructed and compared to the PK data obtained in rats. With good agreement between the simulated and observed data in rats, the model was then scaled-up to compare creatine plasma and tissue levels following various dosing strategies (i.e. once daily vs. 4 times daily, and sustained release (SR) vs. immediate release (IR)) in humans. While the model suggested that SR-CM resulted in comparable plasma area under the curve (AUC_{ss}) with IR-CM, the tissue levels were predicted to be significantly higher following SR-CM (41.3 % and 18.3% increase in brain and muscle concentrations, respectively). The model was also used to predict the impact of other creatine salt forms. For these simulations, CM was compared to creatine hydrochloride (CHCl), creatine citrate (CrC) and creatine pyruvate (CrPyr). Following administration of a large dose (20 g/day), $AUC_{0-\infty}$ in plasma increased by 24.4, 52.1, and 56.3% for CrC, CrPyr, and CHCl, respectively. In the brain, $AUC_{0-\infty}$ increased by 31.0, 55.1, and 70.1%, and

in the muscles by 20.1, 35.1, and 40.1%, for CrC, CrPyr, and CHCl, respectively. Our results suggest that the oral bioavailability of CM is less than complete and is dose-dependent. These studies suggest that newer forms and dosage formulations of creatine will result in superior accumulation of creatine in the tissues.

Acknowledgements

After thanking God, I would like to express my sincere gratitude to my supervisor Dr. Donald Miller for his supervision, dedication, patience, and encouragements throughout my work in his laboratory. I would also like to thank my committee members, Dr. Daniel Sitar, Dr. Ted Lakowski, and Dr. Jun-Feng Wang for their time, thoughtful suggestions, and guidance during the course of my PhD.

To all my lab members, thank you for making the lab environment more enjoyable. Special thanks to Wei Xiong for her support and assistance during my studies.

I would like to thank The Ministry of Higher Education of Saudi Arabia and the Saudi Arabian Culture Bureau in Canada for their generous financial support and for giving me the opportunity to achieve my goal.

To my friends and second family in Winnipeg, thank you for all the good times and memories.

To my family in Saudi Arabia, thank you for your unconditional love and support.

Dedication

Dedicated to

My son Ali

Table of Contents

Abstract	I
Acknowledgements	III
Dedication	IV
List of Tables	IX
List of Figures	XI
List of Abbreviations	XVI

Chapter 1. Introduction

1.1. Introduction	1
1.2. Creatine Storage and Synthesis	2
1.3. Cellular Effects of Creatine	5
1.3.1. Cellular Energetic Effects (Creatine/PCr/CK system)	5
1.3.2. Other Cellular Effects of Creatine	9
1.4. Creatine Transport	10
1.4.1. Creatine Transporter Expression in the Brain	11
1.5. Exogenous Administration of Creatine Supplements	13
1.5.1. Conditions with Increased Energy Requirements: Exercise Performance	14
1.5.2. Conditions Where Creatine is Absent or Reduced: Inborn Errors of Creatine Synthesis or Transport	16
1.5.3. Muscle-related Disorders, Including Muscular Dystrophies (MDs)	17
1.5.4. Neurodegenerative Disorders Such as HD, PD, AD, and ALS.	17

1.5.4.1.	Huntington’s Disease	18
1.5.4.2.	Alzheimer’s Disease	21
1.5.4.3.	Parkinson’s Disease	22
1.5.4.4.	Amyotrophic Lateral Sclerosis	24
1.6.	Dosing and Safety of Creatine Supplementations	25
1.7.	Important Considerations for Creatine Monohydrate Supplementations	26
1.8.	Cellular Mechanisms of Oral Absorption	30
1.9.	Creatine Absorption in the GIT	34
1.10.	Newer Creatine Derivatives	38
1.11.	Physiologically Based Pharmacokinetic Modeling	46
1.12.	Statement of the Problem	50

Chapter 2. Materials and Methods

2.1.	Materials	52
2.2.	PK Study in Rats	52
2.3.	Sample Preparation	56
2.3.1.	Plasma and RBC Samples Preparation	56
2.3.2.	Brain and Muscle Samples Preparation	56
2.4.	LC-MS/MS Analysis	57
2.4.1.	Stock and Working Standard Solutions	58
2.4.2.	Sample Preparation for Standards	59
2.4.3.	Precision, Accuracy, and Recovery	59
2.5.	Physiologically Based Pharmacokinetic Modeling	62
2.5.1.	Structure and Validation of CM Model in Rats and Humans	62

2.6. Creatine Transporter Expression in Caco-2 and MDCK- <i>MDR1</i> Cells .	68
2.7. Permeability Studies	70
2.8. Statistics	71

Chapter 3. Results

3.1. CM PK Study in Rats	72
3.1.1. Plasma Kinetics and Oral Bioavailability of Low Dose and High Dose CM- ¹³ C	72
3.1.2. Tissue Distribution Following Administration of Low Dose and High Dose CM- ¹³ C	76
3.2. Physiologically Based Pharmacokinetic Modeling of Creatine Compounds	79
3.2.1. Examination of Permeability of Creatine in Caco-2 and MDCK- <i>MDR1</i> Monolayers	79
3.2.2. Physiologically Based Pharmacokinetic Modeling of Creatine	89
3.2.2.1. Single Oral Dose CM in Rats	89
3.2.2.2. Single Oral Dose CHCL in Rats	90
3.2.3. Physiologically Based Pharmacokinetic Modeling of Creatine Compounds in Humans	95
3.2.3.1. Single Oral Dose CM in Humans	95
3.2.3.2. Steady-State Oral Dosing of CM in Humans	98
3.2.3.3. Impact of Different Dosing Schedules on Plasma and Tissue Levels of Creatine	101

3.2.3.4. Impact of a Sustained Release Dosage Formulation of CM on Plasma and Tissue Levels of Creatine	110
3.2.3.5. Evaluation of Sex-dependent Differences in Plasma and Tissue Levels of Creatine	114
3.2.3.6. Physiologically Based Pharmacokinetic Modeling of CHCL, CrC, and CrPyr in Humans	116
3.2.3.7. Physiologically Based Pharmacokinetic Modeling of CHCL, CrC, and CrPyr Following Administration of Multiple-Dose in Humans	122
3.3. CEE PK Study in Rats	132

Chapter 4. Discussion

List of Tables

Table 1. Dosing regimen of CM and main findings in the published clinical trials in patients with ALS, PD, or HD	28
Table 2. CRT1 K_m values and serum creatine concentrations in different Species	38
Table 3. Comparison of aqueous solubility of various creatine salt forms and CM	44
Table 4. Comparison of aqueous solubility and octanol-water partitioning of various creatine ester forms and CM	45
Table 5. MRM transitions and collision energies for Creatine- ^{13}C , CRN- ^{13}C , CEE- ^{13}C and the internal standard, Creatine- D_3	58
Table 6. Summary of the key input physicochemical parameters of the various creatine compounds simulated	64
Table 7. Release rate profile for controlled release CM formulation	67
Table 8: Cycling conditions for RT-PCR	69
Table 9: CRT1 primer sequences used for RT-PCR	69
Table 10. Predicted vs. observed PK parameters following administration of bolus iv injection (10 mg/kg) or an oral suspension (70 mg/kg) of CM in rats	94
Table 11. Plasma observed and simulated C_{\max} , T_{\max} , AUC_{0-t} , and $\text{AUC}_{0-\infty}$, following administration of an oral single dose of CM (2, 5, or 20 g)	96
Table 12. Muscles observed and simulated C_{\max} , T_{\max} , and $\text{AUC}_{0-\infty}$, following administration of an oral single dose of CM (5 g)	97
Table 13. Plasma observed and simulated PK parameters following administration of multiple-doses of CM (4 x 5 g oral CM)	99
Table 14. Plasma observed and simulated PK parameters following administration	

of multiple-doses of CM (5, 10, or 15 g twice daily oral CM for 7 days) .. 100

Table 15. Muscle observed and simulated PK parameters following administration of multiple-doses of CM (4 x 5 g oral CM for 7 days) 101

Table 16. The area under the curve at steady state (AUC_{ss}) during 24 hours for plasma, brain, and muscles concentration-time curves following administration of oral CM 20 g/day or 4 x 5 g per day 109

Table 17. Comparison between AUC_{ss} and C_{ss} following administration of 20 g once daily oral CM in SR or IR (suspension) dosage forms for 7 days. $CC_{ss} = AUC_{ss}/\tau$, where τ is the dosing interval (24 hours) 113

Table 18. C_{max} and $AUC_{0-\infty}$ following administration of 20 g oral dose of CM, CrC, CrPyr, or CHCl in plasma, brain, and muscle 121

Table 19. C_{max} and AUC_{ss} at steady state during one dosing interval following administration of 20 g oral dose once daily for 7 days of CM, CrC, CrPyr, or CHCl in plasma, brain, and muscle 131

List of Figures

Figure 1. Endogenous creatine biosynthesis pathway AGAT: L-arginine:glycine amidinotransferase. GAMT: S-adenosyl-L-methionine:N-guanidinoacetate methyltransferase. SAM: S-adenosylmethionine. SAH: S-adenosylhomocysteine	4
Figure 2. Theoretical model of the creatine-PCr-CK system. (Adapted from Walliman et al., 1998) ATP: Adenosine triphosphate. ADP: Adenosine diphosphate. Mi-CK: Mitochondrial creatine kinase. CKc: Cytosolic creatine kinase	8
Figure 3. Schematic representation of different solutes absorption pathways in the GIT tract (Adapted from Alraddadi et al.,)	33
Figure 4. ACAT model used in GastroPlus. (Adapted from Agoram et al.,) ...	49
Figure 5. Schematic presentation of CM- ¹³ C and CEE- ¹³ C PK study treatment groups	55
Figure 6. Representative chromatograms of creatine- ¹³ C (black) and creatine-d ₃ (red) in blank plasma (A), a 10 µg/ml standard sample of creatine- ¹³ C in plasma (B), and an unknown rat plasma sample in similar range as the standard which we measured as 10.7 µg/ml creatine- ¹³ C (C). The assay was developed for the simultaneous measurement of creatine- ¹³ C and creatine-d ₃ (D). Intensity is in counts per minute (CPM)	61
Figure 7. A summary of the simulations of creatine compounds performed in humans	66
Figure 8. Plasma creatine- ¹³ C concentration-time curves following administration of 10 mg/kg iv bolus injection of CM- ¹³ C in adult male rats. The curves are shown in both linear (A) and semi-log (B) formats. Values represent the mean ± SEM. n = 4 rats	74

Figure 9. Plasma creatine-¹³C concentration–time curve following administration of (A) high dose (70 mg/kg) or (B) low dose (10 mg/kg) oral CM-¹³C. Values represent the mean ± SEM. *n* = 4 rats 75

Figure 10. (A) Muscle and (B) brain concentrations of creatine-¹³C 4 hours after administration of iv or oral dose of CM-¹³C. Values represent the mean ± SEM. *n* = 4 rats. Creatine-¹³C content in muscle and brain samples from non-treated rats was below detection limits (0.5 µg/g tissue). ** *p* < 0.01, *** *p* < 0.001, **** *p* < 0.0001 compared to levels in non-treated group (one-way ANOVA). BDL = below detection limit 77

Figure 11. RBC concentrations of creatine-¹³C 4 hours after administration of iv or oral dose of CM-¹³C. Values represent the mean ± SEM. *n* = 4 rats. Creatine-¹³C content in RBC from non-treated rats was below detection limits (0.5 µg/g tissue). NS = non-significant compared to levels in non-treated group (one-way ANOVA). BDL = below detection limit 78

Figure 12. Verification of Creatine Transporter mRNA Expression using RT-PCR in Caco-2 and MDCK-*MDR1* lysates.
 Lane 1: DNA ladder; Lane 2 and 3: Two different samples from Caco-2 lysates; Lane 4 and 5: Two different samples from MDCK-*MDR1* lysates. Arrows indicate bands of interest 80

Figure 13. Permeability of (A) fluorescein, (B) rhodamine 800, and (C) IR dye PEG across Caco-2 monolayers at various time points (0-120 minutes) with or without 10 µM, 100 µM, or 1000 µM CM. Data are presented as % flux. Values represent the mean ± SEM for 3 different monolayers per treatment group . 82

Figure 14. Permeability of (A) fluorescein, (B) rhodamine 800, and (C) IR dye PEG across MDCK-*MDR1* monolayers at various time points (0-120 minutes) with or without 10 µM, 100 µM, or 1000 µM CM. Data are presented as % flux. Values represent the mean ± SEM for 3 different monolayers per treatment group .. 83

Figure 15. Permeability of CM at three different concentrations: 10, 100, or 1000 μ M across (A) Caco-2, or (B) MDCK- <i>MRDI</i> monolayers at various time points (0-120 minutes). Data are presented as % flux. Values represent the mean \pm SEM for 3 different monolayers per treatment group	85
Figure 16. Permeability coefficients of CM at three different concentrations in Caco-2 and MDCK- <i>MDRI</i> monolayers	86
Figure 17. Permeability of CC at three different concentrations: 10, 100, or 1000 μ M across (A) Caco-2, or (B) MDCK- <i>MRDI</i> monolayers at various time points (0-120 minutes). Data are presented as % flux. Values represent the mean \pm SEM for 3 different monolayers per treatment group	87
Figure 18. Permeability coefficients of CC at three different concentrations in Caco-2 and MDCK- <i>MDRI</i> monolayers	88
Figure 19. Simulated (solid line) and observed creatine plasma concentration–time curves obtained from 4 rats, after a single iv dose of CM (10 mg/kg)	91
Figure 20. Simulated creatine concentrations in (A) plasma, (B) muscle and (C) brain following a single oral dose (70 mg/kg) of CM (dashed line) or CHCL (solid line) using GastroPlus compared to observed values	92
Figure 21. Simulated plasma levels of creatine following administration of oral CM (A) 20 g/day for 7 days, or (B) 4 x 5 g for 7 days	103
Figure 22. Simulated plasma levels of creatine at steady state during one dose interval following administration of oral CM (A) 20 g/day for 7 days, or (B) 4 x 5 g for 7 days	104
Figure 23. Simulated brain levels of creatine following administration of oral CM (A) 20 g/day for 7 days, or (B) 4 x 5 g for 7 days	105
Figure 24. Simulated brain levels of creatine at steady state during one dose interval following administration of oral CM (A) 20 g/day for 7 days, or (B) 4 x 5 g for 7 days	106

Figure 25. Simulated muscles levels of creatine following administration of oral CM (A) 20 g/day for 7 days, or (B) 4 x 5 g for 7 days	107
Figure 26. Simulated muscles levels of creatine at steady state during one dose interval following administration of oral CM (A) 20 g/day for 7 days, or (B) 4 x 5g for 7 days	108
Figure 27. (A) Plasma, (B) brain, and (C) skeletal muscle concentration-time curve following administration of 20 g once daily oral CM in SR formulation for 7 days	111
Figure 28. PBPK model simulations of (A) plasma, (B) brain, and (C) muscles concentration-time curves following administration of 20 g once daily oral CM in male (black line) or female (blue line) for 7 days	114
Figure 29. Simulated (A) plasma, (B) brain, and (C) muscles concentrations-time curve following administration of a 5 g oral single dose of CM, CrC, CrPyr, or CHCL	117
Figure 30. Simulated (A) plasma, (B) brain, and (C) muscles concentrations-time curve following administration of a 20 g oral single dose of CM, CrC, CrPyr, or CHCl	119
Figure 31. Simulated (A) plasma, (B) brain, and (C) muscle concentration-time curves following administration of a 4 x 5 g oral of CM, CrC, CrPyr, or CHCl for 7 days	123
Figure 32. Simulated (A) plasma, (B) brain, and (C) muscle concentrations-time curves at steady state during one dosing interval (6 hours) following administration of a 4 x 5 g oral CM, CrC, CrPyr, or CHCl	125
Figure 33. Simulated (A) plasma, (B) brain, and (C) muscle concentration-time curves following administration of a 20 g once daily oral CM, CrC, CrPyr, or CHCl for 7 days	127
Figure 34. Simulated (A) plasma, (B) brain, and (C) muscle concentration-time	

curves at steady state during one dosing interval (24 hours) following administration of a 20 g once daily oral CM, CrC, CrPyr, or CHCl 129

Figure 35. Plasma CEE-¹³C and CRN-¹³C concentration-time curve following iv administration of CEE-¹³C in adult male rats. Values represent the mean ± SEM. *n* = 4 rats 133

Figure 36. Plasma concentration–time curves following administration of (A) high dose (70 mg/kg) or (B) low dose (10 mg/kg) oral CEE-¹³C. Values represent the mean ± SEM. *n* = 4 rats 134

Figure 37. (A) Brain and (B) muscles concentrations of Creatine-¹³C 4 h after administration of iv or oral dose of CEE-¹³C. Values represent the mean ± SEM. *n* = 4 rats. Creatine-¹³C content in muscle and brain samples from non-treated rats was below detection limits (0.5 µg/g tissue). ns= non significant, * *p* < 0.05, ** *p* < 0.01, *** *p* < 0.001, **** *p* < 0.0001 compared to levels in non-treated group (one-way ANOVA). BDL = below detection limit 135

Figure 38. Muscle concentrations of CRN-¹³C 4 h after administration of iv or oral CEE-¹³C. Values represent the mean ± SEM. CRN-¹³C content in muscle samples from non-treated rats was below detection limits (0.5 µg/g tissue). *n* = 4 rats 136

List of Abbreviations

3-NP	3-nitropropionic acid
λ_z	Elimination rate constant
ACAT	Advanced Compartmental Absorption and Transit
AD	Alzheimer's disease
ADP	Adenosine diphosphate
AGAT	L-arginine:glycine amidinotransferase
ALS	Amyotrophic lateral sclerosis
AMP	Adenosine monophosphate
ANT	Adenine nucleotide translocase
ATP	Adenosine triphosphate
AUC	Area under plasma concentration-time curve
AUC_{0-t}	AUC from zero to the last measurable concentration
$AUC_{0-\infty}$	AUC from zero to infinity
AUC_{ss}	AUC at steady state
BBB	Blood-brain barrier
Caco-2	Human epithelial colorectal adenocarcinoma
CAT	Compartmental Absorption and Transit
CC	Cyclocreatine
CCDS	Cerebral creatine deficiency syndromes
CEE	Creatine ethyl ester
$CEE-^{13}C$	Creatine ethyl ester- ^{13}C
CHCl	Creatine hydrochloride
CK	Creatine kinase
CL	Clearance
C_{last}	Last measurable nonzero plasma concentration

CM	Creatine monohydrate
CM- ¹³ C	CM (guanidino- ¹³ C)
C _{max}	Maximum or peak plasma concentration
COX-2	Cyclooxygenase-2
C _{p0}	Initial serum concentration
CR	Controlled release
CrC	Creatine citrate
Creatine-d3	Creatine (methyl-d3)
CRN	Creatinine
CRN- ¹³ C	Creatinine (guanidine- ¹³ C)
CrPyr	Creatine pyruvate
CRT1	Creatine transporter 1
CRT2	Creatine transporter 2
CV	Coefficient of variation
CYP	Cytochrome P450
DAC	Di-acetyl creatine ethyl ester
DDS	Drug delivery systems
F	Absolute oral bioavailability
GAA	Guanidinoacetic acid
GABA	Gamma-Aminobutyric acid
GAMT	S-adenosyl-L-methionine:N-guanidinoacetate
methyltransferase	
GIT	Gastrointestinal tract
GPA	3-guanidinopropionic acid
HD	Huntington's disease
IFNa	Interferon-alpha
IL-1β	Interleukin-1β

IR	Immediate release
iv	Intravenous
K_m	Michaelis constant
LC-MS/MS	Liquid chromatography-tandem mass spectrometry
LDH	Lactate dehydrogenase
LLOQ	Lower limit of quantitation
MDCK- <i>MDR1</i> resistance gene	Madin-Darby canine kidney epithelial cells – multi drug resistance gene
MDs	Muscular dystrophy diseases
Mi-CK	Mitochondrial creatine kinase
MND	Motor neuron disease
MPTP	1-methyl-4-phenyl-1,2,3,6-tetrahydropyridine
mPTP	Mitochondrial permeability transition pore
MRS	Magnetic resonance spectroscopy
MRP2	Multidrug resistance-associated protein 2
NADH	Nicotinamide adenine dinucleotide
NHIS	National Health Interview Survey
P-gp	P-glycoprotein
PBPK	Physiologically based pharmacokinetic
P_c	Permeability coefficient
PCr	Phosphocreatine
PCr-Mg-CPLX	Phosphocreatine-Mg-complex acetate
PD	Parkinson's disease
P_{eff}	Effective permeability
PGE2	Prostaglandin E2
PK	Pharmacokinetic
PTP	Permeability transition pore

REAR	Population Estimates for Age-Related Physiology
RBC	Red blood cell
ROS	Reactive oxygen species
SAH	S-adenosylhomocysteine
SAM	S-adenosylmethionine
SEM	Standard error of the mean
SLC6	Solute carrier 6
SOD1	Superoxide dismutase 1
SR	Sustained release
$T_{1/2}$	Half-life
TLRs	Toll-like receptors
T_{\max}	Time taken to reach C_{\max}
$TNF\alpha$	Tumor necrosis factor-alpha
UHDRS	Unified Huntington Disease Rating Scale
UPDRS	Unified Parkinson Disease Rating Scale
V_d	The apparent volume of distribution

Chapter 1. Introduction

1.1. Introduction

Creatine, is a nitrogenous guanidine compound that is both synthesized endogenously and found exogenously in various food sources such as meat and fish. Since creatine's isolation and extraction from animal skeletal muscle by French chemist Michel Eugène Chevreul in 1832, it has been one of the most extensively studied dietary supplements. (1-3) The earliest reported use of creatine as a potential ergogenic supplement appeared in the early 1990s as studies began to report the beneficial effects of creatine on exercise performance, especially in those sports requiring short, high-intensity exercises. (1, 2, 4-6) In a survey among bodybuilders conducted in 2013, dietary supplements were used by all the respondents, and creatine was among the most popular supplements consumed, with 70% reporting current use of creatine supplements. (7) In 2012, The National Health Interview Survey (NHIS) reported 34% use of creatine among children and adolescents with the purpose of improving sports performance. (8) Creatine is now widely used among recreational and professional athletes as an ergogenic supplement with an annual market of more than 400 million United States dollars worldwide. (9) Creatine monohydrate (CM), first marketed in the early 1990s, is the form most commonly found in dietary supplement/food products and most frequently cited in scientific literature. (10) However, the explosive growth in creatine supplement sales has led to the introduction of many different salt forms of creatine.

1.2. Creatine Storage and Synthesis

In the body, the total amount of creatine is equal to both free creatine and phosphocreatine (PCr), which together comprise the total creatine pool. The total creatine content in the body equals approximately 120 g in a 70 kg adult. (11) About 60% of the total creatine content in the body is PCr, and the remainder is free creatine. (4) Creatine is distributed throughout the body with approximately 95% of creatine stored in skeletal muscle. The remaining 5% is distributed in other tissues with the highest concentrations found in the brain, liver, and kidneys. (11) Creatine and PCr break down (non-enzymatically) to creatinine (CRN), which is then excreted in the urine. (12) Based on CRN excretion in the urine, the daily amount of creatine lost from the body is estimated to be 1.7% (≈ 2 g) of the total body creatine pool. (12) Using this estimate of creatine turnover, the recommended minimum daily requirements of creatine for an average human are around 2 g, to replenish the amount of creatine and PCr converted to CRN. (13)

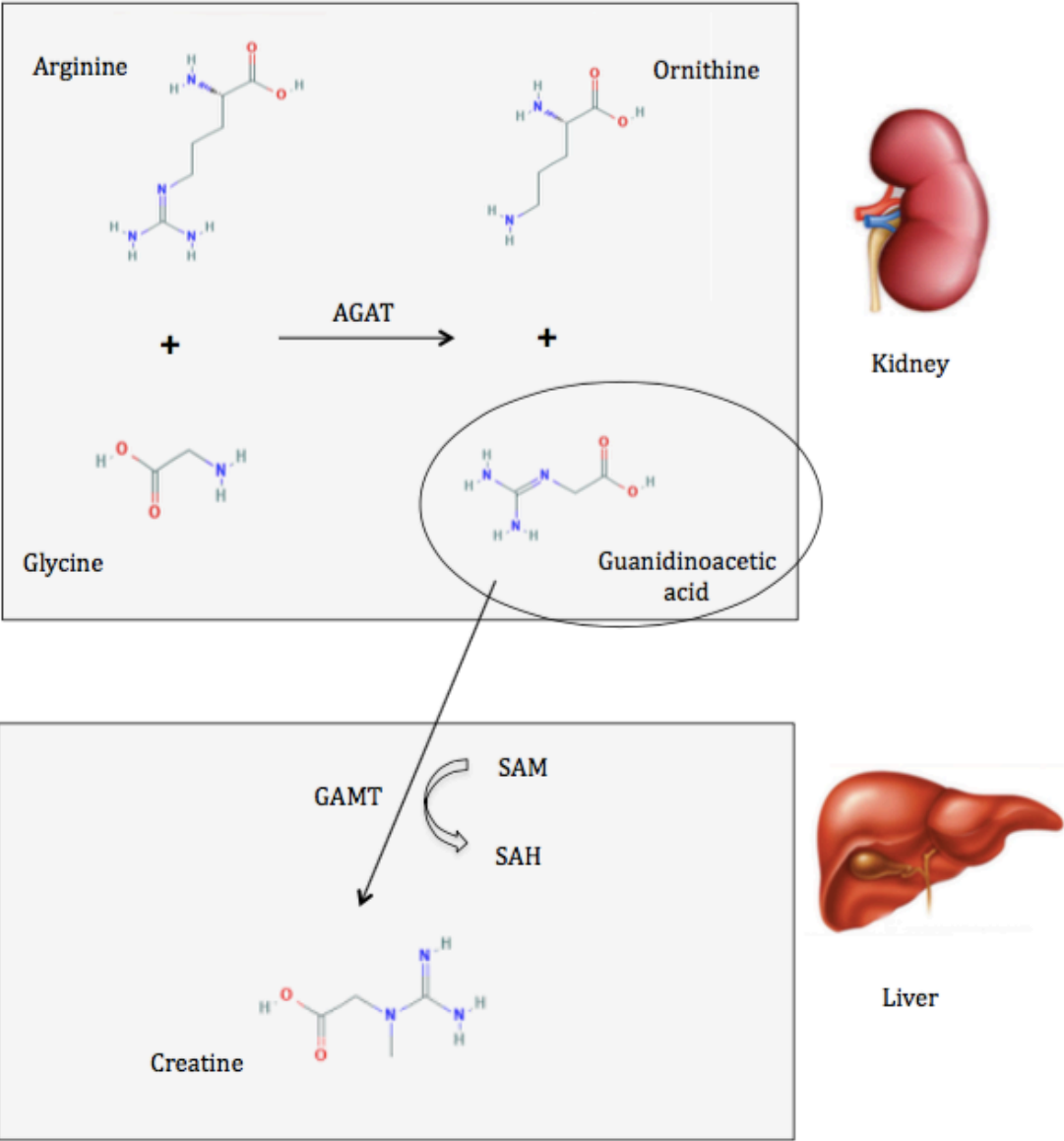
There are two main sources of creatine, exogenous creatine obtained through the diet especially in protein-based foods such as meat, fish, milk, and nuts (4, 13), and endogenous creatine synthesized mainly in the liver and kidney. It is estimated that the normal dietary intake of creatine in an omnivorous diet is around 1 g per day (4, 13) with an additional 1 g coming from endogenous sources, Figure 1. (14) The synthesis of creatine requires three amino acids, L-arginine, glycine, and L-methionine. (14) The first and rate-limiting step of creatine synthesis is the transfer of an amidino group from L-arginine to glycine to yield L-ornithine and guanidinoacetic acid (GAA). (14) This step is catalyzed by the enzyme L-arginine:glycine amidinotransferase (AGAT). (14) GAA is then methylated by the action of a second enzyme, S-adenosyl-L-methionine:N-guanidinoacetate

methyltransferase (GAMT), to produce creatine, Figure 1. (14)

In mammals, the AGAT and GAMT enzymes are expressed in many tissues including the pancreas, liver, kidney, and brain. (15) However, the tissue localization of AGAT and GAMT is complex. In kidneys, AGAT is expressed in high levels, whereas GAMT is expressed in relatively low (or undetectable) levels. (12, 14, 15) In contrast, in the liver, AGAT is not detected, but GAMT is strongly expressed. (14, 15) Based on the expression patterns of AGAT and GAMT and on the fact that the rate of creatine synthesis is significantly reduced with nephrectomy, (16) it is theorized that GAA is first formed in the kidney and then transferred to the liver where creatine is formed. (14) However, the contribution of other tissues to creatine synthesis is uncertain. The mammalian brain is also able to synthesize creatine and all the main cell types of the brain (neurons, oligodendrocytes, and astrocytes) express both AGAT and GAMT. (17-21) However, it is still not known to what extent de novo synthesis of creatine in the brain contributes to the total brain creatine content.

Figure 1. Endogenous creatine biosynthesis pathway. (14)

AGAT: L-arginine:glycine amidinotransferase. GAMT: S-adenosyl-L-methionine:N-guanidinoacetate methyltransferase. SAM: S-adenosylmethionine. SAH: S-adenosylhomocysteine.



1.3. Cellular Effects of Creatine

1.3.1. Cellular Energetic Effects (Creatine/PCr/CK System)

Adenosine triphosphate (ATP) is the universal energy currency for most of the energy requiring processes in biological systems. (22) Excitable cells and tissues, e.g. skeletal and cardiac muscle, all depend on the immediate availability of vast amounts of energy that may be used in a pulsed or fluctuating manner. (22) Simply increasing intracellular concentrations of ATP for energy storage is not the ideal choice to meet the energy requirements of these cells and tissues, since local [ATP], [adenosine diphosphate (ADP)] and [adenosine monophosphate (AMP)], as well as the ATP/ADP ratio, are key regulators influencing many fundamental metabolic processes. (22) Indeed, the level of ATP in excitable cells, such as skeletal muscle, ranges from 2 to 5 mM. Based on these levels of ATP, muscle contraction for example could only be sustained for few seconds. Instead, however, large quantities of PCr are accumulated in these cells or tissues reaching up to 22 to 35 mM, thus providing a relatively large pool of cellular phosphate for replenishing ATP. (11, 23)

The main function of creatine within the cell is to provide a readily available source of phosphate for the replenishment of ATP. This is accomplished through the creatine/PCr/creatine kinase (CK) energy system, which acts as a temporal energy buffer. (14) This system plays an essential role in maintaining high energy levels in the cells, especially under conditions of increased energy demand, where the consumption of ATP exceeds the cells ability to synthesize it (e.g. short intense exercise). (19) The creatine/PCr/CK system also plays an important compensatory role under pathological conditions where reduced cellular oxygen or mitochondrial

dysfunction is present (e.g. myocardial infarction or neurodegenerative disorders).
(24)

Cellular energetics is highly balanced and regulated and capable of rapid response to environmental demands. For instance, the rate of ATP hydrolysis can be increased significantly in cells within seconds, however, even though the cellular pools of ATP are rather small, the level of intracellular ATP remains surprisingly constant. This can be explained by the complex action of the immediately available creatine/PCr/CK system, which represents an extremely efficient energy buffering system. (24) Synthesized creatine is transported through the blood and taken up by tissues with high-energy demands. The enzyme CK, which is a key enzyme in cellular energetics, catalyzes the reversible reaction shown in Figure 2, in which creatine is phosphorylated resulting in PCr. (25, 26) During short intense exercise, when cellular energy in the form of ATP is being consumed, the stores of PCr are hydrolyzed and the phosphate liberated from this reaction is available for phosphorylation converting ADP back into ATP, Figure 2. (13) In muscles, the ATP regeneration capacity of CK is very high and considerably exceeds both ATP utilization as well as ATP replenishment by oxidative phosphorylation and glycolysis. (27)

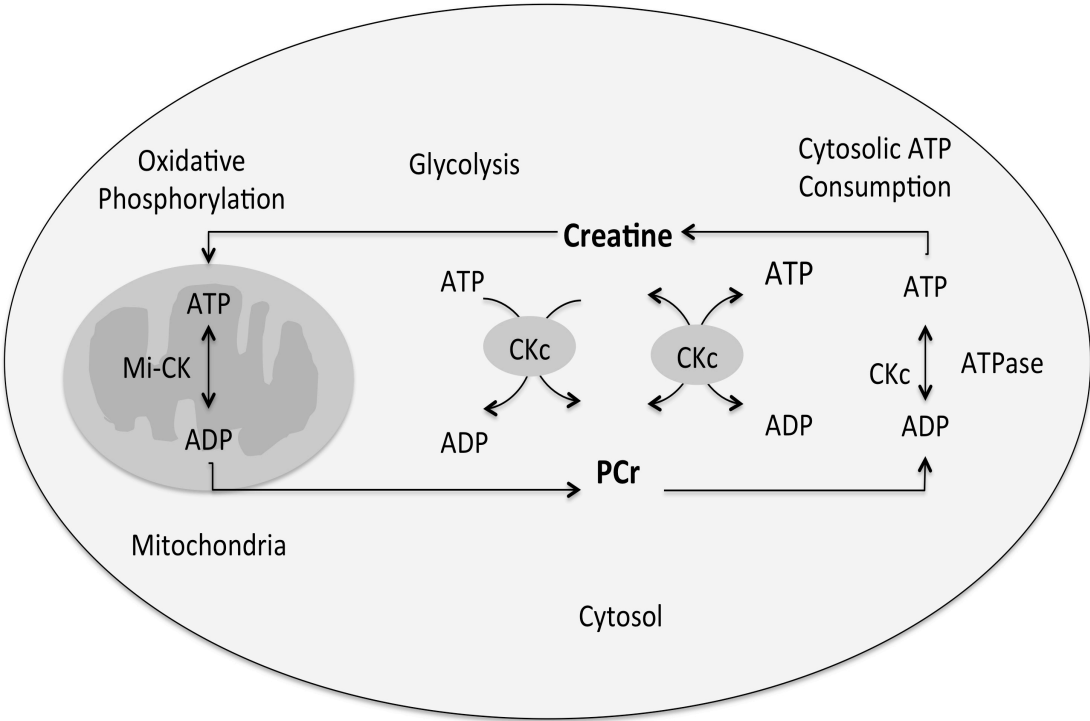
There are 2 types of CK that are co-expressed together in a tissue-specific manner. The first type is cytosolic CK, which consists of 2 subunits, B (brain type) or M (muscle type). The subunit combinations give rise to 3 different dimeric cytoplasmic isoenzymes, CK-MM, CK-BB, and CK-MB. Human M-CK is selectively expressed in adult skeletal muscle and heart tissues, whereas B-CK is expressed in adult heart, colon, and uterus but not skeletal muscle. (28) The second type of CK is mitochondrial CK (Mi-CK), which resides in the mitochondria and has two different isoenzymes, sarcomeric Mi-CK, which is striated muscle specific and ubiquitous Mi-CK, which is found in most other tissues like brain and kidneys.

(14, 23) Cytosolic CK catalyzes the transfer of high-energy phosphate from PCr to ADP, functioning as a temporal energy buffer in times of high ATP turnover. (23) Additionally, some fractions of the cytosolic CK are functionally coupled to glycolysis, and during periods of anaerobic exercise and recovery, preferentially accepts glycolytic ATP to replenish the PCr pool. Moreover, other fractions of cytosolic CK are specifically associated with ATP requiring processes at sites of energy consumption, where ATP is directly regenerated *in situ* by CK, Figure 2. (23)

Beside the function of the creatine/PCr/CK system as a temporal energy buffer, it has been suggested that the creatine/PCr/CK system might also act as an energy shuttle or transporter. (29) Distinct CK isoenzymes are associated with sites of energy production (Mi-CK in the mitochondria) and ATP consumption (Cytosolic CK). Mi-CK is bound to the outer side of the inner mitochondrial membrane (IM) and localized along the cristae membranes. (29) At these sites, Mi-CK octamers are forming micro-compartments with porin and adenine nucleotide translocase (ANT) for energy transfer from ATP to creatine, followed by the transport of PCr into the cytosol. (22, 23) ATP generated by oxidative phosphorylation within the mitochondria is accepted by Mi-CK octamers, transphosphorylated onto creatine, which is entering through the pore, to give PCr, which then is exported into the cytosol to the sites of ATP consumption where it is used to regenerate ATP. (22, 23, 30) Thus, under high workload, high-energy phosphate would be shuttled from mitochondria to sites of energy consumption, where it is then used by cytosolic CK to regenerate ATP locally *in situ* to fuel these ATP-requiring processes and to keep local ATP/ADP ratios very high. (30) ADP liberated by the Mi-CK reaction may directly be transported back to the matrix where it is rephosphorylated to ATP. Creatine liberated through this reaction diffuses back to the mitochondria, thereby completing the cycle. (14)

Figure 2. Theoretical model of the creatine-PCr-CK system. (Adapted from Walliman et al., 1998). (23)

ATP: Adenosine triphosphate. ADP: Adenosine diphosphate. Mi-CK: Mitochondrial creatine kinase. CKc: Cytosolic creatine kinase.



1.3.2. Other Cellular Effects of Creatine

In addition to helping maintain cellular energetics, several other beneficial effects of creatine have been suggested. One of the possible beneficial cellular effects of creatine is stabilizing the mitochondrial permeability transition pore (mPTP), thus preventing mitochondrial dysfunction. (30-33) The permeability transition is an abrupt increase of the inner mitochondrial membrane permeability to solutes. PTP opening is traditionally linked to mitochondrial dysfunction because its occurrence leads to mitochondrial depolarization, cessation of ATP synthesis, calcium release, inhibition of respiration, and activation of apoptosis. (32) It should be mentioned that these detrimental effects on cell viability are only seen for long-lasting openings of the PTP, while short-term openings, may be involved in physiological regulation of calcium and reactive oxygen species (ROS) homeostasis, and provide mitochondria with a fast mechanism for calcium release. (31)

Mi-CK interacts with the proteins of both inner and outer mitochondrial membranes that contribute to mPTP formation. It was suggested that creatine converts Mi-CK from its dimeric form to the more stable octameric form that stabilizes mPTP, thus preventing its opening. (32)

In addition, creatine was shown to have the ability of directly scavenging free radical species. (34) Creatine treatment in cultured mammalian cells exposed to different oxidative agents exerted a dose-dependent (up to 10 mM) antioxidant activity via a mechanism dependent on direct scavenging of reactive oxygen and nitrogen species. (34) Moreover, recently, several studies have reported interest in the anti-inflammatory effects of creatine. Evidence in support of the anti-inflammatory effects of creatine include reduced production of inflammatory

markers, such as prostaglandin E2 (PGE2), tumor necrosis factor-alpha (TNF α), and lactate dehydrogenase (LDH), associated with intense exercise upon supplementation with oral creatine in athletes. (35-37) In addition, many *in-vitro* studies have shown that creatine reduces inflammatory mediators and markers including PGE2, cyclooxygenase-2 (COX-2), TNF α , and toll-like receptors (TLRs) in various cell lines. (38-40) Alraddadi et al., showed creatine to be protective against interleukin-1 β (IL-1 β) insult in canine chondrocytes, used as an *in-vitro* model of osteoarthritis, reducing TNF α , PGE2 and COX-2 production. (38) Together, these studies suggest that creatine has several potential beneficial effects in a variety of cells and tissues.

1.4. Creatine Transport

Given the tissue distribution of the enzymes required for synthesis of creatine, it is likely that most endogenous creatine is produced in different tissues than the ones that ultimately utilize creatine. Evidence for this is the observation that in mammals the organs likely responsible for creatine synthesis (i.e. liver and kidneys) contain the highest levels of AGAT and/or GAMT but have the lowest levels of CK, the enzyme responsible for phosphorylation of creatine to PCr. (11) Based on this observation, synthesized creatine must be transported from tissues that produce the nutrient (mainly liver and kidneys) to tissues with high and fluctuating energy demands for storage and utilization, such as skeletal muscle, brain, and the heart. It is transported into tissues against a concentration gradient through a specific sodium- and chloride- dependent creatine transporter (CRT1). (13)

CRT1 belongs to the solute carrier 6 (SLC6) family of membrane transport proteins. (41) SLC6 represents a large family of membrane transporters that facilitate the transport of many solutes including neurotransmitters, such as dopamine, and amino acids across the plasma membrane of cells. (41) CRT1 is encoded by the SLC6A8 gene located on chromosome Xq28. (42) At the mRNA level, the tissue expression of CRT1 matches that of CK, predominantly in muscles, kidney, heart, brain, colon, and testes. (43-45) In addition to CRT1, an additional creatine transporter has been identified, creatine transporter 2 (CRT2), which is encoded by the SLC6A10 gene, located on chromosome 16p11 and is expressed in the testes only. (46) The physiological significance of this particular isoform is still not clear.

CRT1 is a saturable sodium- and chloride- dependent transporter that transports creatine with high specificity against its concentration gradient. (42) The cellular uptake of creatine depends on the sequential binding and co-transport of Na^+ and Cl^- ions with a coupling ratio of 2 Na^+ : 1 Cl^- : 1 creatine molecule. (47) The ion concentration gradient generated by the plasma membrane Na^+/K^+ ATPase provides the driving force for creatine uptake into the cell. (47)

1.4.1. Creatine Transporter Expression in the Brain

Although creatine is synthesized in the liver and kidney, creatine concentrations in the mammalian brain is 4- to 20- fold greater than that in the liver. (48) In the brain, CRT1 is expressed on both the luminal and abluminal sides of the capillary endothelial cells suggesting the blood-brain barrier (BBB) permeability of creatine is dependent on transporter activity. (49) Moreover, CRT1

is also widely expressed in neurons and oligodendrocytes. However, it does not appear to be highly expressed in the astrocytic feet processes, which cover more than 98% of the surface of the capillary endothelial cells. (49, 50) While AGAT and GAMT are expressed in almost all the cells in the brain, including neurons and astrocytes, it is still not known to what extent de novo synthesis of creatine in the brain contributes to the total brain creatine content.

In contrast, there is supportive evidence of the important role of creatine transport at the BBB in meeting the creatine requirements of the brain. In *in-vitro* mouse hippocampal slices, the creatine transporter was required for creatine uptake through the plasma membrane. Incubation with creatine increased creatine and PCr content of the tissue. On the other hand, inhibition of the creatine transporter with 3-guanidinopropionic acid (GPA) dose-dependently prevented this increase. (51) In addition, The presence of a creatine transport system from the blood to the brain across the BBB has been demonstrated in mouse capillaries and has been shown to be saturable by endogenous plasma creatine. (49)

Perhaps the most compelling evidence supporting the important role of BBB creatine transport is from the study of genetic mutations within the CRT1 transporter. Individuals with CRT1 deficiency, caused by mutations in the SLC6A8 gene, have reduced levels of creatine in the brain despite normal functioning of AGAT and GAMT. (43) The loss of CRT1 function leads to neurological symptoms, including intellectual disability, delays in speech, autism, and seizures. (52) Patients deficient in CRT1 seem to be unresponsive to exogenously administered creatine and did not display any creatine signal according to proton magnetic resonance spectroscopy. (47) On the other hand, AGAT and GAMT deficient patients that have reduced ability for de novo synthesis of creatine, can be successfully treated with oral creatine

supplementation, although very high doses of creatine are used and the replenishment of cerebral creatine takes months and may only achieve partial restoration of the cerebral creatine pool. (53-55) This highlights the importance of peripheral and exogenously administered sources of creatine as determinants of brain levels of creatine and has fueled interest in potential benefits of creatine supplementation in the treatment of creatine deficient syndromes and neurodegenerative diseases.

1.5. Exogenous Administration of Creatine Supplements

As mentioned before, in situations of increased energy demands or reduced energy production, exogenous creatine supplementation might be beneficial. The loss of creatine due to degradation to CRN is around 2 g daily. This amount is replenished by endogenous synthesis and through creatine present in the diet. (13) However, in case of high-energy requirements or reduced energy production, large amounts of creatine are required to produce beneficial effects that can only be obtained through dietary supplementation. (56) Exogenously administered creatine must first be absorbed into the bloodstream across the intestinal wall. It is then delivered to target organs and taken up by CRT1 to be stored or utilized by the various tissues. (56) To date, creatine supplementation, in the form of CM, has been exploited mainly by athletes and bodybuilders. However, interest in the potential use of creatine supplementation in many diseases where cellular energy production is compromised has increased dramatically. Conditions for which creatine supplementation is being actively examined as either as a stand-alone nutritional supplement or combination therapy include:

- 1) Conditions with increased energy requirements or consumption: Exercise, bodybuilding, and sports performance
- 2) Conditions where endogenous creatine is absent or reduced due to inborn errors in genes responsible for creatine synthesis and/or transport
- 3) Muscle-related disorders, including muscular dystrophy diseases (MD)
- 4) Various neurodegenerative disorders such as Huntington's disease (HD), Parkinson's disease (PD), Alzheimer's disease (AD) and amyotrophic lateral sclerosis (ALS)

1.5.1. Conditions with Increased Energy Requirements: Exercise Performance

The creatine-PCr pool is a readily available source of high-energy phosphagen for cellular energy during strenuous exercise and muscle function, especially under anaerobic conditions. (57) During short-duration, high-intensity exercises, cellular ATP requirements are met by both anaerobic glycolysis and the scavenging of high-energy phosphagen from the PCr system. (1) Skeletal muscle at maximal effort relies on anaerobic glycolysis as the dominant form of ATP production. However there is a time lag before anaerobic glycolysis can be fully activated (around 10 seconds) and there is a limit to how long it can be sustained (approximately 30 seconds). Thus the PCr shuttle provides the source of high-energy phosphate required for ATP replenishment during those times that anaerobic glycolysis is unavailable. (58, 59) By increasing the muscle stores of PCr with oral creatine supplementation, the PCr shuttle can be prolonged, leading

to less dependence on the glycolytic pathway. (60) The performance benefits that result from creatine supplementation include more cellular energy for short-duration, high-intensity exercise, improved energy transfer in muscle cells, greater buffering capacity resulting in less fatigue and shorter recovery time following intense exercise. (60)

Studies have demonstrated that dietary supplementation with CM is correlated with increases in total skeletal muscle creatine levels by approximately 20%, with large inter-individual variation (5-30%). (61-64) Of the increased deposition of creatine in the muscle following supplementation, approximately one-third is in the form of PCr and available for immediate use (61, 65, 66). The observed increase in total creatine in skeletal muscle following oral supplementation was correlated with improved anaerobic exercise performance as measured by increased work output, strength, exercise capacity, and muscle mass. (59, 66-68)

In addition to the well-known effects of creatine supplementation on muscle performance, more recent studies have reported potential use of creatine supplements in muscle repair following injury (69, 70), as well as for its anti-inflammatory effects (35, 36, 71, 72) that apply to both the endurance and power sports athlete. Evidence in support of the anti-inflammatory effects of creatine supplementation includes reduced production of inflammatory markers associated with intense exercise upon supplementation with oral CM. (35-37)

Studies by Santos et al. evaluated the effect of creatine supplementation on the levels of inflammatory markers and muscle soreness in athletes after running 30 km. They found that supplementation with CM (20 g daily), 5 days prior to the 30 km race, significantly attenuated the increases in plasma PGE₂ and TNF α (by 60.9% and 33.7%, respectively), and abolished the increase in plasma LDH concentrations observed after running 30 km compared to the placebo group. (35) Similarly, using the same creatine supplementation protocol, Bassit and colleagues

found that CM significantly reduced the plasma levels of TNF α , interferon-alpha (IFN α), IL-1 β , and PGE2 after a half-iron man competition. (36) These results suggest that creatine supplementation during a short period of five days before intense exercise may attenuate the increase in plasma levels of pro-inflammatory cytokines and PGE2.

1.5.2. Conditions Where Creatine is Absent or Reduced: Inborn Errors of Creatine Synthesis or Transport

Inborn genetic errors collectively referred to as cerebral creatine deficiency syndromes (CCDS) are due to deficiencies in either the enzymes required to produce creatine (i.e. AGAT and GAMT), or the transporter required for cell accumulation of creatine (i.e. CRT1 (SLC6A8)). (18) The AGAT and GAMT deficiencies are autosomal recessive diseases, while SLC6A8 deficiency is an x-linked disorder. (18) Patients with CCDS have significantly reduced levels of cerebral creatine, leading to developmental delay, intellectual disabilities, movement disorders, epilepsy, and mental retardation. (47)

Pediatric patients with GAMT or AGAT deficiency treated with very high doses, ranging from 0.35-2 g/kg/day, of exogenous CM show improved neurological outcomes. (53, 55, 56) However, treatment is more effective the earlier it started, and replenishment of cerebral creatine can take months and may only achieve partial restoration of the cerebral creatine pool. (56) In contrast, SLC6A8 deficient patients do not respond favorably to exogenous CM supplementation, as the exogenous creatine cannot reach the brain in sufficient amounts due to the absence of the transporter in the BBB necessary to facilitate

creatine delivery to the brain. (47). This lack of effective treatment has spurred interest in newer forms of creatine that can penetrate the BBB without the aid of the CRT1 transporter, which will be, discussed later.

1.5.3. Muscle-related Disorders, Including Muscular Dystrophies (MDs)

Studies have shown that exogenous creatine supplementation might be beneficial in certain hereditary muscular disorders characterized by progressive muscle wasting and weakness. (73) The more common hereditary myopathies are the MDs encompassing 30 different genetic disorders. (73) Patients with MD have lower skeletal muscle creatine and PCr concentrations compared to healthy subjects, which may be a function of lower creatine transporter content. (73) Despite the reductions in CRT1 expression, meta-analysis of all randomized controlled trials of creatine supplementation in MD revealed significant increases in muscle strength with exogenous CM supplementation compared to control group and improvements in functional performance. (73)

1.5.4 Neurodegenerative Disorders Such as HD, PD, AD and ALS

Although the majority of studies on creatine supplementation have focused on exercise performance, recent evidence suggests creatine might be beneficial in certain neurodegenerative diseases that involve impaired energy production and/or mitochondrial dysfunction. (24, 74) CM supplementation has been shown to be

neuroprotective in many cellular and animal models of neurodegenerative diseases including HD, AD, PD, and ALS. (74-78) The exact molecular mechanism by which creatine exerts its neuroprotective effect is not clearly understood. However, several potential mechanisms of neuroprotection of creatine have been suggested including buffering of intracellular energy reserves, improved mitochondrial function, stabilization of the mitochondrial permeability transition pore, reduced excitotoxicity, and increased antioxidant activity. (74-78)

1.5.4.1. Huntington's Disease

HD is a progressive autosomal dominant inherited neurodegenerative disorder. It is caused by an unstable expansion of CAG trinucleotide repeat in the huntingtin gene, which is located on chromosome 4, resulting in mutated elongated poly-glutamine stretches in the huntingtin protein. (79) The behavior of the mutated protein is not completely understood, but it is toxic to certain cell types, particularly brain cells. Early damage is most evident in the subcortical basal ganglia, initially in the striatum, but as the disease progresses, other areas of the brain are also affected, including regions of the cerebral cortex. (79)

HD is characterized by degeneration of the gamma-aminobutyric acid (GABA)-ergic medium-sized spiny projection neurons within the striatum in the basal ganglia leading to progressive development of motor incoordination and loss of cognitive function. (80, 81)

There is increasing evidence suggesting a role of cellular energetics and mitochondrial dysfunction in HD. (82-88) Several studies have shown elevated levels of lactate in the cerebral cortex and basal ganglia of patients with HD. Also,

there is reduced PCr/inorganic phosphate in the resting muscle of HD patients and reductions in mitochondrial electron transport enzymes found in HD postmortem tissue. (86, 89-91) Additional evidence for altered cellular energetics and potential role for creatine supplementation in HD comes from studies in various animal models of HD. Matthews et al. used two neurotoxins, malonate and 3-nitropropionic acid (3-NP) in rats; these are reversible and irreversible inhibitors of succinate dehydrogenase (complex II), respectively. (92) These neurotoxins induced striatal lesions and abnormal motor behavior that closely resembled that seen in HD patients. (92) Investigators found that administration of 1% dietary CM (w/w diet) for 2 weeks resulted in significant reductions in lesion volume produced by malonate and 3-NP. (92) In addition CM supplementation increased brain concentrations of PCr and protected against depletion of PCr and ATP produced by 3-NP. CM also protected against 3-NP induced increases in striatal lactate levels. (92) Using the same HD model in a different study, Shear and colleagues showed that addition of 1% CM to the rats chow for 2 weeks prior to 3-NP administration, attenuated striatal lesions, striatal atrophy, ventricular enlargement, cognitive deficits, and motor abnormalities compared to rats fed normal chow. (93)

Ferrante et al. used the transgenic R6/2 mouse model of HD. This model has a CAG repeat length of 141-157 (normal < 35) and develops a progressive neurological HD phenotype. (75) At 4.5-6 weeks, R6/2 mice showed a loss of brain and body weight as well as neuronal intra-nuclear inclusions that were immune-positive for huntingtin. Additionally, at 9-11 weeks the mice develop many of the neurological features associated with HD including irregular gait, stereotypic movements, and resting tremors. (75) Using this transgenic mouse model, investigators found that dietary supplementation with 1 or 2% CM at 21 days of age significantly increased survival compared to the control group (by 9.4 and 17.4% in mice supplemented with 1 or 2% creatine, respectively). In addition,

CM administration significantly slowed motor deterioration, reduced gross brain atrophy, and delayed striatal neuron atrophy. (75)

Moreover, Dedeoglu et al. examined the effect of administration of creatine after onset of clinical symptoms in a transgenic mice model of HD. (94) They showed that supplementation of the diet with 2% CM, starting at 6, 8, and 10 weeks of age, analogous to early, middle, and late stages of human HD, significantly extended survival, improved motor performance, and delayed neuronal atrophy. (94) Together, these results suggested beneficial effects of creatine supplementation in mitigating the effects of HD.

Due to the fact that oral creatine supplementation had produced significant neuroprotection in both neurotoxin-induced and transgenic animal models of HD, small pilot studies were conducted to assess the safety, tolerability, and efficacy of creatine supplementation in patients with HD. Verbessem et al. conducted a double-blind placebo-controlled pilot study over a 1-year period. A total of 41 patients ingested 5 g of CM or a matching placebo. (95) In the same year, Tabrizi et al. conducted an open label pilot study with 13 HD patients given 10 g of CM per day for 12 months. (96) In both of these studies, CM administration was safe and well tolerated, however, no improvement in cognitive function was found.

In 2014, The Huntington study group (HSG) published the results of PRECREST, a 18-month, randomized, placebo-controlled, phase II, secondary prevention in at-risk, patients that carried the gene mutation, and presymptomatic HD participants. (97) They showed that high dose CM (up to 30 g daily) was safe and well tolerated. In addition, creatine supplementation significantly slowed that rate of cortical thinning, and reduced the change in white matter, grey matter, and basal ganglia volumes compared to the placebo group. (97)

Based on these positive results, CREST-E, a large multicenter, phase III, randomized, double-blind, placebo-controlled trial of high dose creatine treatment

(up to 40 g daily) in patients with HD (stage I or II) was initiated. The aim of this study was to assess the efficacy of high doses of CM for slowing the progressive functional decline of patients with early manifest HD. The CREST-E trial was to cover a period of 3 years. Unfortunately, it was terminated (October 2014) at the halfway mark due to lack of effectiveness in the creatine supplementation group. (98) While disappointing, possible explanations for the failure of CM to show beneficial effects in the CREST-E trial compared to PRECREST include the inclusion of later stages of HD in the trial and the need for earlier intervention with creatine supplementation, before the onset of symptoms, to prevent or delay the progression of the disease as opposed to using creatine after the onset of symptoms.

1.5.4.2. Alzheimer's Disease

AD is a late-onset, age-dependent, progressive neurodegenerative disease characterized by progressive cognitive decline. (99) The most important pathological features of AD are significant loss of neurons and cortical atrophy, intracellular neurofibrillary tangles, and deposits of extracellular plaques rich in insoluble β -amyloid protein. (100) It is known that abnormalities in energy metabolism and mitochondrial function are one of the earliest detectable defects in patients with AD. (101-103)

Clinically, reductions in glucose metabolism in the brains of patients with AD have been reported and the changes in glucose utilization usually preceded the cognitive defects observed in those patients. (101, 104) The finding that glucose metabolism was decreased suggested that defects in the respiratory chain might

contribute in the pathogenesis of AD. In addition, a selective reduction of cytochrome c oxidase activity (complex IV) in the mitochondria has been reported. (102, 103) Another biochemical signature of AD brain tissue as shown in many *in-vitro* and post-mortem studies is a higher level of oxidatively damaged mitochondrial DNA, lipids, and proteins when compared to controls. (105, 106)

So far, very few studies have been conducted to examine the neuroprotective effect of creatine in AD. Brewer and Wallimann have shown that CM at concentrations ranging from 0.125 and 2 mM protected against glutamate and β -amyloid toxicity in cultured rat hippocampal neurons. (76) The mechanism by which creatine exerted its neuroprotective effect might be partially through increased levels of ATP and PCr. (76) Considering the neuroprotective effects of creatine against β -amyloid toxicity *in-vitro*, two *in-vivo* studies investigated the effects of creatine supplementation in a rat model of β -amyloid- induced AD. However, no beneficial effect of dietary supplementation with 2% CM were found in terms of leaning and memory, nor did it protect against β -amyloid-induced neuronal apoptosis. (107, 108)

1.5.4.3. Parkinson's Disease

PD is a chronic, progressive, age-dependent neurodegenerative disorder. It is characterized by progressive bradykinesia, muscle rigidity, tremors, and gait abnormalities. The main cause of PD is the extensive loss of the dopaminergic neurons in the substantia nigra of the brain. (109) The histological hallmark of PD is the presence of fibrillar aggregates called Lewy Bodies and the accumulation of the protein alpha-synuclein inclusions in neurons. (110)

The exact molecular mechanism that contributes to the loss of dopaminergic neurons in PD remains elusive. However, interrelated processes including inflammation, oxidative stress, and mitochondrial dysfunction play a role in the pathogenesis of PD. (111) Studies have reported that the activity of nicotinamide adenine dinucleotide (NADH)-ubiquinone reductase (complex I) in the electron transport chain is reduced in the substantia nigra in patients with PD. (112, 113) In addition, the neurotoxin 1-methyl-4-phenyl-1,2,3,6-tetrahydropyridine (MPTP), which is a known inhibitor of complex I activity of the mitochondrial electron transport chain, produces neurological damage that resemble that seen in patients with PD and it has been used as a model of PD in many studies. (99) Moreover, a significant decrease of ATP levels was observed in the brains of mice after treatment with MPTP. (114) These findings suggest a role of cellular energetics and mitochondrial dysfunction in PD.

Matthews et al demonstrated that CM supplementation at doses of 0.25 to 0.1% of diet produced dose-dependent neuroprotective effects in an MPTP mouse model of PD. (78) They also found that creatine supplementation protected against the loss of neurons in the substantia nigra region. (78) In addition, using the same PD mouse model, Yang et al., found that supplementing the diet with 2% CM 1-week prior to administering MPTP, significantly attenuated dopaminergic neuron loss in the substantia nigra. (115)

Since creatine supplementation has shown strong neuroprotective effects in animal models of PD, the National Institute of Neurological Disorders and Stroke (NINDS) conducted a phase II, randomized, double-blind, clinical trial of creatine supplementation and showed that creatine is not futile and should be considered for Phase III clinical trials. (116) Due to this finding, NINDS conducted a phase III, double-blind, placebo-controlled clinical trial (NET-PD LS-1 study) in 2007. This study was one of the largest clinical trials in PD. It was a multicenter trial

conducted in 51 centers across the United States and Canada with an enrollment of 1720 patients with early-stage PD. Participants were randomized to receive CM at a dose of 5 g twice daily or a matching placebo for up to 5 years. However, in September 11, 2013, the NINDS terminated the NET-PD LS-1 study for futility.

1.5.4.4. Amyotrophic Lateral Sclerosis

ALS is a chronic, progressive, and usually fatal neurodegenerative disease. The terms motor neuron disease (MND) or Lou Gehrig's disease are sometimes used interchangeably with ALS. (117) The defining feature of ALS is the progressive degeneration and loss of upper and lower motor neurons in the motor cortex of the brain, the brainstem, and the spinal cord and it is characterized by muscle spasticity, rapidly progressive weakness, and atrophy. (117)

Mitochondrial and energetic defects are implicated in the pathogenesis of ALS. The cause of mitochondrial dysfunction in ALS is still not clear, however, evidence suggests that superoxide dismutase 1 (SOD1), a cytoplasmic enzyme and one of the main free radical scavenging enzymes that protects cells against oxidative damage, is trans-located to the mitochondria forming protein aggregates, that leads to mitochondrial dysfunction. (118) Browne et al., reported an early reduction in ATP levels in the cerebral cortex of a transgenic animal model of ALS and the changes in ATP were readily detectable before any pathological changes and the onset of symptoms. Reduced levels of ATP were also accompanied by impaired glucose utilization. (6) Moreover, the activity of the mitochondrial respiratory chain enzymes was also altered in the ALS animal model. (119, 120)

These findings combined suggest a role of cellular energetics and mitochondrial dysfunction in ALS.

Creatine supplementation has been suggested to be a potential therapeutic strategy for ALS. Studies have shown that oral administration of 1-2% dietary CM results in an increase in survival and in a significant improvement of the motor performance in mouse models of ALS compared to controls. (77) Additionally, 2% dietary CM supplementation protected against the loss of neurons in both the substantia nigra and motor cortex and also reduced the level of oxidative damage in a mouse model of ALS. (77)

Based on the success of creatine supplementation in animal studies, small clinical trials were conducted to examine the effect of creatine in patients with ALS. In these studies, CM was given at a dose of 5 g per day and patients were followed up for a period of 6-9 months. However, CM at this specific dosage regimen failed to demonstrate any therapeutic benefits in all the outcome measures. (121-123)

1.6. Dosing and Safety of Creatine Supplementations

CM is the standard and most commonly used form of creatine and it is the most commonly cited form of creatine in the scientific literature. Dietary supplementation with CM for improved athletic performance typically involves a loading dose of 20 g per day (4 x 5 g) over a five-day period, followed by a daily maintenance dose of 3-5 g. (13) This regiment has been reported to result in an approximately 20% increase in intramuscular creatine levels after 2-5 days of receiving the loading dose. (11, 13, 124) Studies suggest this dosing level is safe

and well tolerated with minimal side effects. (68, 125-127)

On the other hand, supplementation with CM for therapeutic indications typically involves daily doses that exceed 20 g. Indeed, the recent HD clinical trials had a targeted daily dose of 30-40 g. (97) Even at these higher doses, creatine supplementation appeared to be relatively safe and well tolerated and no significant adverse events were reported. The most common adverse effects reported after 18 months of treatment were mild gastrointestinal discomfort, diarrhea and nausea (22-50% in creatine treated group compared to 3-16% in placebo). (97) Moreover, supplementation with high dose creatine had no adverse effects on renal, hepatic, or cardiovascular function. (97) In a double-blinded, placebo-controlled, 12-week study, 34 subjects were given 20 g of CM per day for 5 days and 10 g per day for 51 days. No significant changes in total protein, serum CRN, bilirubin and blood urea nitrogen, or in serum enzymes aspartate transaminase, alkaline phosphatase, gamma-glutamyl transpeptidase, LDH, and creatine phosphokinase were reported, indicating minimal changes in clinical markers of renal and hepatic function. (4) However, it is important to note that long-term studies examining the safety of high dose (>20 g/day) creatine supplementation are lacking and the potential risks of long-term supplementation need to be determined.

1.7. Important Considerations for Creatine Monohydrate Supplementations

CM supplementation has shown strong neuroprotective effects in many *in-vitro* and animal models of neurodegenerative diseases. However, most of the clinical trials in humans have failed to show neuroprotective effects of creatine,

Table 1. The lack of beneficial effects might be due to the doses used in most of the human studies, which were substantially lower than the allometric dose equivalent given in the pre-clinical studies. In most of the successful animal studies, CM was given at doses ranging from approximately 0.2 to 0.6 g per day. Based on allometric dosing, this would require a 20-40 g daily dose in human studies, which is substantially larger than the doses used in most of the clinical trials, Table 1.

In addition, it is known that CM, which is the form of creatine supplement that is used in most of the current human trials, has a relatively low aqueous solubility (~ 16.6 mg/ml). (128) Since it is usually given at high doses (5-25 g/day for athletes, and > 25 g/day for therapeutic applications), it is likely administered as an oral suspension. As only the solubilized creatine is available for absorption in the intestines, such a dosing practice would suggest that a substantial portion of the creatine consumed is unabsorbed. Aside from diminished beneficial responses, the unabsorbed creatine in the intestines could contribute to water retention and gastrointestinal discomfort reported in many studies with creatine supplementation.

The relatively large doses of creatine required to produce the desired therapeutic effects suggests inefficiencies in either bioavailability and/or tissue distribution of current creatine products. This highlights the importance of finding alternative creatine forms with improved and more efficient dosage formulations.

Table 1. Dosing regimen of CM and main findings in the published clinical trials in patients with ALS, PD, or HD.

UPDRS: Unified Parkinson Disease Rating Scale. UHDRS: Unified Huntington Disease Rating Scale.

Study	Application	Dose of CM	Main Findings
Groeneveld et al. (122)	ALS	5 g twice daily for 16 months, starting after the onset of symptoms	No evidence of a beneficial effect of CM on survival or disease progression
Shefner et al. (121)	ALS	20 g/day for 5 days as loading dose, followed by 5 g/day for 6 months, starting after the onset of symptoms	No beneficial effect of CM was demonstrated in any of the outcome measures
Rosenfeld et al. (123)	ALS	10 g/day for 5 days as loading dose, followed by 5 g/day for 9 months, starting after the onset of symptoms	There was a trend toward improved survival, but no beneficial effect on the markers of disease progression measured

NINDS NET-PD Investigators (futility trial) (116)	PD	10 g/day for 12 months, starting after the onset of symptoms	CM should not be rejected as futile in a 12-month evaluation of the clinical progression of PD and should be considered for a phase III clinical trial
Bender et al. (129)	PD	20 g/day for 6 days as loading dose, followed by 2 g/day for 6 months, then 4 g/day for a total of 2 years.	CM improved patient mood and led to a smaller dose increase of dopaminergic therapy but had no effect on overall UPDRS scores
NET-PD investigators (130)	PD	5 g twice daily for a minimum of 5 years	CM did not improve clinical outcomes. The trial was terminated early for futility.
Tabrizi et al. (96)	HD	10 g/day for 12 months	No improvement in UHDRS scores after 12 months
Verbessem et al. (95)	HD	5 g/day for 12 months	CM did not improve functional, neuromuscular, or cognitive status in

			patients with HD.
Rosas et al. (PRECREST) (97)	HD	15 g twice daily for 18 months, starting before the onset of clinical symptoms (pre-manifest HD)	CM at a dose of 30 g/day was safe and well tolerated and slowed cortical and striatal atrophy at 6 and 18 months compared to controls.
Hersch et al. (CREST-E) (98)	HD	Up to 40 g/day for 48 months, starting after the clinical onset of symptoms.	CM was not beneficial in slowing functional decline in early symptomatic HD patients.

1.8. Cellular Mechanisms of Intestinal Absorption

The gastrointestinal tract (GIT) is responsible for the digestion and absorption of nutrients. (131) The main structures of the digestive tract include the oral cavity, esophagus, and stomach (collectively referred to as the upper digestive tract), and the small and large intestines (lower digestive tract). The small intestine measures approximately 6 m in length, while the large intestine measures around 1.5 m. (132) The epithelial enterocytes that line the small intestine are characterized by a large surface area ($\approx 300 \text{ m}^2$) due to the presence of villi and microvilli, and represent the main site for nutrient and drug absorption. (132) The small intestine

is divided into three segments: The duodenum (less than 1 ft long), which is the first part of the small intestine, the jejunum, which is the middle segment and the ileum, the third and final segment adjacent to the large intestine (jejunum and ileum together are approximately 9 ft long). (133) After passing the oral cavity and the esophagus, ingested material first enters the stomach where excreted enzymes and the low pH environment begin breaking down the ingested material into more absorbable nutritional units such as glucose, amino acids and di- and tri-peptides that can be easily absorbed in the small intestines. (133)

Absorption describes the transfer of a compound from its site of administration to the bloodstream. For any compound to be absorbed in the GIT, whether it is a nutrient, drug, or potential toxin, it must be in solution. (60) The rate and efficiency of absorption depend on factors related to the site where the compound is absorbed and the compound's physicochemical characteristics. (134) There are two basic absorption pathways by which a compound can be taken up from the GIT and enter into the systemic circulation. These include passive diffusion or active transcellular transport, Figure 3. (134)

The passive absorption process is governed by two factors: the concentration gradient across the membrane that exists for the solute of interest, which is the driving force for passive diffusion, and the permeability of the solute across lipid bilayers. (60) Permeability describes how well solutes move across biological interfaces and is determined by the distance a solute can penetrate into the lipid bilayer (in this case the intestinal wall) per unit time. (135) Permeability is determined by the physicochemical properties of the solute, with parameters such as size/surface area, lipophilicity, charge and hydrogen bonding potential of the solute influencing passive diffusion across the cellular interface. (135)

The first type of passive diffusion is simple diffusion, which can be transcellular or paracellular. In transcellular simple diffusion, the solute can readily

pass across the biological membrane from area of high solute concentration to areas of low concentration, Figure 3. The ideal properties for high bioavailability through the transcellular route include molecular weight less than 300 daltons, a log P value (measure of lipophilicity) between 1-3, and nonionized functional groups with fewer than 5 hydrogen-bond acceptors. (136)

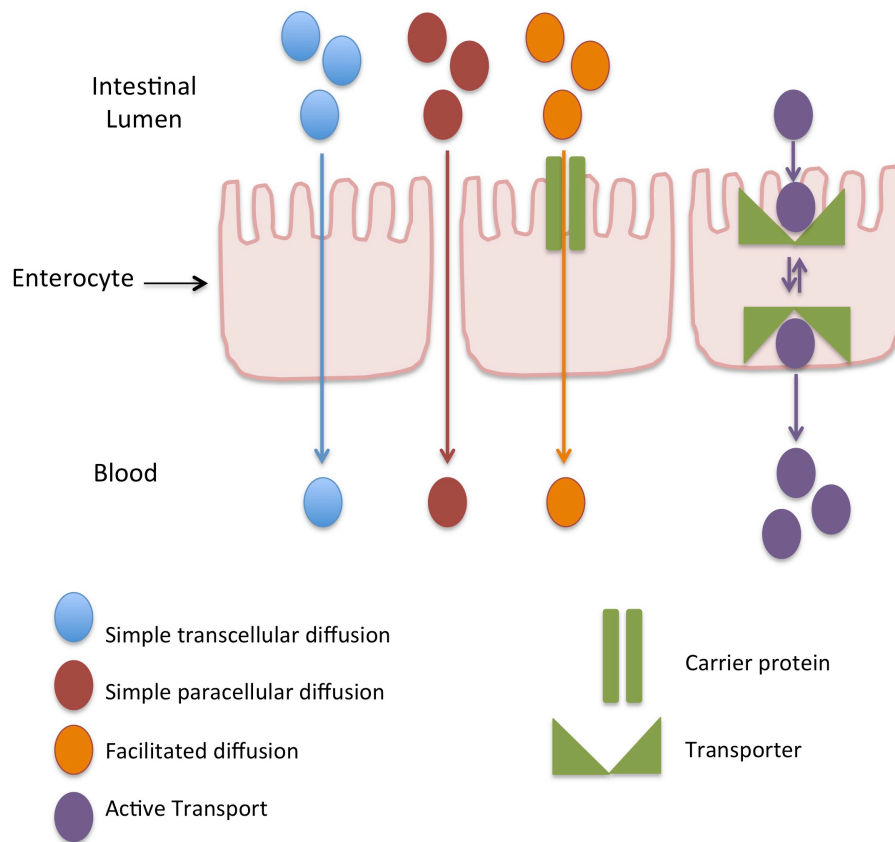
On the other hand, in paracellular simple diffusion, solutes move through spaces (tight junctions) that exist between the epithelial cells, Figure 3. (137) While the bulk flow movement of solutes through the tight junctions is restricted, the complexity and restrictiveness of the tight junctions vary depending on the location within the small intestine. Thus, tight junctions between epithelial cells in the duodenum and jejunum have a larger pore opening (approximately 8-13 Ångstroms in diameter) than in the ileum, where pore sizes of approximately 4 Ångstroms in diameter are observed. (138) Ideal properties for solutes to be absorbed via paracellular route include molecular weight of less than 250 daltons, positive charge, and log P of less than zero. (137)

The second type of passive diffusion is facilitated diffusion. Facilitated diffusion is the process of moving molecules or ions across a biological membrane via specific transmembrane proteins along its concentration gradient. (134) Being passive, facilitated diffusion does not require energy from ATP hydrolysis in the transport step. The main differences between simple and facilitated diffusion is that the latter relies on the molecular binding between the solute and the membrane-embedded channel or carrier protein. In addition, the rate of the facilitated diffusion is saturable unlike passive diffusion. (134)

Active transport involves specific transporters that span the membrane to facilitate the movement of the solutes into or out of the cell against its concentration gradient (from areas of low concentrations to areas of high concentrations), Figure 3. There are two types of active transport, primary active

transport that is driven by the hydrolysis of ATP, or secondary active transport that is often coupled with the movement of ions in either a co-transport or counter-transport fashion. (139) Active transport systems are chemically selective and show saturation kinetics for transported substrates. (139)

Figure 3. Schematic representation of different solutes absorption pathways in the GIT tract (Adapted from Alraddadi et al.,) (140)



1.9. Creatine Absorption in the GIT

To date, the exact mechanism by which creatine is absorbed through the GIT is unknown. Creatine is a zwitterion with a positively charged guanidine functional group and a negatively charged carboxylic acid functional group. (128) When ingested, creatine usually exists as a charged molecule depending on its location within the GIT. (60) In the stomach and the upper part of the small intestine with low pH, the carboxylic acid functional group is likely to be protonated and the predominant form of creatine is the positively charged species. On the other hand, as the ingested creatine progresses down the intestinal lumen the pH becomes neutral and the zwitterion and negative charged species will become more predominant. (60) Because creatine exists primarily as a charged molecule with a logP value of - 0.1 for CM, (128) its ability to partition into a lipophilic environment such as the plasma membrane of the intestinal epithelial cell is limited. In fact, only solutes displaying LogP values between 1 and 3 are likely to be absorbed by passive transcellular diffusion in the GIT. (136) Thus, in considering the absorption of creatine from the GIT, passive diffusion via the transcellular route is likely to be minimal.

Another possibility for solute absorption through the GIT is via transcellular transport via CRT1. However, there are some considerations regarding CRT1 that suggest active transport of creatine is likely to be minimal. First of all, expression of CRT1 at both the mRNA and protein level has been reported in epithelial cells of the intestine. (141) Recent studies examining the expression and function of CRT1 during development in the rat, showed multiple forms of CRT1 within the colon during development. (141) However, the activity and expression level of CRT1 in the colon diminished during maturation, with little CRT1 activity

observed in the adult rat. (141) If similar developmental patterns exist in humans, this would suggest that creatine absorption through CRT1 in the GIT is lower in adulthood.

An additional consideration is the localization of CRT1 within the GIT. Previous studies have reported brush border expression of CRT1 in the jejunal and ileal segments of the small intestine. (142, 143) However, while brush border CRT1 is the first step in absorbing exogenous creatine, there would need to be transporters positioned on the basolateral membrane of the intestinal epithelial cells to move the absorbed creatine into the bloodstream. While an extensive search for CRT1 on the basolateral membrane did reveal a sodium dependent transporter for creatine, the direction of the transport was inward. (144) This means that the transporter, under normal physiological conditions, would likely be transporting creatine from the blood into the intestinal epithelial cell, and thus would not aid in the oral absorption of creatine.

A final consideration for transporter-mediated absorption of creatine is the kinetics of the CRT1. As absorption through CRT1 is saturable at high concentrations, the extent to which CRT1 can efficiently absorb creatine will be dependent on the amount of creatine in the gastrointestinal fluid. Michaelis constant (K_m) values of CRT1 and serum creatine concentrations in different species are shown in Table 2. (13, 47) By definition, the K_m represents the substrate concentration at which the reaction rate is half maximal. It is important to note that these K_m values are gathered from studies done on different tissues and cell types. However, based on blood concentrations of creatine, it is apparent from these K_m values that CRT1 is working close to saturation suggesting a possible limitation of creatine accumulation by the amount of CRT1 protein in the cell membrane. (47) For example, in un-supplemented humans, the normal plasma levels of creatine range from 50 to 100 μM and with K_m values of 15-77 μM , this

suggests that the transporter is working near saturation and any further increase in the plasma concentrations of creatine would most likely saturate the transporter resulting in limited entry into the cell via CRT1. Considering that supplementation with 5 g of creatine, which is typically the lowest dose used by athletes, results in maximal plasma creatine concentrations of around 800 μM , (145), it is most likely that these plasma concentrations are well above those required to saturate the creatine transporter. For this reason, and those discussed above, active transcellular transport pathways for the absorption and tissue distribution of creatine supplements, under the current dosing strategies, are likely to be minimal.

As creatine has a molecular weight of 149.1 g/mole (below the 250 dalton cut-off for paracellular diffusion), and is positively charged in the upper part of the GIT, with a logP value of -1, (128) absorption of creatine through the paracellular route may be the predominant absorption pathway. A paracellular diffusion pathway for creatine absorption in the GIT is also supported by creatine permeability studies conducted in various intestinal models. (144, 146) Studies by Orsenigo and colleagues examined creatine permeability across inverted jejunal segments of the rat intestine. (144) While transporter mediated uptake of creatine was observed in both brush border and basolateral intestinal membrane preparations, permeability across intact intestinal tissue was not transporter dependent, as demonstrated by the absence of concentration dependency and the inability to influence transcellular creatine permeability with various CRT1 inhibitors. (144)

A paracellular diffusion pathway for creatine absorption in the GIT is also supported by permeability studies in human epithelial colorectal adenocarcinoma (Caco-2) monolayers. (128, 146, 147) The Caco-2 cell line is a human intestinal epithelial cell line derived from human colon carcinoma. It is a well-established cell line that is widely used to examine and predict oral absorption within the

pharmaceutical industry. (148) Caco-2 cells express CRT1 at the mRNA level, (149) although potential changes in expression were observed during differentiation, (141) consistent with the developmental expression analysis reported for CRT1 in rats. Dash and colleagues examined the permeability of radiolabeled CM in Caco-2 monolayers; the reported low permeability observed was consistent with a solute with poor oral absorption profile. (146) Additional studies comparing the permeability of various creatine analogs and salt forms across Caco-2 monolayers were also consistent with minimal permeability. (128) As Caco-2 cells have highly developed tight junctions, paracellular diffusion would be limited, and solutes undergoing paracellular diffusion would be expected to have low permeability. (60) Together, these studies provide compelling evidence for paracellular diffusion of creatine as the primary mechanism for oral absorption.

Table 2. CRT1 K_m values and serum creatine concentrations in different species. (13, 47).

Species	K_m (μM)	Serum creatine concentration (μM)
Human	15-77	50-100
Rat	22-46	140
Rabbit	35	150
Mouse	110	200

1.10. Newer Creatine Derivatives:

Bioavailability of a drug is defined as the amount of the administered drug that is absorbed and available within the systemic circulation for producing a response and is expressed as percentage of the drug administered. (150) Oral bioavailability of a compound is determined by measuring the area under plasma concentration-time curve (AUC) after oral administration of the compound and comparing it to the resulting AUC following intravenous (iv) administration. (150)

While there has been much research devoted to understanding the uptake of creatine into skeletal muscles and to exploring the effects of creatine on exercise performance, few studies have examined the oral bioavailability and the pharmacokinetic (PK) profile of creatine supplements. Given the physicochemical properties of CM, the relatively high doses required, and the previously discussed studies in the various intestinal absorption models that report low permeability of creatine, the oral absorption of CM based supplements is likely to be incomplete.

In addition, if paracellular diffusion is the primary absorption route for creatine in the GIT, formulations that improve the aqueous solubility of the creatine, should have a substantial impact on oral bioavailability.

Due in large part to the inefficiencies in current creatine supplement formulations there has been growing interest in new and improved forms of creatine with improved aqueous solubility and bioavailability. The approaches taken have involved identification of different creatine salt forms, Table 3, with improved aqueous solubility properties and the design of ester derivatives of creatine, Table 4, with either improved solubility and/or cell permeability properties. The importance of the formulation and its impact on oral absorption is often under appreciated. Given that the aqueous solubility of CM is approximately 16.6 mg/ml, athletes taking a standard dose of CM (ranging from 5-10 g) would require 400-800 ml of fluid to ensure the dose is completely solubilized. As a result of this, most CM products are taken as suspensions and would be incompletely absorbed in the GIT. Even in those cases where CM is consumed completely in solution, the doses are such that conditions are at or near super-saturation solubility and will likely result in precipitation of creatine out of solution during transit through the GIT. As creatine can only be absorbed when in solution with the contents of the GIT, there is likely to be significant reductions in oral bioavailability with standard doses of CM based supplements consumed.

Of the many different creatine salt forms, there are three: creatine pyruvate (CrPyr), creatine citrate (CrC), and creatine hydrochloride (CHCl), for which human oral bioavailability studies have been reported. (145, 151) The most convincing evidence that the oral absorption of CM in humans is less than complete comes from studies by Jager and colleagues. (145) In their study, they compared the oral bioavailability of CrPyr and CrC to that of CM. Subjects were given 5 g doses of CrC, CrPyr or CM as an aqueous solution and the resulting

plasma creatine concentrations were measured over time. For CrC, which has a slightly greater solubility than CM, there was a small increase (approximately 10%) in oral bioavailability compared to CM. For CrPyr, which has an approximately 6-fold higher aqueous solubility, there was a modest, approximately 25%, increase in oral bioavailability compared with CM. (145) Interestingly, in the studies by Jager et al, the improved oral absorption observed with CrPyr and CrC was statistically significant, though the differences were not considered important, primarily due to the perceived complete oral absorption of CM. (145) In this respect, regulatory standards indicate that different salt forms of a compound are considered bioequivalent when the relative bioavailability of one salt form is 75-120 % of that observed with another salt form. Under this criterion, CrPyr, with an approximately 25% increase in oral bioavailability, would not be considered to have the same oral absorption properties as CM and would not be considered bioequivalent.

While the increases in oral bioavailability observed with CrC and CrPyr could be classified as relatively modest, oral absorption studies with CHCl provide even more compelling evidence to suggest that improvements in bioavailability of creatine supplements are possible. (151) In these studies volunteers were given a 5-g dose of either CM or CHCl in 8 ounces of water. A crossover design was employed to allow direct comparisons of differences in oral absorption of the two creatine salts within the same subject. The results of these studies reported an approximately 60% increase in oral absorption of CHCl compared with CM. (151) With such increases in bioavailability observed with CHCl, it is difficult to claim complete oral absorption of CM. Together, these studies provide two important and fundamental findings. First, with increased oral absorption of the various creatine salts ranging from 10% to 60% over that of CM, it is clear that the bioavailability of CM is not nearly complete. Second, as CM bioavailability is not complete, there

is potential for development of creatine supplements with improved oral absorption, which in turn could provide significant advancements in performance benefits, and allow for reduced dosages and more flexible dosing formulations (sports drinks and bars, fortified foods, etc.).

In addition to the multiple salt forms of creatine, there are modified ester forms of creatine such as creatine ethyl ester (CEE). In addition to having improved aqueous solubility compared with CM, the ester form of creatine also has improved octanol-water partitioning, an index of cell permeability, Table 4. As there are esterases throughout the blood and tissue, CEE was designed to be a pronutrient with enhanced oral absorption, which could then be hydrolyzed to creatine once absorbed into the body. Gufford and colleagues evaluated the permeability of CM, CRN, and CEE using Caco-2 cell line. They reported that of the three compounds examined, CM had the lowest permeability in Caco-2 monolayers and that CEE permeability was approximately 3.6 fold higher than that of CM. (147)

There are few studies examining either the biological effects or oral absorption properties of CEE. The only direct comparison study of CEE and CM reported that CEE was not as effective at increasing serum and muscle creatine levels or in improving body composition, muscle mass, strength, and power. (152) The study followed healthy volunteers over a 48-day period in which subjects were supplemented daily with 300 mg/kg of CM, CEE or placebo and underwent an exercise weight training regimen. Furthermore, the study reported high levels of CRN in serum samples from the CEE-supplemented treatment group. However, re-examination of the data, looking at changes in muscle creatine and peak and mean power measurements in the CEE, CM and placebo groups over the course of the 48-day study showed CEE performance was as good or better than CM. This is due in part to the lower starting values for subjects in the CEE treatment group in terms

of muscle creatine levels and power assessments. (152) As for the high serum CRN levels in the CEE group, recent reports demonstrate that CEE is rapidly converted to CRN in aqueous solutions at neutral pH. (147) Interestingly, CEE is very stable in aqueous solutions at low pH and appears to be more stable in lipophilic environments at neutral pH ranges, (147) suggesting that CEE may be largely intact during absorption in the GIT and stable within the membrane environment of cells. Thus, while initial findings suggested CEE is less effective, more studies are required to definitively address the issue.

In addition to potentially improved oral absorption with newer creatine forms, effort has been made to improve the delivery of creatine to the brain especially in conditions of hereditary CRT1 deficiency and in neurodegenerative disorders. CM is a polar molecule, thus it would not be expected to cross well either the BBB or the cell plasma membrane in the absence of a transporter. (51) A possible way to improve delivery of creatine to the brain is to modify this molecule to render it lipophilic enough to cross BBB and plasma membranes in a carrier-independent way. (51)

Interestingly, in *in-vitro* mouse hippocampal slices, two creatine derivatives, creatine benzyl ester and phosphocreatine-Mg-complex acetate (PCr-Mg-CPLX) were able to increase the creatine content of the tissue. This increase was not prevented by GPA, a creatine transporter blocker, suggesting a crossing of the plasma membranes in a transporter-independent way. On the other hand, the increase in creatine content of the tissue caused by incubation with CM was prevented by GPA. (51) Thus, CRT1 is required for CM uptake through the plasma membrane and this might explain why hereditary transporter deficiency is attended by severe brain damage despite the possibility of an endogenous synthesis. Creatine benzyl ester and and PCr-Mg-CPLX cross the plasma membrane in a transporter-independent way, and might be useful in the therapy of hereditary

creatine transporter deficiency. They may also prove useful in the therapy of brain anoxia or ischemia and/or neurodegenerative disorders.

Another lipophilic molecule that has been synthesized in an attempt to cross the BBB and plasma membrane in a transporter independent way is di-acetyl creatine ethyl ester (DAC). DAC was able to increase creatine content in mouse hippocampal slices even when CRT1 was blocked. Interestingly, it did so in micromolar concentrations (1-2 μM), at variance with all the other creatine derivatives. (153)

Table 3. Comparison of aqueous solubility of various creatine salt forms and CM.

	CM	CrC	CrPyr	CHCl
Molecular weight (g/mol)	149.7	202	219	169
Aqueous solubility (mg/ml)	18 ± 2	52 ± 7	107 ± 8	708 ± 34
Ratio of solubility (relative to CM)	1.0	2.8	5.9	39.3

Table 4. Comparison of Aqueous Solubility and Octanol-Water Partitioning of various creatine ester forms and CM.

	CM	CEE	Creatine <i>t</i>-butyl Ester HCl (CE3)
Molecular weight (g/mol)	149.7	195.6	223.7
Aqueous solubility 25 °C mg/mL	21.0 ± 1.9	970.8 ± 14.3	389.0 ± 10.6
Ratio of solubility (Relative to CM)	1.00	46.2	18.4
Partition coefficient 25 °C	0.10 ± 0.02	0.21 ± 0.13	0.06 ± 0.07
Ratio of Partition coefficient (Relative to CM)	1.00	2.01	0.61

1.11. Physiologically Based Pharmacokinetic Modeling

Physiologically based pharmacokinetic (PBPK) modeling is a mathematical model that integrates physiological and anatomical parameters related to the body, physicochemical properties related to the drug, and formulation properties of the compound to predict the *in-vivo* PK profile of the compound. (154) PBPK models are increasingly applied during pharmaceutical development and discovery because of their strength in data integration, delivery of mechanistic insights, and superior predictive power. (155) While classical compartmental PK models simply describe absorption as a single first-order process, PBPK models differ in that they are mechanistic in nature and incorporate physiological processes such as gastrointestinal transit time and blood flow to the different organs and tissue. (156)

PBPK models are made of compartments corresponding to the different physiological organs of the body, linked together by the circulating blood system. Each compartment is described by tissue volume and blood flow rate that is specific to the species of interest. (157) Each tissue is defined with assumptions of either perfusion-rate limited or permeability-rate limited. Perfusion-rate limited kinetics tends to apply to small lipophilic molecules where the blood-flow to the tissue is considered the limiting process of the absorption. Permeability-rate limited kinetics is important for hydrophilic and larger molecules where the permeability across the cell membrane becomes the limiting process of absorption. (157)

The original Compartmental Absorption and Transit (CAT) model was the first physiologically based absorption model developed by Yu and Amidon in 1999. (158) In this model, the GIT is divided into a set of seven small intestinal compartments. The first compartment represents the duodenum, the next two

represent the jejunum, and the final four represent the ileum with equal flow transit times. The stomach and colon were not modeled in the original CAT model. (158) The general assumption of the CAT model is that a drug is passing through the GIT and the dissolved fraction is absorbed in each compartment into the portal vein. This model takes into account three factors: physicochemical properties of the drug, such as pKa and solubility, physiological factors such as pH of GIT and gastric emptying, and formulation properties, such as particle size and surface area. (159)

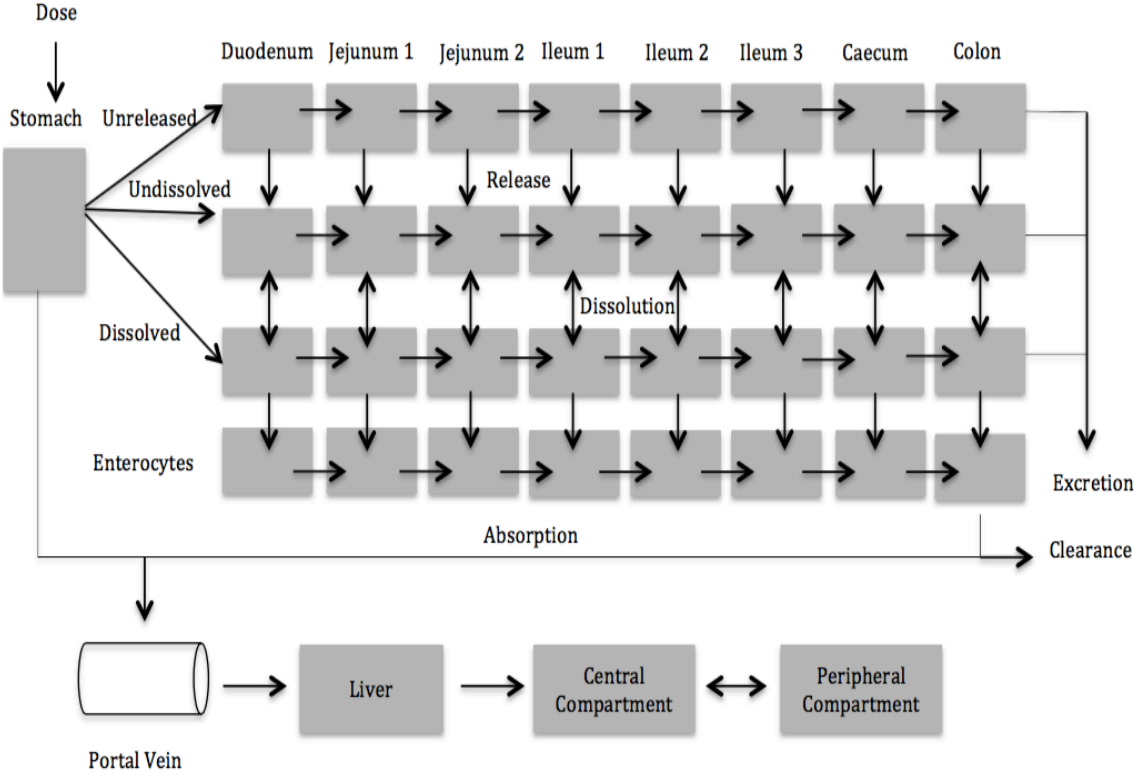
GastroPlusTM is the first physiologically based absorption model to be produced as a commercial software tool. Starting with Yu and Amidon's model, the company, Simulation Plus, Inc, incorporated additional features to the CAT model naming it the Advanced CAT (ACAT) model. (160) Features in the GastroPlusTM model not present in the original CAT model include dissolution rate, pH-dependent solubility, controlled release, absorption in the stomach or colon, gut metabolism, influx or efflux transporters, exsorption/secretion, and other factors within the intestinal tract. (159) In the ACAT model, there are a total of eighteen compartments, nine gastrointestinal compartments: stomach, seven small intestinal compartments, and colon, and nine enterocyte compartments, Figure 4, and three different drug states, unreleased, undissolved, and dissolved. Compartment properties are set by default to published experimental data, accounting for pH, volume, and permeability characteristics in the corresponding intestinal region. (159)

An advantage of GastroPlusTM for controlled release oral formulations is being able to model drug in formulation matrix (unreleased) as well as both the dissolved and un-dissolved drug fractions. This is important for controlled release formulations as the drug can be released into solution (dissolved) or as solid particles (undissolved). Undissolved drug undergoes dissolution and becomes

available for absorption, carrier-mediated transport, and luminal degradation. Undissolved (solid particles) and dissolved (drug in solution) drug undergoes first order transit through the GIT. Drug is eventually excreted from the colon if it is not absorbed before the end of the transit process. The kinetics associated with these processes are modeled by a system of coupled linear and non-linear equations. The total amount of absorbed material is summed over the integrated amounts being absorbed/exsorbed from each absorption/transit compartment. The theoretical basis and mathematical description of the ACAT model are described further in detail by Agoram et al. (159)

PBPK modeling can also be used to predict plasma concentrations of compounds following any route of administration and dosage forms (e.g. oral tablet, oral solution, iv route) under different conditions (e.g. fed vs. fasting, healthy vs. diseases). In addition to predicting plasma concentrations, an advantage of PBPK models is the ability to predict tissue distribution and concentrations of the compound in various organs of interest. (161) While direct measurement of drug concentrations in tissue homogenates is possible, it is generally only feasible in animals, and tissue samples are usually taken post-mortem. Therefore, only one time-point is available per animal. Defining the time-course of tissue concentrations requires the sacrifice of a number of animals at different time points. However, PBPK modeling, tissue concentrations at any given time point, as well as the steady-state tissue concentration can be predicted. (161)

Figure 4. ACAT model used in GastroPlus. (Adapted from Agoram et al., (159))



1.12. Statement of the Problem:

Creatine, in the form of CM, has been consumed in large doses (> 10 g/day) for years by athletes and bodybuilders without exact knowledge of its PK profile and oral bioavailability. In addition, the use of CM as a therapeutic agent requires relatively large doses (> 30 g/day) for beneficial effects to manifest. The large doses of CM required and the fact that the aqueous solubility of CM is low (around 17/mg/ml) suggest a substantial amount of CM dietary supplements may be undissolved within the GIT and thus have reduced oral absorption.

The research objective of this dissertation is to determine the oral bioavailability and PK profile of CM and to identify through *in-vitro*, *in-vivo* and *in-silico* simulations, alternative dosing strategies and alternative forms of creatine that result in improved oral bioavailability and/or tissue distribution.

The main objectives are:

- 1- To examine the oral bioavailability, PK properties and tissue distribution of CM following single oral dose administration in rats. As single doses in humans can vary from 1 g to more than 20 g, the potential influence of dose on oral absorption will also be examined.
- 2- To examine the impact of different dosing schedules on plasma and tissue, especially brain, levels of creatine using larger doses of CM (i.e. 20 g daily dose) for impacting brain function.
- 3- To determine whether there are sex-dependent differences in blood and tissue levels of creatine.
- 4- Predict the impact of other creatine salt forms, with improved physicochemical properties, on plasma and tissue levels of creatine following administration of single or multiple oral doses in humans and

compare that to CM.

Chapter 2. Materials and Methods

2.1. Materials

Creatine (*methyl-d₃*) (creatine-d₃) was obtained from Cambridge Isotope Laboratories, Inc. (Tewksbury, MA, USA). CM (guanidino-¹³C) (CM-¹³C) and Creatinine (guanidine-¹³C) (CRN-¹³C) were purchased from Sigma Aldrich (St. Louis, MO, USA). Creatine ethyl ester-¹³C (CEE-¹³C) was obtained from Dr. Jonathan Vennerstrom, University of Nebraska Medical Center (Omaha, NE, USA). Catheter locking solution was purchased from SAI infusion technologies (Lake Villa, IL, USA). Madin-Darby canine kidney epithelial cells – multi drug resistance gene (MDCK-*MDR1*) and Caco-2 cell line were purchased from American Type Tissue Culture Collection (Manassas, VA, USA). PureLink[®] RNA Mini Kit and iTaq[™] Universal SYBR[®] Green One-Step RT PCR Kit were purchased from Invitrogen (Carlsbad, CA, USA) and Bio-rad (Hercules, CA, USA), respectively. Transwell Polycarbonate Membrane Inserts (12 mm diameter, 0.4 μm pore size) were obtained from Corning (NY, NY, USA). Rhodamine 800 and sodium fluorescein were purchased from Sigma Aldrich (St. Louis, MO, USA). IR Dye 800 CW PEG fluorescent contrast agent was obtained from Licor (Lincoln, NB, USA). All other reagents and chemicals were purchased from Sigma–Aldrich (St. Louis, MO) and cell culture reagents from Invitrogen Canada Inc. (Burlington, ON, Canada) unless otherwise specified.

2.2. PK Studies in Rats

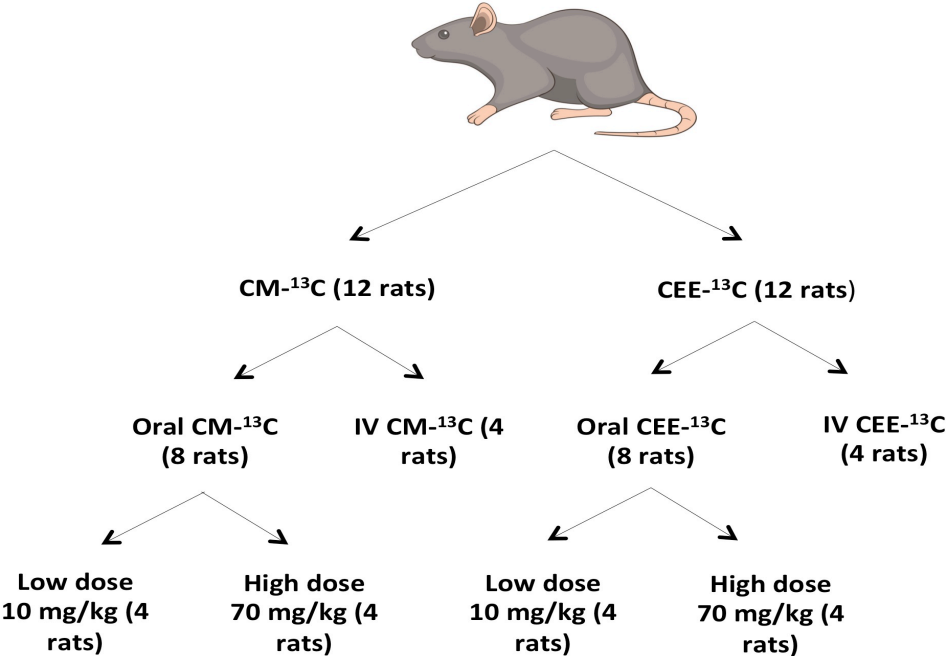
The studies examining the PK profile of CM and CEE following oral or iv dosing were approved by the University of Manitoba Animal Care Committee (Protocol 14-010; 27 January 2014) and were performed in accordance with the Canadian Council on Animal Care guidelines. Twenty-four adult male Sprague–Dawley rats weighing 280–310 g and implanted with jugular vein catheters (Charles River Laboratories, Wilmington, MA, USA) were included in this study. The catheters were externalized and secured on the dorsal side of the neck. Rats were allowed to recover and acclimatize for at least 7 days before the start of the study. During this period, the catheters were flushed with heparinized saline every other day. In addition, the rats had free access to food and water and were kept in the central animal care facility at the University of Manitoba with a 12-hour light/dark cycle, controlled humidity ($55 \pm 5\%$), and controlled temperature (21 ± 2 °C). Food was withheld 12 hours prior to the PK studies.

Rats were randomly assigned to 6 treatment groups (4 rats in each group), Figure 5. The first 4 groups were given either oral low dose (10 mg/kg) or high dose (70 mg/kg) of either CM-¹³C or CEE-¹³C dissolved in normal saline solution. Doses (1 ml/kg) were administered via oral gavage. The final 2 groups received bolus iv injection (10 mg/kg) of either CM-¹³C or CEE-¹³C, Figure 5. Serial blood samples (0.2 ml) were collected at various time points (0–240 min) following oral or iv administration of CM-¹³C or CEE-¹³C in tubes containing citrate buffer. Following the last blood sampling (i.e., 240 minutes after creatine administration), rats were anesthetized and euthanized by decapitation; muscle and brain tissue samples were collected and immediately freeze-clamped in liquid nitrogen. Following liquid nitrogen freezing, tissue was weighed, and stored at -80 °C. Plasma fractions were immediately obtained from blood samples by centrifugation (15 minutes at 2000 x g) and stored at -80 °C until further processing for analysis by liquid chromatography-tandem mass spectrometry (LC-MS/MS).

All the figures of the PK study were obtained using Excel or GraphPad Prism Version 6.0c. The initial serum concentration (C_{p0}) of creatine- ^{13}C was obtained directly from the plasma concentration (log scale)–time curve. The maximum or peak plasma concentration (C_{max}) and time taken to reach C_{max} (T_{max}) were estimated directly from the plasma concentration–time curves. The terminal elimination constant (k_{el}) was determined by linear regression analysis of the terminal phase of the plasma concentration (log scale)–time curve. The AUC from zero to the last measurable concentration (AUC_{0-t}) was calculated using the linear trapezoidal method. (162) The remaining PK parameters were calculated according to the following formulas:

- The AUC from zero to infinity ($\text{AUC}_{0-\infty}$) = $\text{AUC}_{0-t} + C_{\text{last}} / k_{\text{el}}$; where C_{last} is the last measurable nonzero plasma concentration.
- Absolute oral bioavailability (F) = $(\text{AUC}_{\text{oral}} / \text{AUC}_{\text{IV}}) \times (\text{Dose}_{\text{IV}} / \text{Dose}_{\text{oral}})$.
- Half-life ($T_{1/2}$) = $\ln 2 / k_{\text{el}}$.
- Clearance (CL) = $\text{dose} / \text{AUC}_{0-\infty}$.
- The apparent volume of distribution (V_d) = $\text{CL} / k_{\text{el}}$.

Figure 5. Schematic presentation of CM-¹³C and CEE-¹³C PK study treatment groups.



2.3. Sample Preparation

2.3.1. Plasma and Red Blood Cells (RBC) Samples Preparation

For LC-MS/MS analysis, 10 µg/ml (10 µl) of the internal standard, creatine-d₃, dissolved in citrate buffer (0.13 g citrate/ml distilled water, pH 4.3), was added to 100 µl of plasma from each sample. After that, 1 ml of ice-cold acetonitrile (with 0.3% formic acid, pH 3) was added to each sample to precipitate the protein. Then, the samples were vortexed for 2 minutes and centrifuged at 15,000 x g for 5 minutes. The supernatant was collected and transferred to new tubes and the samples were vacuum centrifuged to dryness at 45 °C using a Savant SPD1010 SpeedVac Vacuum Centrifuge (SpeedVac) (Thermo Fisher Scientific, Inc., Asheville, NC, USA).

The cell fraction from the collected blood was thawed and the lysed cells were then processed as described above for plasma samples.

2.3.2. Brain and Muscle Samples Preparation

Brain and muscle tissue were homogenized in citrate buffer (1.3 g tissue/7 ml citrate buffer) using an electric homogenizer. 10 µl internal standard (10 µg/ml) was added to a 100 µl aliquot of tissue homogenate and vortexed. After mixing, 1 ml of ice-cold acetonitrile was added and the samples were centrifuged at 15,000 rpm for 5 minutes at 4 °C. Supernatants were collected and transferred to a clean tube and evaporated using SpeedVac.

2.4. LC-MS/MS Analysis (These studies were performed by Dr. Ryan Lillico and Wenxia Luo in Dr. Lakowski's lab)

The analytical system used was a Shimadzu LCMS-8040 triple-quadrupole mass spectrometer; LC-MS/MS (Shimadzu, Kyoto, Japan) coupled to a Nexera ultra high performance liquid chromatograph (Shimadzu, Kyoto, Japan) and data were analyzed using Shimadzu LabSolutions software (Version 5.72). The LC-MS/MS was operated in DUIS mode (electrospray ionization and atmospheric pressure chemical ionization (ESI/APCI)) using multiple reaction monitoring (MRM). The LC-MS/MS conditions consisted of a desolvation line temperature of 250 °C and heating block temperature of 400 °C. Nebulizing gas flow was 2 l/min and drying gas was 15 l/min.

The analytical system described above was used for the analysis of isotope labeled creatine-¹³C, CRN-¹³C, and CEE-¹³C in tissue and plasma samples. The analytical column used was a Primesep 200 (3 μm, 2.1 x 100 mm) (SIELC Technologies, Wheeling, IL, USA) mixed function cation exchange column. The mobile phase consisted of A (0.05% aqueous formic acid) and B (1% formic acid in acetonitrile). A linear gradient was applied from 0% to 85% B over 4 minutes, held at 85% B for 2 minutes followed by a step down to 0% B and held for 4 minutes to recondition and equilibrate the column prior to the next injection. The total flow rate of the system was 0.4 ml/min and the column oven was set at 40 °C. Creatine-¹³C, CRN-¹³C, CEE-¹³C and the internal standard, creatine-D₃, were monitored in positive MRM mode. Table 5 describes the precursor and product ion mass to charge ratios (m/z) with the collision energy of each compound.

Table 5. MRM transitions and collision energies for Creatine-¹³C, CRN-¹³C, CEE-¹³C and the internal standard, Creatine-D₃.

Compound	Precursor Ion <i>m/z</i>	Product Ion <i>m/z</i>	Collision Energy (eV)
Creatine- ¹³ C	133.1	90.1	-15
CRN- ¹³ C	115.2	44.3	-20
CEE- ¹³ C	161.1	118.1	-15
	161.1	44.1	-20
Creatine-D ₃	135.1	93.1	-15
	135.1	47.2	-20

2.4.1. Stock and Working Standard Solutions

All stock solutions were prepared at 1, 10, 100 and 1000 µg/ml concentrations in citrate buffer (0.13 g/ml, pH 4.3). These solutions were stored at -20 °C and remade after 3 freeze–thaw cycles. Calibration standards containing 10 µg/ml internal standard in rat plasma, muscle or brain homogenate were prepared from stock solutions by dilution to a series of concentrations as 0.01, 0.05, 0.1, 0.5, 1.0, 5.0, 10 and 50 µg/ml. Plasma and tissue samples from untreated rats were prepared containing 10 µg/ml internal standard to evaluate background signal.

2.4.2. Sample Preparation for Standards

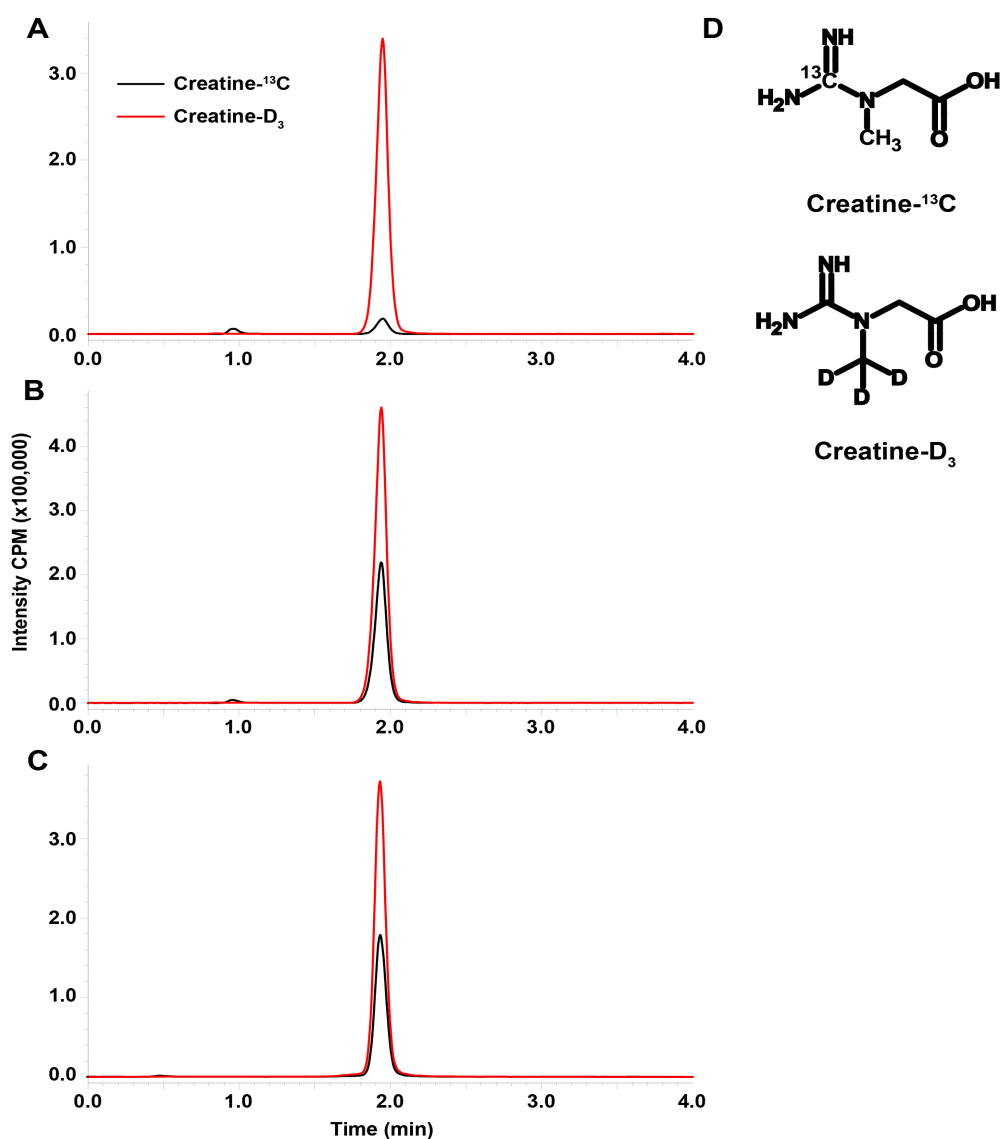
The working standards were added to 100 μl plasma, muscle homogenate or brain homogenate (homogenized at 1.3 g tissue/7 ml citrate buffer) containing 10 $\mu\text{g}/\text{ml}$ internal standard in micro-centrifuge tubes for concentrations described above. Cold acetonitrile with 0.3% formic acid (1 ml at $-20\text{ }^{\circ}\text{C}$) was promptly added to the samples to precipitate proteins. The samples were vortexed for 2 minutes and centrifuged at 15,000 \times g for 5 minutes. The supernatant was transferred to new tubes and vacuum centrifuged to dryness using SpeedVac at $45\text{ }^{\circ}\text{C}$. The dried samples were reconstituted in 50 μl of 0.05% aqueous formic acid and 3 μl were injected into the LC-MS/MS system.

2.4.3. Precision, Accuracy, and Recovery

The assay limits and accuracy were determined by inter-day analysis of standard curves prepared in rat plasma ($n = 4$). The lower limit of quantitation (LLOQ) was defined as the lowest point on the standard curve to achieve a coefficient of variation (CV) no higher than 20%. This was calculated to be $0.551 \pm 0.098\text{ }\mu\text{g}/\text{ml}$ (CV of 17.8%). The standard curve was linear between 0.551 and 50 $\mu\text{g}/\text{ml}$ with no point other than LLOQ exceeding 15% CV. Quality control samples of 2.5 and 10 $\mu\text{g}/\text{ml}$ were measured during analysis and their recoveries were $98.0 \pm 3.76\%$ and $99.6 \pm 1.09\%$ respectively. Unknown samples exceeding 50 $\mu\text{g}/\text{ml}$ were diluted using mobile phase containing 10 $\mu\text{g}/\text{ml}$ internal standard and calculated based on the dilution factor. All back-calculated samples were within 15% agreement with their original extrapolated values.

Blank plasma containing 10 $\mu\text{g/ml}$ internal standard (Figure 6A) showed trace amounts of creatine- ^{13}C from endogenous creatine due to the natural abundance of ^{13}C . This was accounted for since the curve was generated in plasma; however, this is a limitation to the assay with respect to the LLOQ in comparison to other LC-MS/MS assays for creatine. (163, 164) Standard in plasma at 10.0 $\mu\text{g/ml}$ and an unknown measured to be 10.7 $\mu\text{g/ml}$ (Figure 6B and 6C, respectively) show consistency in retention time and ionization demonstrating the robustness of the assay. The choice of stable isotope labeled internal standards was made based on the similarity of the internal standard to the analyte (Figure 6D).

Figure 6. Representative chromatograms of creatine-¹³C (black) and creatine-d₃ (red) in blank plasma (A), a 10 µg/ml standard sample of creatine-¹³C in plasma (B), and an unknown rat plasma sample in similar range as the standard which we measured as 10.7 µg/ml creatine-¹³C (C). The assay was developed for the simultaneous measurement of creatine-¹³C and creatine-d₃ (D). Intensity is in counts per minute (CPM).



2.5. Physiologically Based Pharmacokinetic Modeling

All PBPK and simulations in rats and humans were performed using GastroPlus™, version 9.0 (Simulations Plus Inc., Lancaster, CA, USA). This module incorporates a whole-body PBPK model and simulates PK profiles and tissue distribution of compounds using input parameters based on the physicochemical properties of the compound of interest (e.g., solubility, partition coefficient (LogP), pKa) and disposition data (e.g., tissue-to-plasma partition coefficient (Kp) and clearance).

2.5.1 Structure and Validation of CM model in Rats and Humans

The default rat (0.3 kg) and human (30-year old American healthy male and female weighing 70 kg and 60 kg, respectively) fasted physiology in GastroPlus were used for the simulations. CM model in rats and humans consisted of 14 tissue compartments, including heart, lung, liver, spleen, GIT, adipose tissue, skeletal muscle, brain, kidney, skin, reproductive organs, red marrow, and yellow marrow linked together by venous and arterial blood circulation. Species-dependent physiological parameters, including tissue volume and weights, blood flow, and Kp, were generated by GastroPlus built-in Population Estimates for Age-Related Physiology (REAR) module. Intestinal absorption of CM was simulated using the default ACAT model in fasted state.

The drug distribution between tissue and blood was assumed to be perfusion rate limited, except in the muscle and brain, which were set as permeability rate limited and the kinetics for CRT1 were added.

The key physicochemical parameters required to construct CM model were obtained from experiments, published literature, or from a built-in ADMET predictor in GastroPlus and are shown in Table 6. For CM simulations, measured solubility-pH data obtained from the literature (128) were used and the data were fitted using the built-in pKa-based solubility model.

First, a model for CM in rats was built and the simulations were run using 2 formulations: 70 mg/kg oral (suspension form) or 10 mg/kg iv bolus injection of CM. The observed PK values from our CM PK study in rats were used to compare to and validate our simulated parameter. The same base model in rats was used to simulate 70 mg/kg oral (solution form) CHCl by changing the physicochemical properties as shown in Table 6. The PK profile of CHCl was compared to that of CM. A summary of the simulations of creatine compounds performed in human is shown in Figure 7.

Table 6. Summary of the key input physicochemical parameters of the various creatine compounds simulated

Parameter	CM	CCit	CPyr	CHCl
Molecular weight (g/mol)	149.15	202	219.2	167.6
LogP	-3.5	-3.2	-3.3	-3.2
Solubility (mg/ml)	17.1 ± 0.4	52 ± 7	91.6 ± 7.7	709 ± 7
Diffusion Coefficient (predicted by GastroPlus based on molecular weight) (cm ² /s x 10 ⁶)	1.1177	0.9494	0.9087	1.0494
Mean precipitation time (s)	900 (default)	900 (default)	900 (default)	900 (default)
Drug particle density (g/ml)	1.2 (default)	1.2 (default)	1.2 (default)	1.2 (default)

Particle radius (μm)	25	25	25	25
Effective GI Permeability (P_{eff}) ($\text{cm/s} \times 10^5$)	1.41	1.41	1.41	1.41

Figure 7. A summary of the simulations of creatine compounds performed in humans

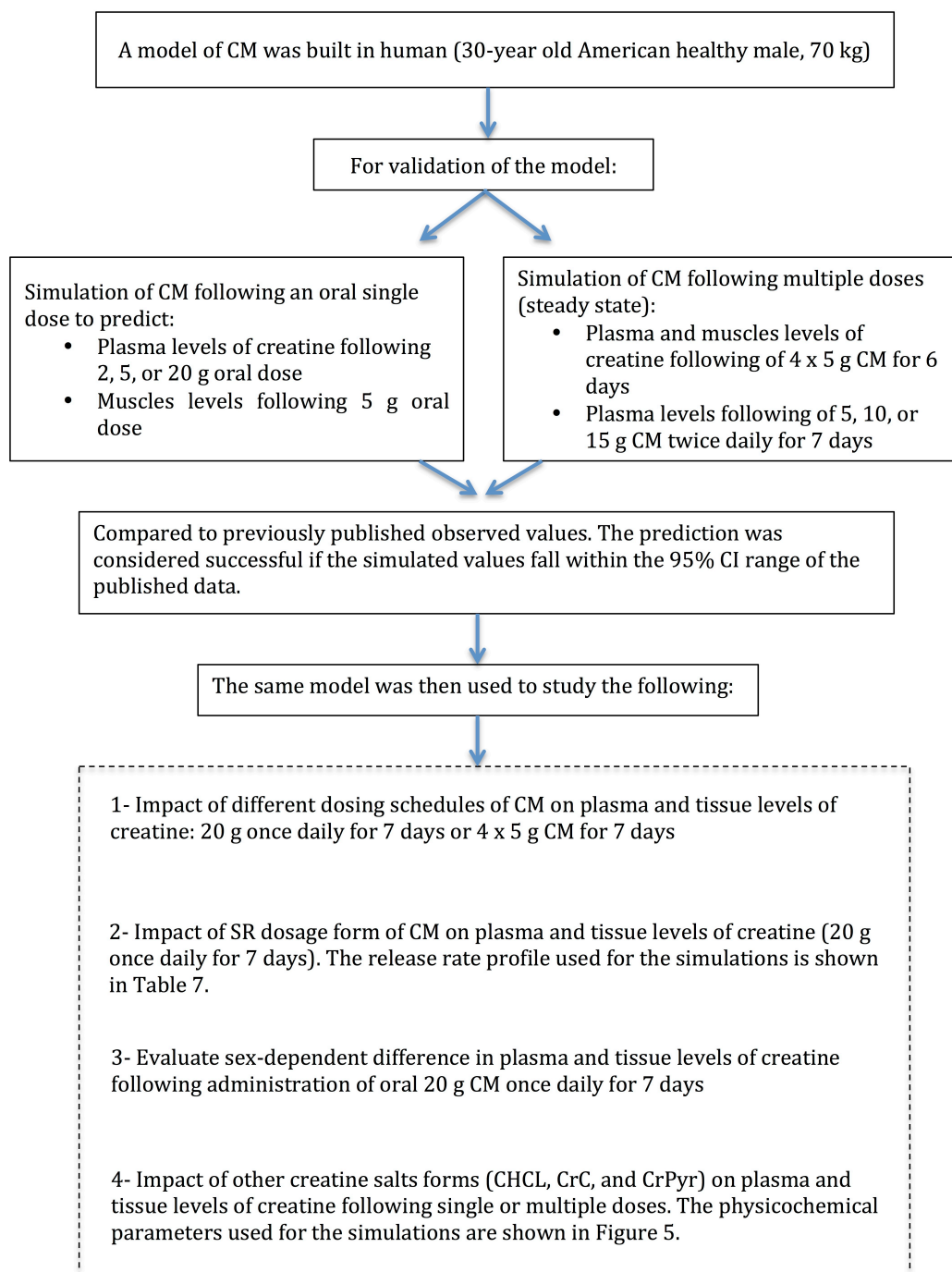
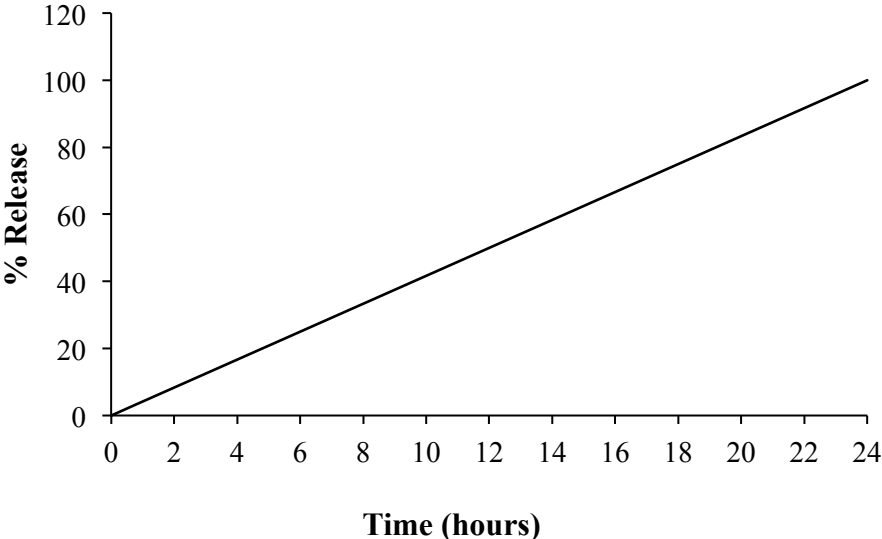


Table 7. Release rate profile for controlled release CM formulation.



2.6. Creatine Transporter Expression in Caco-2 and MDCK-*MDR1* Cells

Caco-2 and MDCK-*MDR1* cells were seeded in 100 mm cell culture dishes. After 24 hours, cells were harvested and total RNA was obtained using PureLink[®] RNA Mini Kit according to the manufacturer's instructions. The concentration of RNA in the samples was determined using Eppendorf BioPhotometer Plus spectrophotometer (Eppendorf, Hamburg, Germany). Total RNA samples were stored at -80 °C until further analysis.

Reverse transcription and amplification of complementary DNA (cDNA) was carried out using iTaq[™] Universal SYBR[®] Green One-Step RT PCR Kit. Each RT reaction contained 2 µg of total RNA. RT-PCR reactions were carried out in a PTC-100 Programmable Thermal Controller (MJ Research Inc., St. Bruno, Quebec, Canada). The cycle conditions are shown in Table 8. The primers for creatine transporter were designed using NCBI/Primer-Blast and were synthesized by Invitrogen (Ontario, Canada), Table 9. Reaction products were separated by electrophoresis on 2% agarose gel along with a 300 bp DNA molecular weight marker. The bands were visualized under UV light exposure. The predicted size of the PCR product was 111 and 176 bp, for human and canine CRT1, respectively.

Table 8: Cycling conditions for RT-PCR

Step	Time	Temperature
Reverse Transcription	15 minutes	50°C
PCR initial heat activation	2 minutes	95°C
Denaturing	15 seconds	95°C
Combined annealing/extension	60 seconds	60°C
Number of cycles: 45		

Table 9: CRT1 primer sequences used for RT-PCR

Primer	Forward Primer	Revers Primer	Product Length
Human	GTGTGGATAGATGCGG GGAC	TGGTCCCATTGTAGCA GTTGT	111
Canine	GTCGACGGGAAAGATC GTGT	GCCGATGGCGTAGGAA AAGA	176

2.7. Permeability studies

Permeability of CM and cyclocreatine (CC) were assessed over a 120-minute period on confluent monolayers of both MDCK-*MDR1* and Caco-2 cells grown on 12 well Transwell polycarbonate membrane inserts (24 mm diameter; 0.4 μm pore size) in the apical to basolateral (A-B) direction. MDCK-*MDR1* and Caco-2 were seeded at a density of 60000 cell/cm². Volume of media in the apical and basolateral compartments was 0.5 and 1.5 ml, respectively. The monolayers were used upon reaching confluency (4 days for MDCK-*MDR1* and 15 days for Caco-2).

On the day of the experiment, the media was replaced with assay buffer (122 mM sodium chloride, 3 mM potassium chloride, 1.4 mM calcium chloride, 1.2 mM magnesium sulfate, 25 mM sodium bicarbonate, 10 mM 4-(2-hydroxyethyl)-1-piperazineethanesulfonic acid (HEPES), 10 mM glucose and 0.4 mM dipotassium phosphate, pH 7.4) in both apical and basolateral compartments. The assay buffer in the apical compartment also contained 3.2 μM rhodamine 800, 1 μM IR Dye 800 CW PEG and 1 μM sodium fluorescein to assess monolayer integrity, with or without 10 μM , 100 μM , or 1000 μM CM or CC.

Samples (10 μl) were removed from the apical (donor) compartment at the start and conclusion of the permeability study. Samples (100 μl) were removed from the receiver compartments at various time points (0-120 minutes) and replaced with equal volumes of fresh assay buffer. The samples from the apical and basolateral compartments were placed in black 96-well plates. Quantitative analysis of the samples were performed using an Odyssey Near Infrared Imager (700 nm channel for rhodamine 800 and 800 nm channel for IR Dye 800 CW PEG)

and Biotek Synergy HT Microplate Reader at excitation 485 nm and emission 528 nm for sodium fluorescein.

The concentrations of the fluorescent permeability markers were quantitated using standard curves for each fluorescent compound. Permeability data were presented as the percent flux. Passage of creatine from the donor to the receiver compartment was analyzed using the HPLC method described above.

The permeability coefficient for CM and CC were calculated using the following equation:

$$P_{app} = (dCr/dt) \times (Vd/(A \times Cd))$$

Where:

dCr: Concentration in receiver compartment at any given time-point (μM)

dt: Time (sec)

Vd: Volume in the donor compartment (ml)

A: Area (cm^2)

Cd: Concentration in donor compartment at time 0 (μM).

2.8. Statistics

All PK data were expressed as mean \pm standard error of the mean (SEM). Statistical significance was evaluated using one-way ANOVA with Tukey post-hoc comparison of the mean.

Chapter 3. Results

3.1. CM PK Study in Rats

3.1.1. Plasma Kinetics and Oral Bioavailability of Low Dose and High Dose CM-¹³C

Linear and semi-log mean plasma concentration–time curves following administration of a 10 mg/kg iv bolus injection of CM-¹³C are shown in Figure 8A and Figure 8B, respectively. The C_{\max} of creatine-¹³C was obtained from visual inspection of the plasma concentration-time curve and was $76 \pm 15 \mu\text{g/mL}$ (Figure 8A) peaking at 3 minutes (T_{\max}). The shape of the semi-log curve shown in Figure 8B indicates that removal of creatine-¹³C from the plasma compartment following iv bolus injection followed a multiple compartment PK model with a rapid distribution phase followed by a slow terminal elimination phase.

Plasma creatine was also assessed following oral administration of CM-¹³C. The mean plasma concentration–time curves following high dose (70 mg/kg) and low dose (10 mg/kg) oral administration of CM-¹³C are shown in Figure 9A and Figure 9B, respectively. For both high dose and low dose CM-¹³C, the time for absorption was similar with T_{\max} occurring around 60 minutes post-administration. However, the amount of creatine absorbed was dose-dependent with C_{\max} reaching 14 ± 4 and $7 \pm 2 \mu\text{g/mL}$, for 70 mg/kg and 10 mg/kg doses, respectively. The $AUC_{0-\infty}$ for oral high dose (70 mg/kg), low dose (10 mg/kg), and iv (10 mg/kg)

CM-¹³C were 2501 ± 378 , 1139 ± 488 , and 2450 ± 110 $\mu\text{g}\cdot\text{min}/\text{mL}$, respectively. The oral bioavailability was dose-dependent with high dose CM-¹³C having oral bioavailability of 15.7 ± 3.4 % and low dose CM having oral bioavailability of 53.2 ± 11.2 %. While CRN-¹³C was also analyzed in these studies, the amount of CRN-¹³C was unchanged from baseline values at all time points examined (data not shown).

Figure 8. Plasma creatine-¹³C concentration-time curves following administration of 10 mg/kg iv bolus injection of CM-¹³C in adult male rats. The curves are shown in both linear (A) and semi-log (B) formats. Values represent the mean ± SEM. *n* = 4 rats.

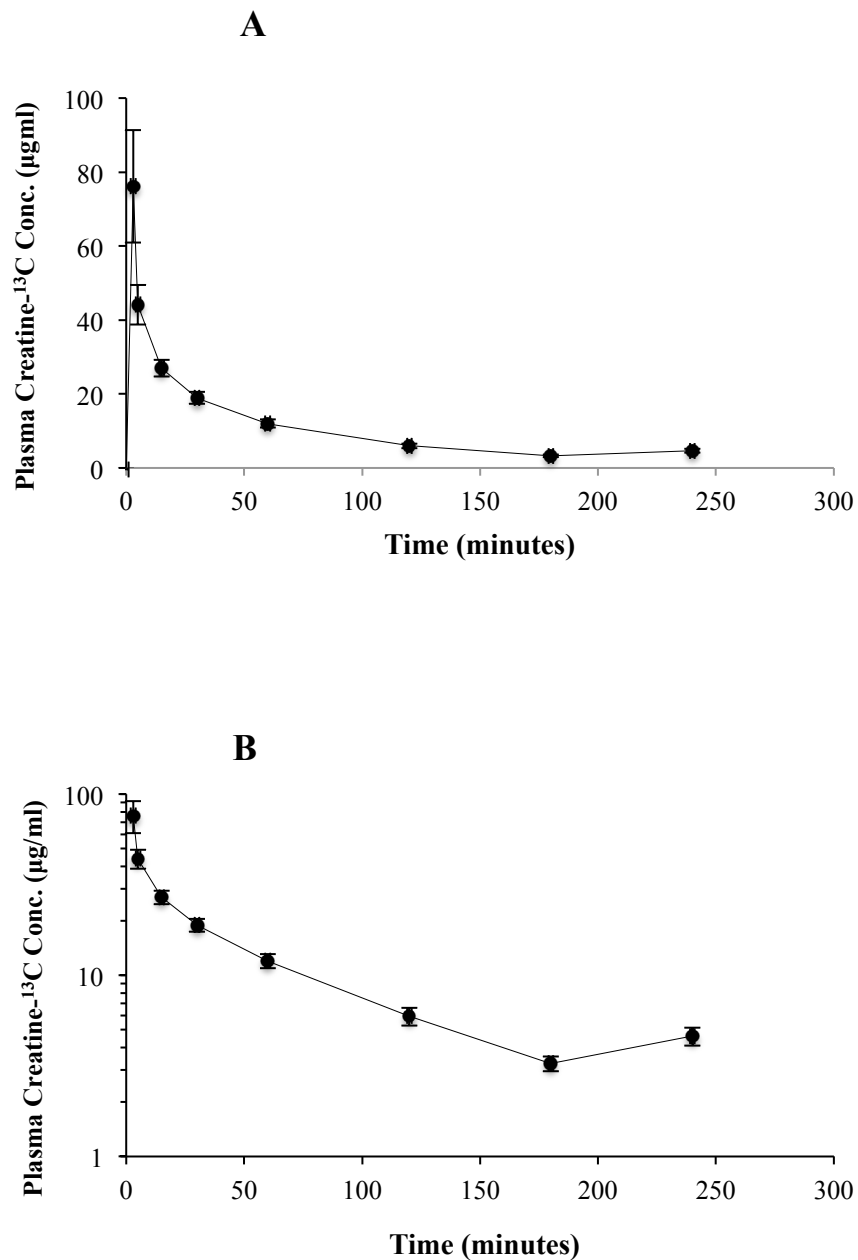
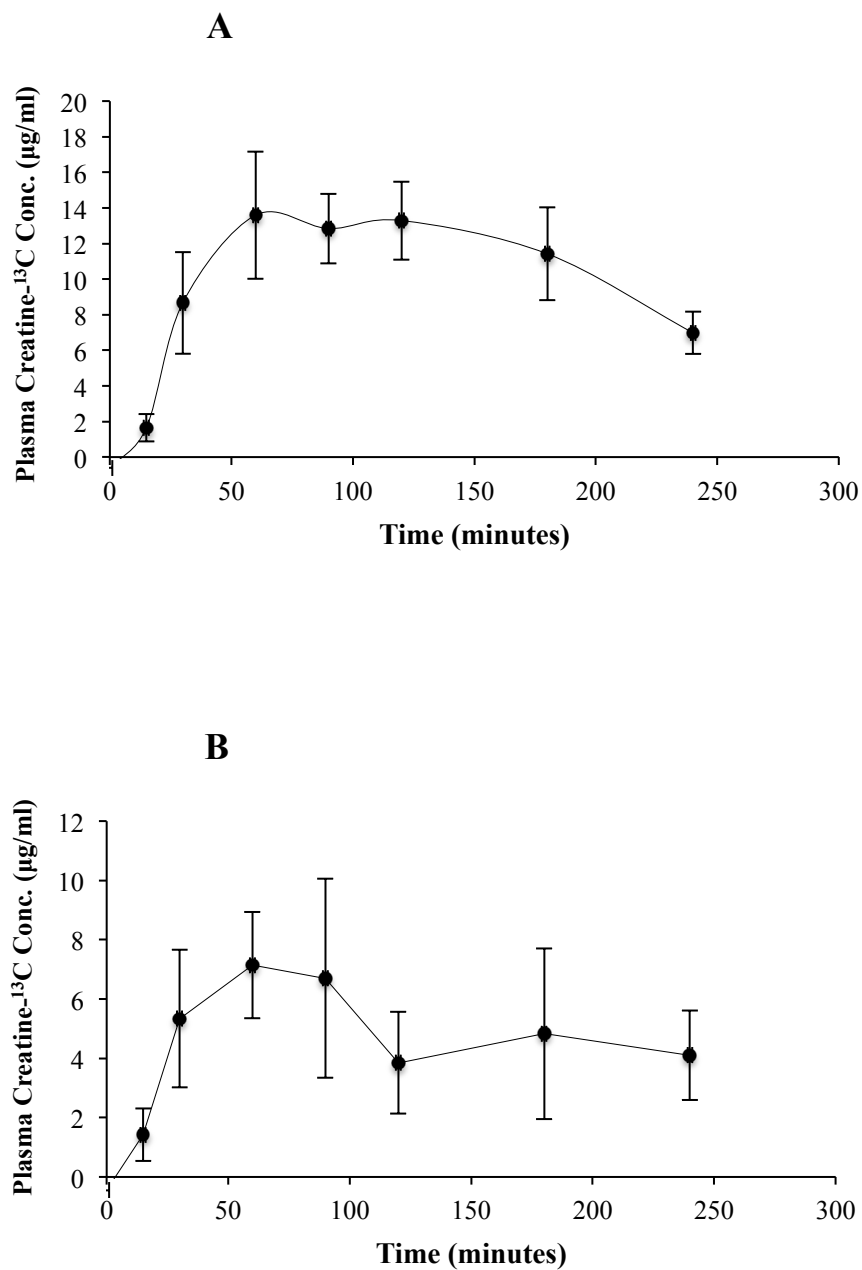


Figure 9. Plasma creatine-¹³C concentration–time curve following administration of (A) high dose (70 mg/kg) or (B) low dose (10 mg/kg) oral CM-¹³C. Values represent the mean ± SEM. *n* = 4 rats.



3.1.2. Tissue Distribution Following Administration of Low Dose and High Dose CM-¹³C

Tissue distribution of creatine-¹³C following administration of iv and oral CM-¹³C was also quantified using LC-MS/MS. Tissue accrual was the highest in the muscle samples reaching approximately 16 µg/g at four hours following either oral or iv CM-¹³C, Figure 10A. While increases in creatine-¹³C were also detected in the brain, the levels were about a third of that observed in muscle, Figure 10B. Muscle and brain concentrations of creatine-¹³C were compared to tissue concentrations from non-treated rats.

Creatine-¹³C content in the red blood cell (RBC) samples following oral administration showed little change from baseline levels taken prior to administration of CM-¹³C. However, RBC levels of creatine-¹³C following iv injection peaked at three minutes and were at or near baseline levels at four hours, Figure 11.

Figure 10. (A) Muscle and (B) brain concentrations of creatine-¹³C 4 hours after administration of iv or oral dose of CM-¹³C. Values represent the mean ± SEM. *n* = 4 rats. Creatine-¹³C content in muscle and brain samples from non-treated rats was below detection limits (0.5 µg/g tissue). ** *p* < 0.01, *** *p* < 0.001, **** *p* < 0.0001 compared to levels in non-treated group (one-way ANOVA). BDL = below detection limit.

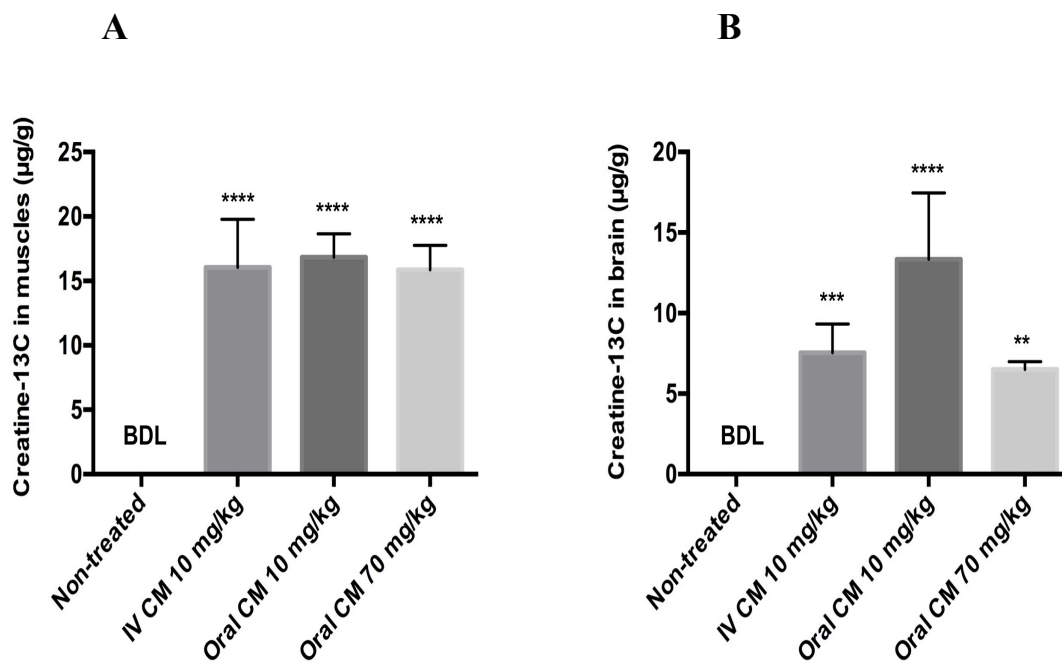
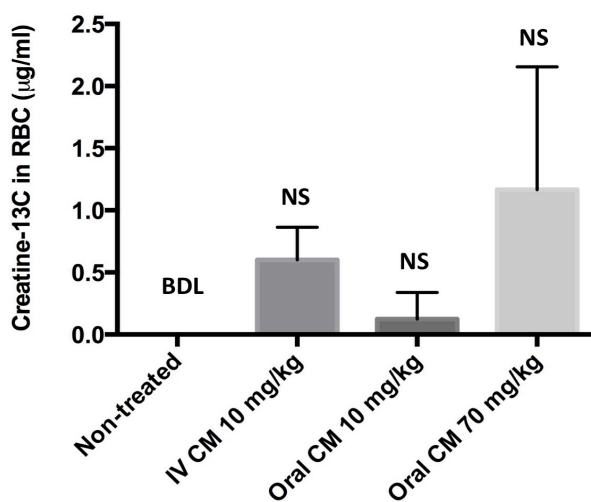


Figure 11. RBC concentrations of creatine-¹³C 4 hours after administration of iv or oral dose of CM-¹³C. Values represent the mean ± SEM. *n* = 4 rats. Creatine-¹³C content in RBC from non-treated rats was below detection limits (0.5 µg/g tissue). NS = non-significant compared to levels in non-treated group (one-way ANOVA). BDL = below detection limit.



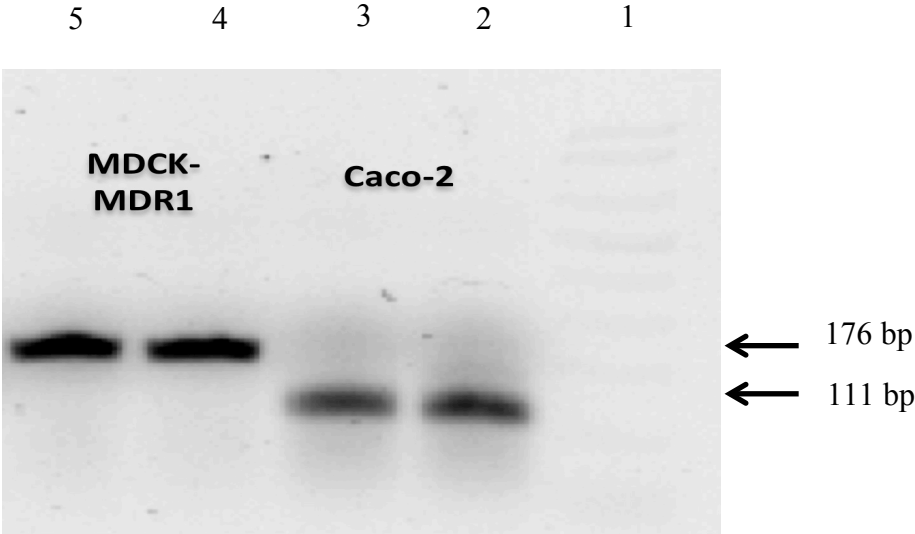
3.2. Physiologically Based Pharmacokinetic Modeling of Creatine Compounds

3.2.1 Examination of Permeability of CM in Caco-2 and MDCK-*MDR1* Monolayers

The permeability coefficient of the compound of interest is one of the main input parameters required for PBPK simulations. Caco-2 and MDCK-*MDR1* are two of the most commonly used cell lines for *in-vitro* permeability testing of compounds. (165) Permeability in both cell lines is well documented to correlate with human intestinal absorption. (165) CM permeability across MDCK-*MDR1* and Caco-2 monolayers was examined at various concentrations and the permeability coefficients obtained from these studies were used for the PBPK simulations. In addition, the expression of CRT1 was examined at the mRNA level in Caco-2 and MDCK-*MDR1* cell lines using RT-PCR in order to confirm the presence of CRT1 in these 2 cell lines for creatine permeability experiments. Creatine transporter gene expression was detected in both cell culture preparations, appearing as a distinct band at the predicted size (111 and 176 bp for Caco-2 and MDCK-*MDR1*, respectively), Figure 12.

Figure 12. Verification of Creatine Transporter mRNA Expression using RT-PCR in Caco-2 and MDCK-*MDR1* lysates.

Lane 1: DNA ladder; Lane 2 and 3: Two different samples from Caco-2 lysates; Lane 4 and 5: Two different samples from MDCK-*MDR1* lysates. Arrows indicate bands of interest.



For the permeability studies, three different fluorescent probes were used to assess cell monolayer integrity with or without CM or CC. The fluorescent permeability markers included fluorescein (MW 332.31) which is a small hydrophilic probe, IR dye 800 CW PEG (MW 35,000), a large hydrophilic probe, and rhodamine 800, which is a P-glycoprotein probe. The permeability of all three probes examined in Caco-2 and MDCK-*MDR1* monolayers was low (less than 5-10% over 120 minutes) suggesting intact and tight monolayers, Figure 13 and Figure 14. The permeability of fluorescein in Caco-2 monolayers was below the level of detection at all the time points examined (data not shown). In addition, none of the creatine compounds examined altered the permeability of these three probes, suggesting monolayer integrity was not influenced by the creatine compounds used, Figures 13 and 14.

The permeability of CM across Caco-2 and MDCK-*MDR1* is shown in Figure 15 and the permeability coefficients (P_c) are shown in Figure 16. There was a concentration-dependent effect on CM permeability, with the lowest concentration (10 μM) of CM having a higher permeability compared to 100 or 1000 μM examined. The concentration dependent effect on permeability was most apparent in the Caco-2 monolayers where P_c were 10 μM > 100 μM > 1000 μM (Figure 16). With respect to the MDCK-*MDR1*, there was also a concentration dependent effect on permeability with 10 and 100 μM being greater than 1000 μM , Figure 16. The permeability of CC across Caco-2 and MDCK-*MDR1* were lower and lacking the concentration dependent effect in comparison with CM, Figure 17 and Figure 18.

Figure 13. Permeability of (A) rhodamine 800, and (B) IR dye PEG across Caco-2 monolayers at various time points (30-120 minutes) with or without 10 μ M, 100 μ M, or 1000 μ M CM. Data are presented as % flux. Values represent the mean \pm SEM for 3 different monolayers per treatment group

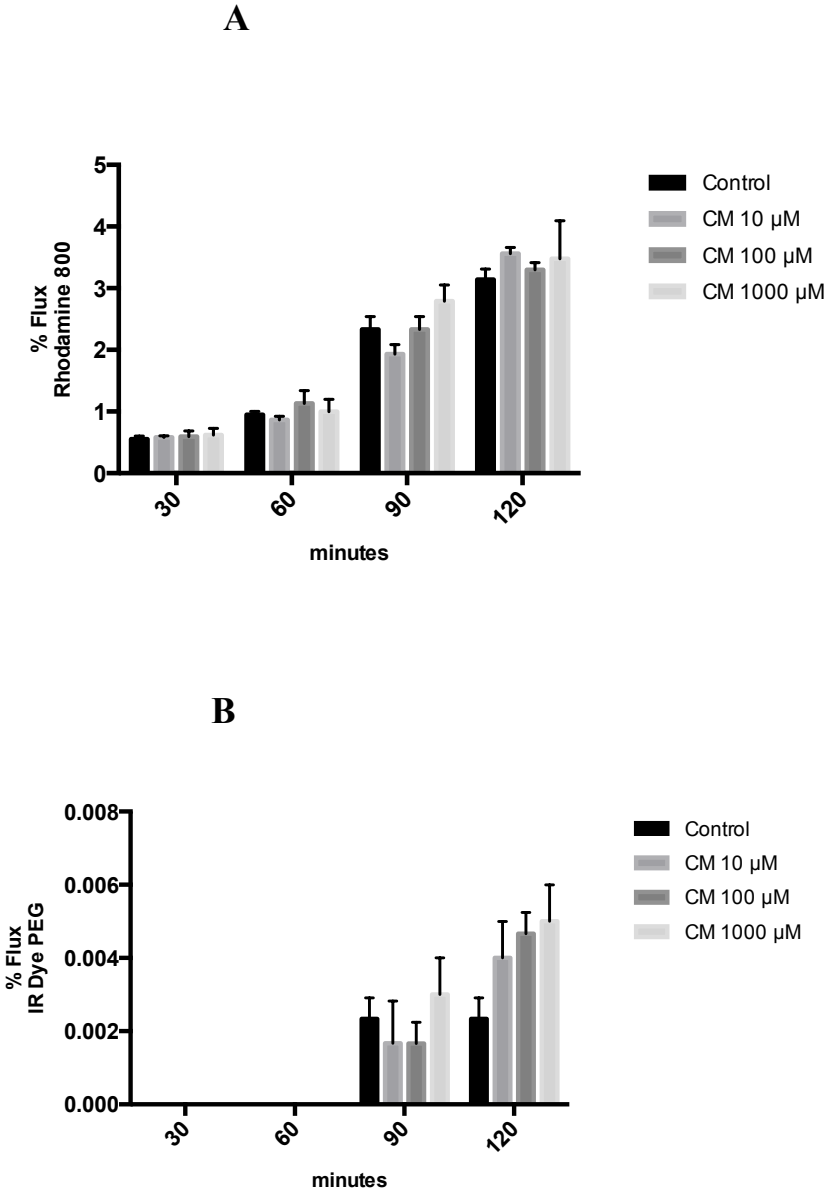
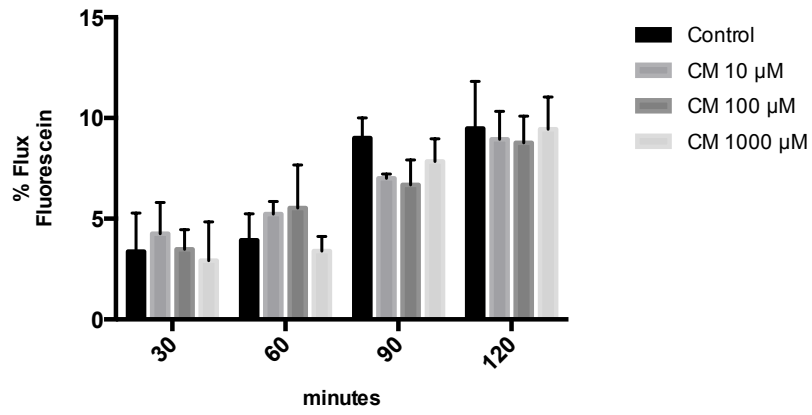
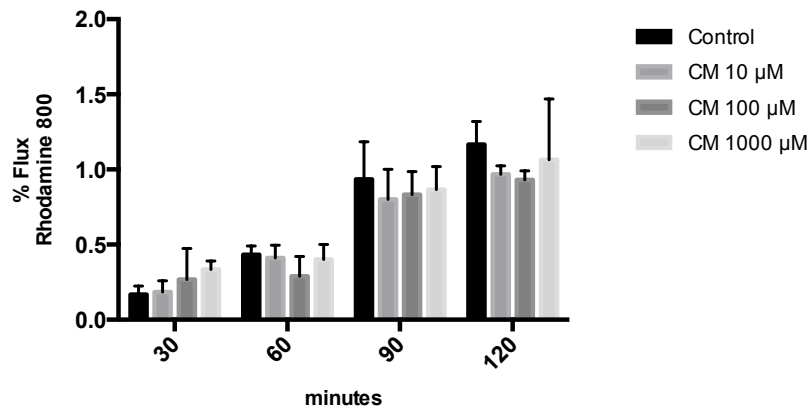


Figure 14. Permeability of (A) fluorescein, (B) rhodamine 800, and (C) IR dye PEG across MDCK-*MDR1* monolayers at various time points (30-120 minutes) with or without 10 μ M, 100 μ M, or 1000 μ M CM. Data are presented as % flux. Values represent the mean \pm SEM for 3 different monolayers per treatment group.

A



B



C

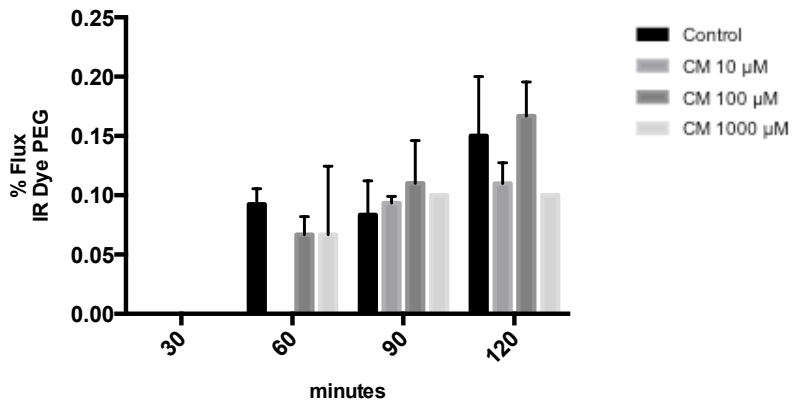


Figure 15. Permeability of CM at three different concentrations: 10, 100, or 1000 μM across (A) Caco-2, or (B) MDCK-*MRDI* monolayers at various time points (30-120 minutes). Data are presented as % flux. Values represent the mean \pm SEM for 3 different monolayers per treatment group.

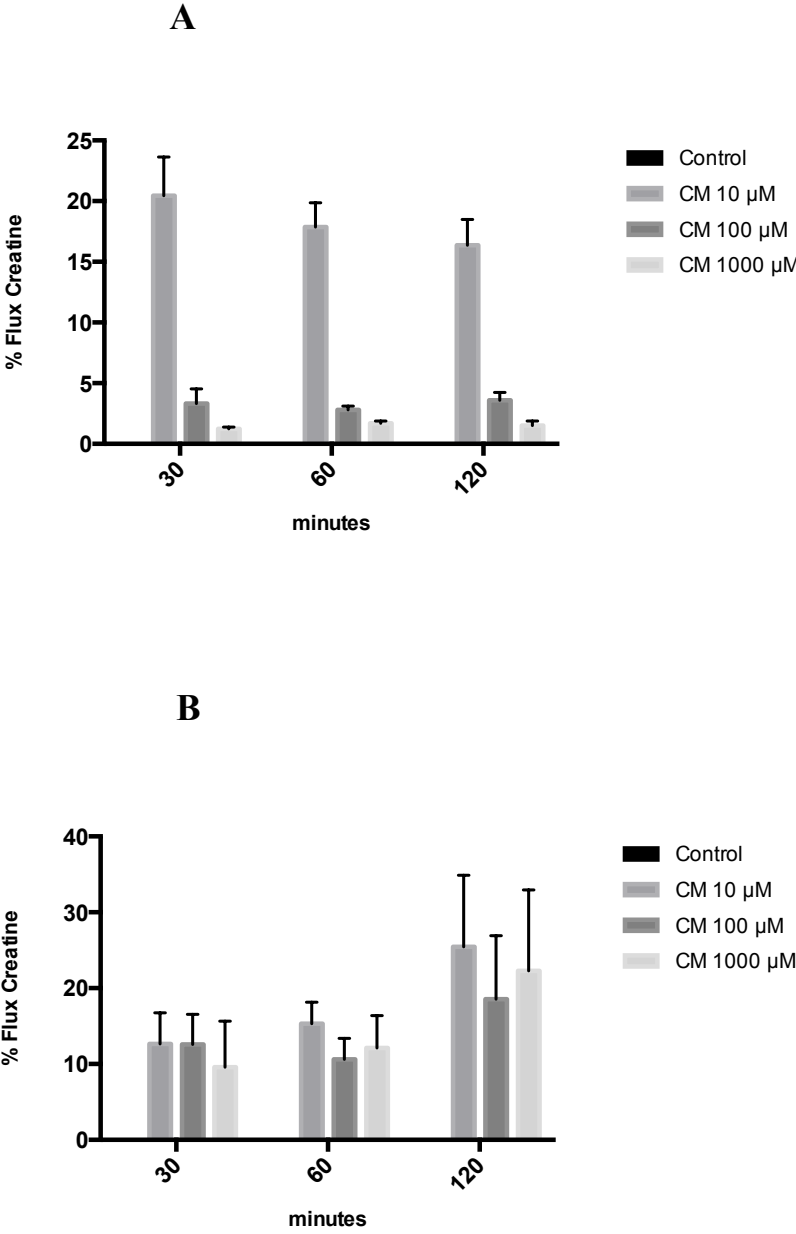


Figure 16. Permeability coefficients of CM at three different concentrations in Caco-2 and MDCK-MDR1 monolayers.

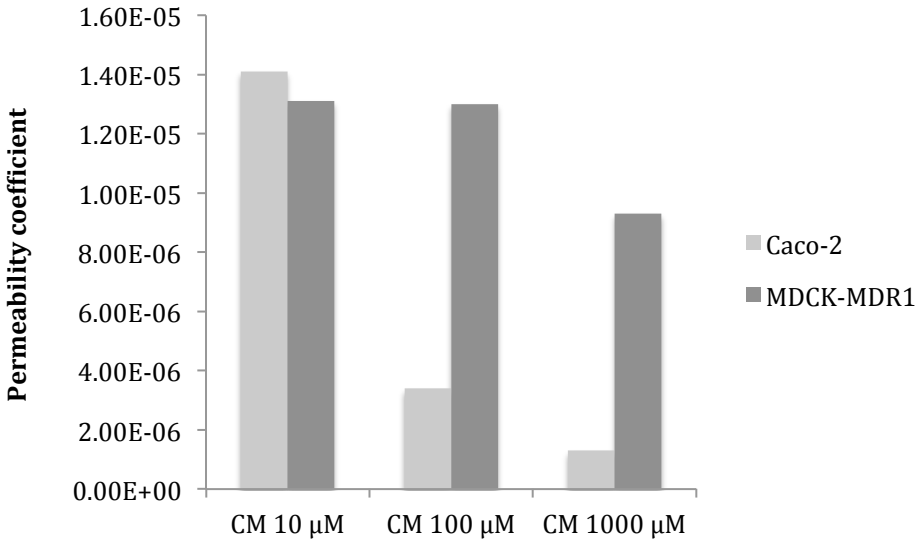


Figure 17. Permeability of CC at three different concentrations: 10, 100, or 1000 μM across (A) Caco-2, or (B) MDCK-*MRDI* monolayers at various time points (30-120 minutes). Data are presented as % flux. Values represent the mean \pm SEM for 3 different monolayers per treatment group.

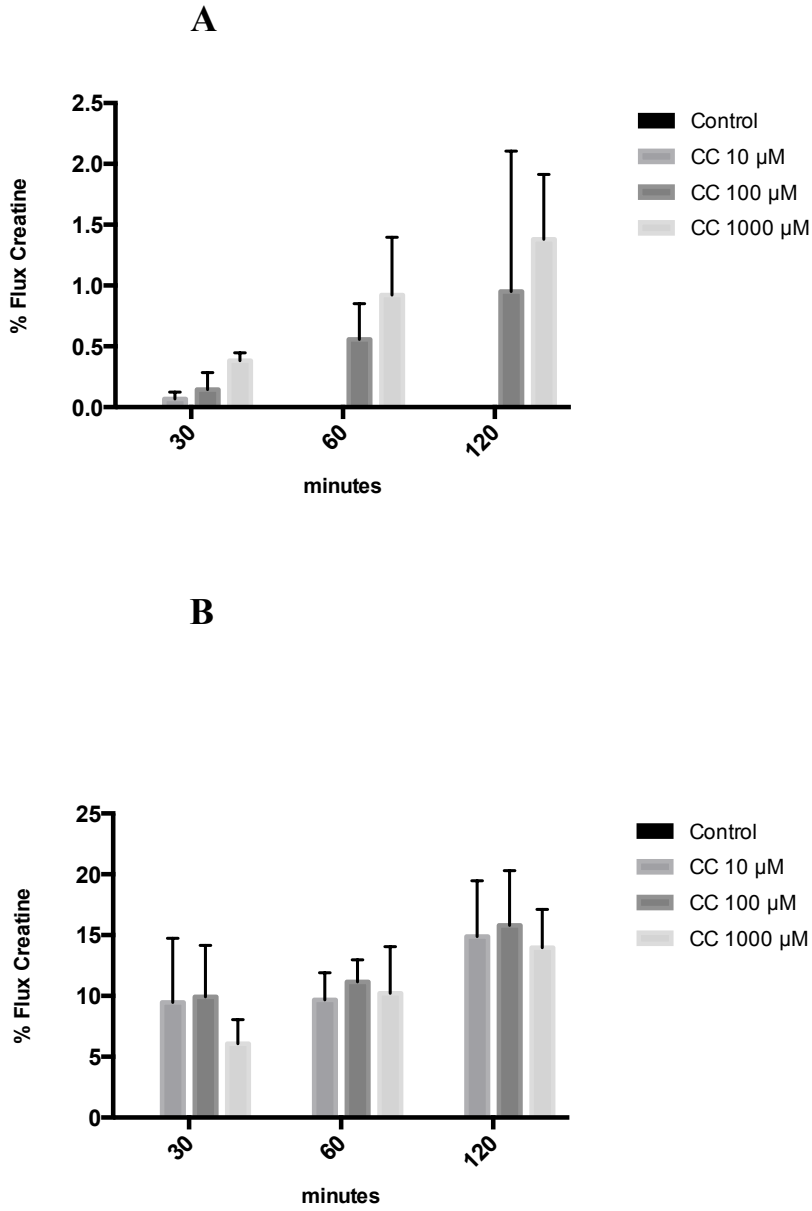
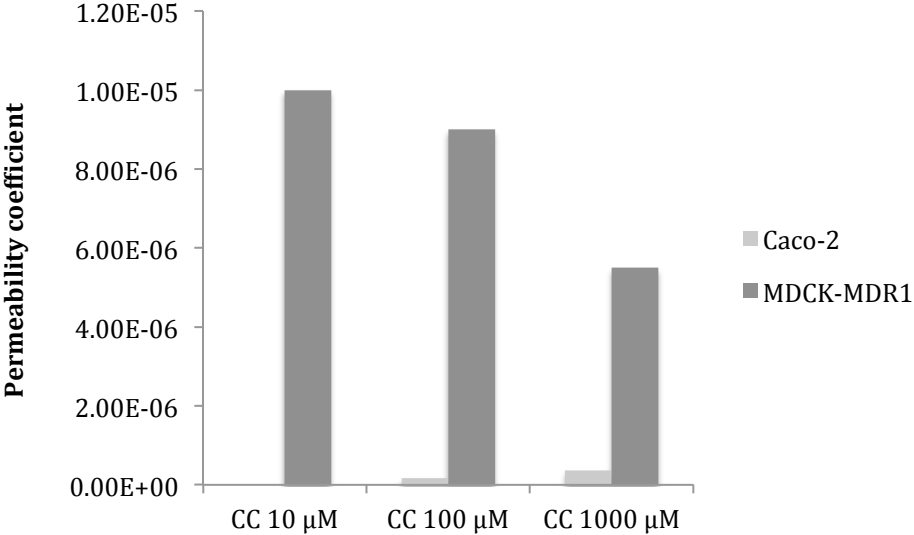


Figure 18. Permeability coefficients of CC at three different concentrations in Caco-2 and MDCK-*MDR1* monolayers.



3.2.2. Physiologically Based Pharmacokinetic Modeling of Creatine

3.2.2.1. Single Oral Dose CM in Rats

Using the permeability coefficients from the Caco-2 and MDCK-*MDR1* monolayers, the physicochemical properties of CM and physiological parameters such as tissue blood flow and organ size, the PK profile of CM following administration of a bolus iv injection (10 mg/kg) or oral dose (70 mg/kg) in rats was simulated using GastroPlusTM. The oral dose (70 mg/kg) of CM was simulated in suspension form since the aqueous solubility of CM is around 17 mg/kg and the oral dose given in rats was dissolved in 0.25 ml of PBS. The simulated plasma concentration-time curves following administration of bolus iv injection or oral CM are shown in Figure 19 and Figure 20A, respectively.

To compare the appropriateness of the PBPK model, the simulation curves generated using GastroPlus were compared to the experimental values. The predicted PK parameters from the modeling program and the observed experimental values are shown in Table 10. For the iv injection route, there was very good agreement between the observed and simulated values with an R-squared value (R^2) = 0.99. The same PBPK model displayed some divergence from observed values in the high dose oral absorption (especially at the later time points) group, Figure 20A. However, the R^2 value for the oral administration route was still 0.84, Table 10. Considering the variability within the data set, the PBPK model provided a very good approximation of PK parameters for oral dosing of CM, Table 10.

3.2.2.2. Single Oral Dose CHCl in Rats

Given the good agreement between the PBPK model estimates for CM and the PK profile determined experimentally, the same model was also used to predict the impact of other creatine salt forms on plasma and tissue levels of creatine in rats. For these simulations, CM was compared to CHCl, a newer salt form of creatine with higher aqueous solubility (approximately 709 mg/mL) compared to 17 mg/ml for CM. (128) The predicted plasma concentration-time curves and tissue (brain and muscles) concentrations following administration of 70 mg/kg oral CHCl were compared to a similar dose of CM (Figure 20). The predicted C_{\max} of CHCl in plasma was around 35 $\mu\text{g/mL}$ compared to 14 $\mu\text{g/mL}$ for CM, and the predicted oral bioavailability was 66% compared to approximately 17% with CM, Figure 20A. The substantial differences in plasma creatine levels with CM and CHCl were attributed to the enhanced aqueous solubility of CHCl. As the aqueous solubility of CHCl is around 709 mg/ml, a dose of 70 mg/kg is completely dissolved in 0.25 ml compared to a similar dose of CM that is given as a suspension due to the low aqueous solubility of CM.

In addition to increased plasma levels of creatine, an increase in tissue levels of creatine in muscles and the brain were also predicted when CHCl was used compared to CM, Figure 20B and 20C, respectively. The simulated muscle concentrations of creatine peaked at approximately 34 $\mu\text{g/mL}$ for CHCl compared to approximately 17 $\mu\text{g/mL}$ with a similar dose of CM, Figure 20B. For the brain, predicted levels of creatine reached approximately 15 $\mu\text{g/mL}$ (115 μM) with CHCl compared to approximately 8 $\mu\text{g/mL}$ (61 μM) with CM, Figure 20C.

Figure 19. Simulated (solid line) and observed creatine plasma concentration–time curves obtained from 4 rats, after a single iv dose of CM (10 mg/kg).

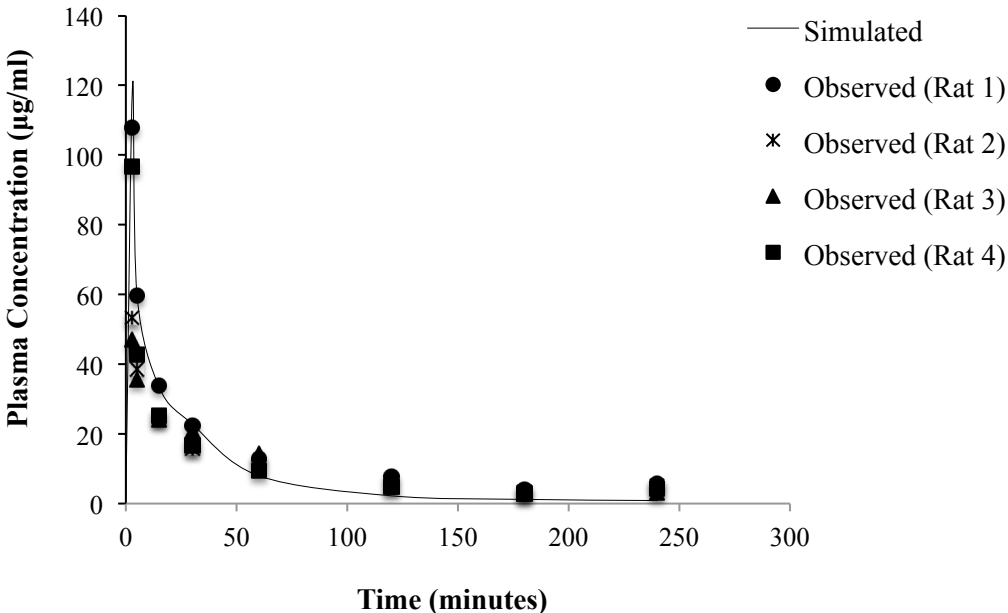


Figure 20. Simulated creatine concentrations in (A) plasma, (B) muscle and (C) brain following a single oral dose (70 mg/kg) of CM (dashed line) or CHCl (solid line) using GastroPlus compared to observed values.

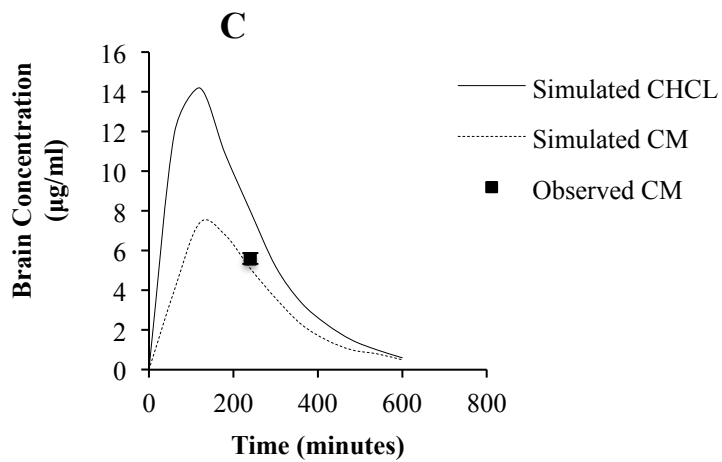
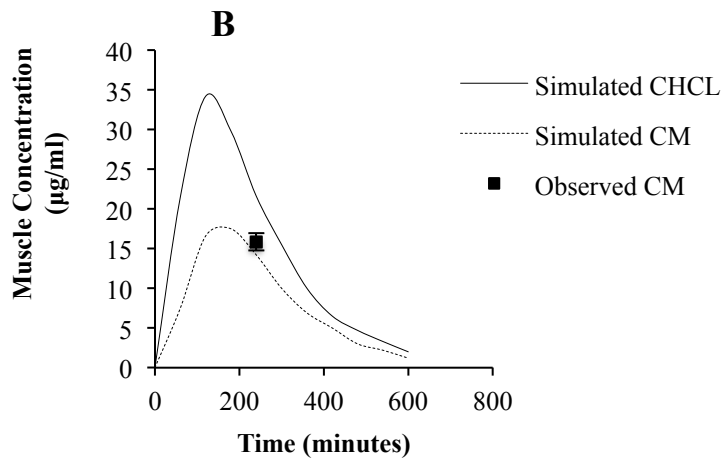
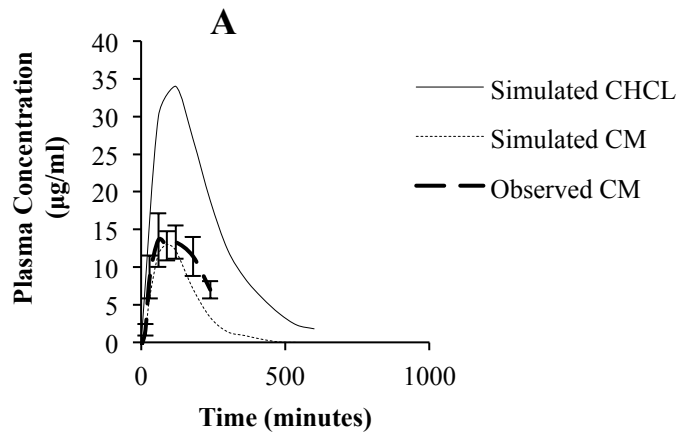


Table 10. Predicted vs. observed PK parameters following administration of bolus iv injection (10 mg/kg) or an oral suspension (70 mg/kg) of CM in rats.

Parameter	IV Bolus Injection of CM (10 mg/kg)		Oral Suspension of CM (70 mg/kg)	
	Simulated	Observed	Simulated	Observed
C _{max} (µg/ml)	122	76 ± 15	14	14 ± 3
T _{max} (min)	3	3	87	60
V _d (L/kg)	0.2	0.3 ± 0.1	-	-
T _{1/2} (min)	64	69 ± 4	-	-
CL (L/hr)	0.04	0.05 ± 0.01	-	-
AUC _{0-∞} (µg.min/ml)	2279	2450 ± 110	2286	2501 ± 378
F (%)	-	-	17	16 ± 4
R ² value (model vs. observed)	0.99	-	0.84	-

3.2.3. Physiologically Based Pharmacokinetic Modeling of Creatine Compounds in Humans

3.2.3.1. Single Oral Dose CM in Humans

Using GastroPlus software, we were able to model the plasma concentration-time profile for CM in rats with good agreement to the observed values. In addition, the PBPK model was also able to predict concentrations of creatine in various tissue compartments. Given the agreement of the established PBPK model with observed PK values in rats, our model was further extrapolated to humans. Comparison of the PBPK model simulation parameters with published PK data following administration of an oral single dose of CM in humans were used to validate the PBPK model. The *in-vivo* PK data obtained from literature and used to evaluate the accuracy of the PBPK model included plasma concentration-time profiles following oral administration of 3 different doses (2, 5 and 20 g) of CM (61, 145, 166-170) and muscle concentration-time profiles following oral administration of 5 g CM. (168) Both plasma and muscle observed and simulated C_{max} , T_{max} , AUC_{0-t} , and $AUC_{0-\infty}$, following administration of an oral single dose of CM are presented in Table 11 and Table 12. There was reasonable agreement between the observed and simulated values with the values predicted from the PBPK model falling within the confidence intervals of the previously published values.

Table 11. Plasma observed and simulated C_{\max} , T_{\max} , AUC_{0-t} , and $AUC_{0-\infty}$, following administration of an oral single dose of CM (2, 5, or 20 g).

Dose	Data Source	C_{\max} ($\mu\text{g/ml}$)	T_{\max} (h)	$AUC_{0-\infty}$ ($\mu\text{g.h/ml}$)
2 g CM	Observed ($n=5$) (166)	42 ± 17 95% CI: [27,57]	1	76 ± 31 95% CI: [49,103]
	Observed ($n=17$) (167)	45 ± 3 95% CI: [44,46]	1	81 ± 5 95% CI: [79,83]
	Simulated	34	1	83
5 g CM	Observed ($n=3$) (61)	118 ± 16 95% CI: [100,136]	1	-
	Observed ($n=6$) (168)	102 ± 11 95% CI: [93,111]	2 ± 1	392 ± 98 95% CI: [314,470]
	Observed ($n=6$) (145)	114 ± 16 95% CI: [101,127]	1	356 ± 56 95% CI: [311,400]
	Simulated	97	1	336
20 g CM	Observed ($n=15$)	324 ± 99 95% CI:	2	-

	(169)	[274,374]		
	Observed (<i>n</i> =6) (170)	477	2	-
	Simulated	302	2	1761

Table 12. Muscles observed and simulated C_{\max} , T_{\max} , and $AUC_{0-\infty}$, following administration of an oral single dose of CM (5 g)

Dose	Data Source	C_{\max} ($\mu\text{g/ml}$)	T_{\max} (h)	$AUC_{0-\infty}$ ($\mu\text{g}\cdot\text{h/ml}$)
5 g CM	Observed (<i>n</i> =6) (168)	48 ± 16 95% CI: [35,61]	2 ± 1	162 ± 64 95% CI: [111,213]
	Simulated	52.8	2	219

3.2.3.2. Steady-State Oral Dosing of CM in Humans

As the biological effects of creatine supplementation are based on multiple dosing, PK profiles following administration of multiple-doses of oral CM in humans were simulated and compared to published values. The *in-vivo* PK data obtained from literature and used for comparison with the current simulations included plasma and muscle concentration-time profiles after oral administration of 5 g CM four times daily for 6 days in healthy volunteers, (168, 170) and plasma concentration-time profile of CM following administration of 5, 10, or 15 g oral CM twice daily for 7 days. (171) The PK parameters generated using GastroPlus were compared to these observed published values. The plasma and muscle concentrations of creatine from published studies and from the simulated PK profiles are listed in Tables 13-15.

Table 13 and Table 15 show the plasma and muscle observed and simulated PK parameters following administration of multiple-doses of CM (4 x 5 g oral CM). Table 14 shows plasma observed and simulated PK parameters following administration of multiple-doses of CM (5, 10, or 15 g twice daily for 7 days). As with the single dose PK simulations, for the steady-state oral dosing of CM, there was reasonable agreement between the observed and simulated values with the values predicted from the PBPK model falling within the confidence intervals of the observed values.

Table 13. Plasma observed and simulated PK parameters following administration of multiple-doses of CM (4 x 5 g oral CM).

Parameter	Observed (168) 4 x 5 g for 6 days (n=6)	Observed (170) 4 x 5 g for 4 weeks (n=6)	Simulated 4 x 5 g for 6 days
C_{\max} ($\mu\text{g/ml}$)	162 \pm 30 95% CI: [138,186]	-	151
T_{\max} (h)	2 \pm 1	-	1
AUC_{ss} ($\mu\text{g}\cdot\text{h/ml}$)	-	-	2420
C_{ss} ($\mu\text{g/ml}$)	97 \pm 13 95% CI: [87,107]	119	104

Table 14. Plasma observed and simulated PK parameters following administration of multiple-doses of CM (5, 10, or 15 g twice daily oral CM for 7 days).

Dose	Data Source	Pre-dose concentration (trough) at steady state ($\mu\text{g/ml}$)	AUC₀₋₅ ($\mu\text{g.h/ml}$)
5 g BID CM	Observed (171) (n=6)	20 \pm 1 95% CI: [19,21]	333 \pm 24 95% CI: [313,352]
	Simulated	18	308
10 g BID CM	Observed (171) (n=6)	39 \pm 4 95% CI: [36,42]	632 \pm 110 95% CI: [544,720]
	Simulated	35	614
15 g BID CM	Observed (171) (n=6)	62 \pm 8 95% CI: [55,68]	857 \pm 66 95% CI: [804,910]
	Simulated	55	837

Table 15. Muscle observed and simulated PK parameters following administration of multiple-doses of CM (4 x 5 g oral CM for 7 days).

Dose	Data Source	C_{max} (µg/ml)	T_{max} (h)	AUC_{0-∞} (µg.h/ml)
4 x 5 g CM for 7 days	Observed (168) (n=3)	52 ± 30 95% CI: [1,131]	2	197 ± 125 95% CI: [0,520]
	Simulated	108	2	577

3.2.3.3. Impact of Different Dosing Schedules on Plasma and Tissue Levels of Creatine

In most of the clinical trials of CM for therapeutic applications (e.g. HD and PD), high doses of CM (> 20 g/day) were used in an attempt to increase the levels of creatine in the brain to achieve levels sufficient for beneficial therapeutic effects. Using the modeling parameters established for single dose CM, additional simulations were performed to examine and compare the plasma and tissue levels of creatine following administration of different oral dosage regimens. The first dosing consideration was to examine one large 20 g/day dose of CM versus a 20 g daily dose of CM divided into smaller doses given multiple times per day (4 x 5 g) to determine their impact on plasma and tissue levels of creatine.

Figures 21-26 show the simulated plasma, brain, or muscles concentration-time curves following administration of either 20 g once daily or 4 x 5 g per day CM. Table 16 compares the resultant AUC_{ss} at steady state during 24 hours.

As expected, the simulated peak or C_{max} at steady state in plasma and tissue was higher following administration of 20 g CM compared to the smaller dose of CM (5 g), Figures 21-26. However, there was no significant difference in the resultant AUC_{ss} in plasma and tissue following administration of one large 20 g dose compared to smaller doses, Table 16.

Figure 21. Simulated plasma levels of creatine following administration of oral CM (A) 20 g/day for 7 days, or (B) 4 x 5 g for 7 days.

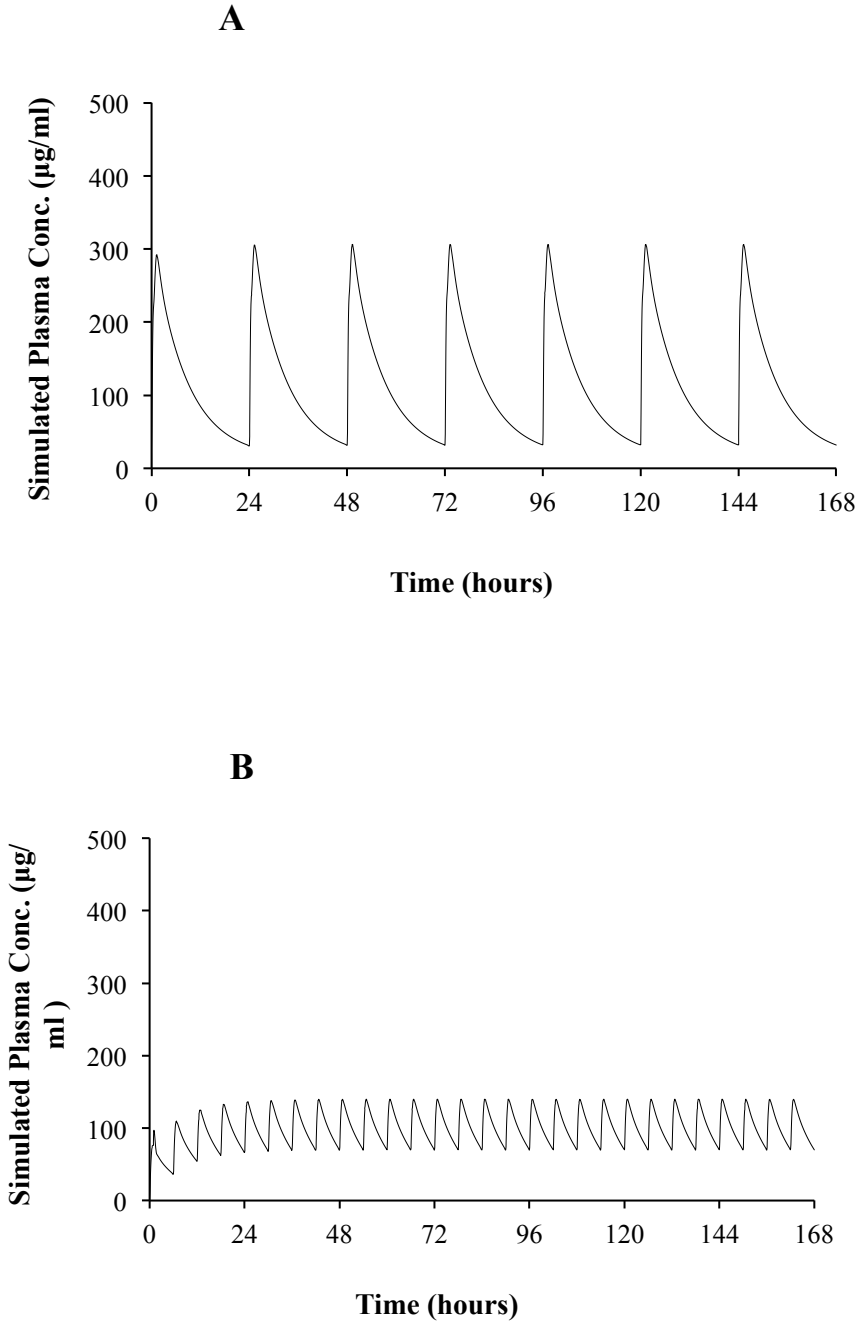


Figure 22. Simulated plasma levels of creatine at steady state during 24 hours following administration of oral CM (A) 20 g/day for 7 days, or (B) 4 x 5 g for 7 days.

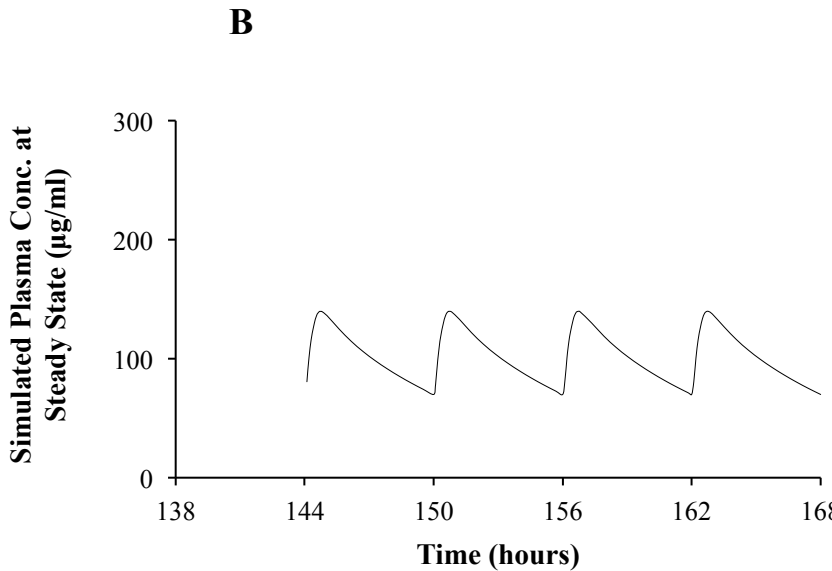
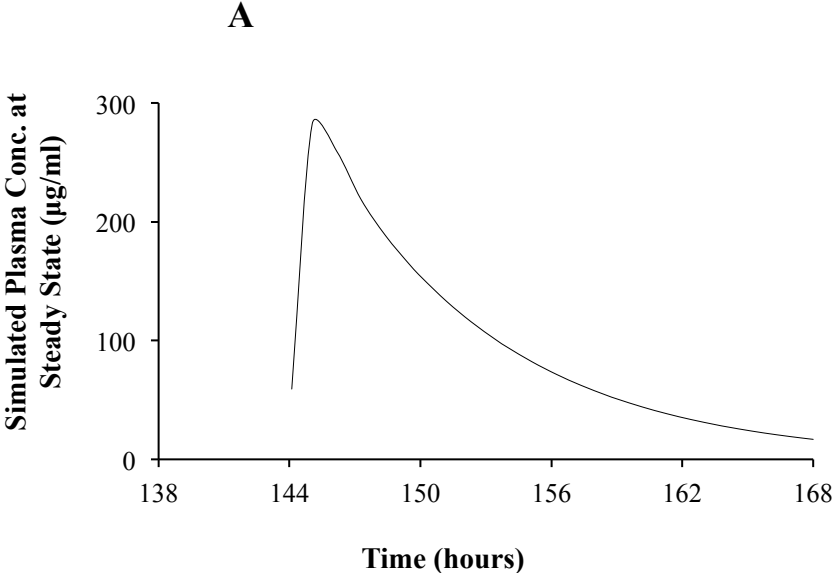


Figure 23. Simulated brain levels of creatine following administration of oral CM (A) 20 g/day for 7 days, or (B) 4 x 5 g for 7 days.

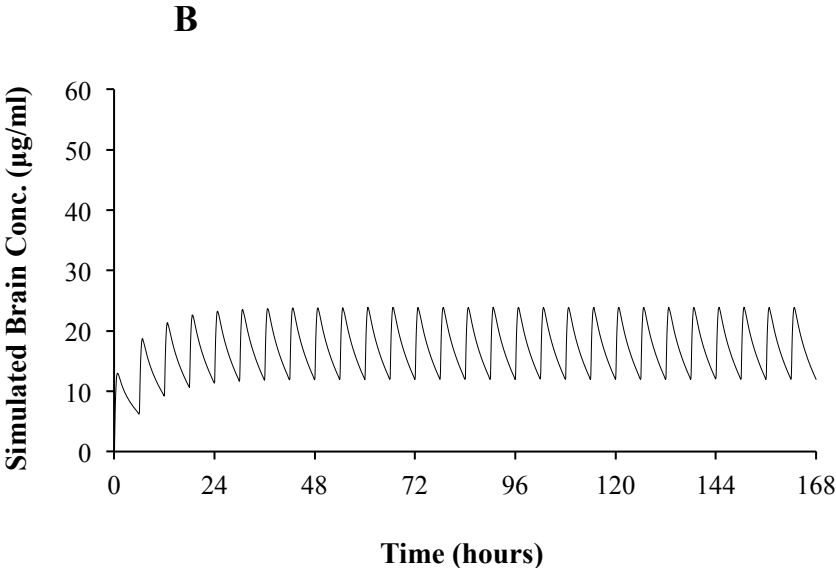
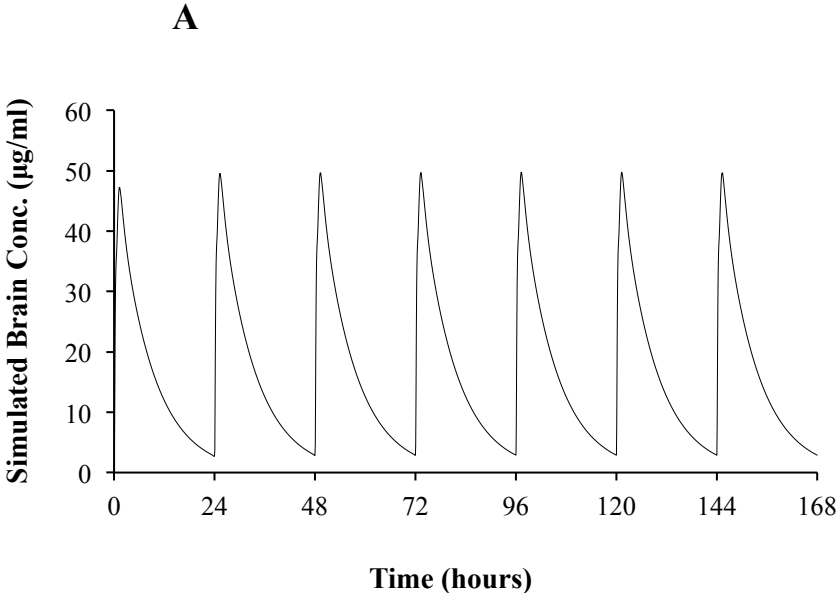


Figure 24. Simulated brain levels of creatine at steady state during 24 hours following administration of oral CM (A) 20 g/day for 7 days, or (B) 4 x 5 g for 7 days.

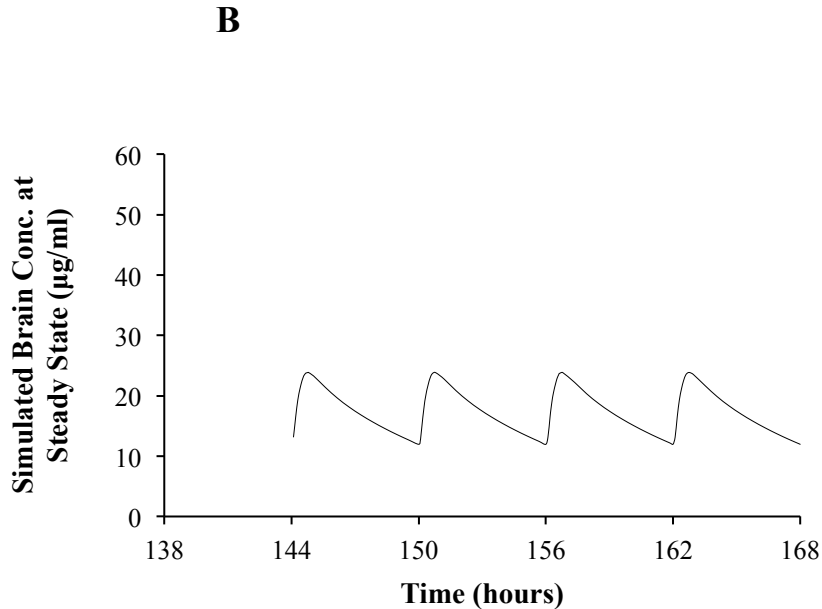
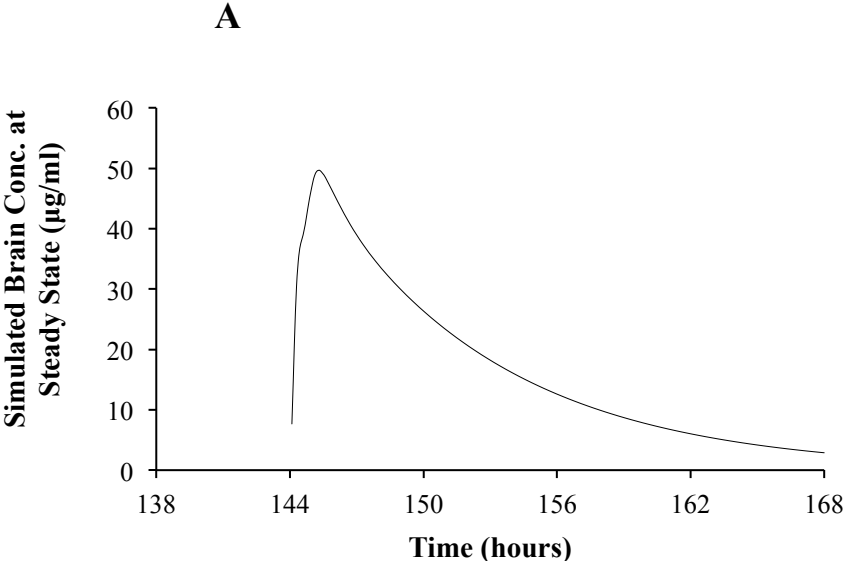


Figure 25. Simulated muscles levels of creatine following administration of oral CM (A) 20 g/day for 7 days, or (B) 4 x 5 g for 7 days.

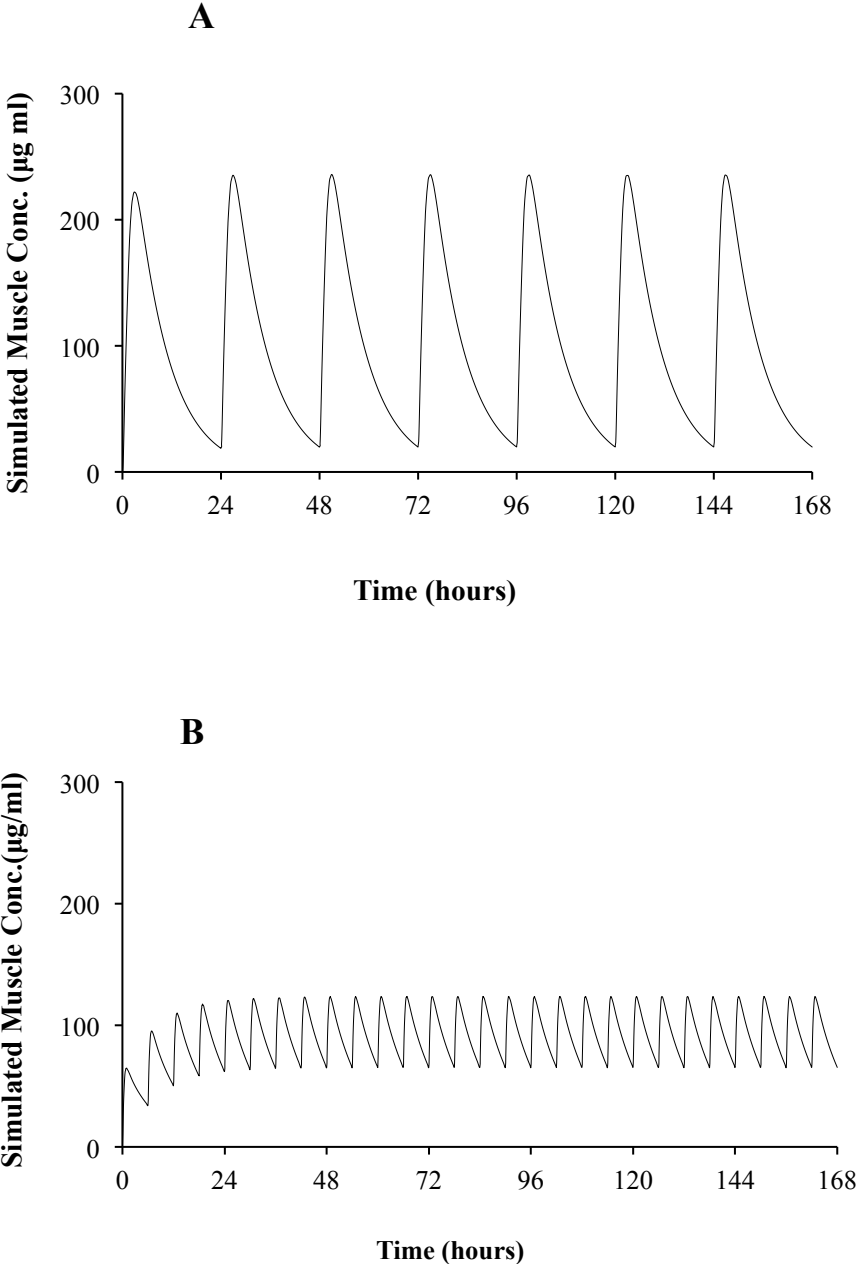


Figure 26. Simulated muscles levels of creatine at steady state during 24 hours following administration of oral CM (A) 20 g/day for 7 days, or (B) 4 x 5g for 7 days.

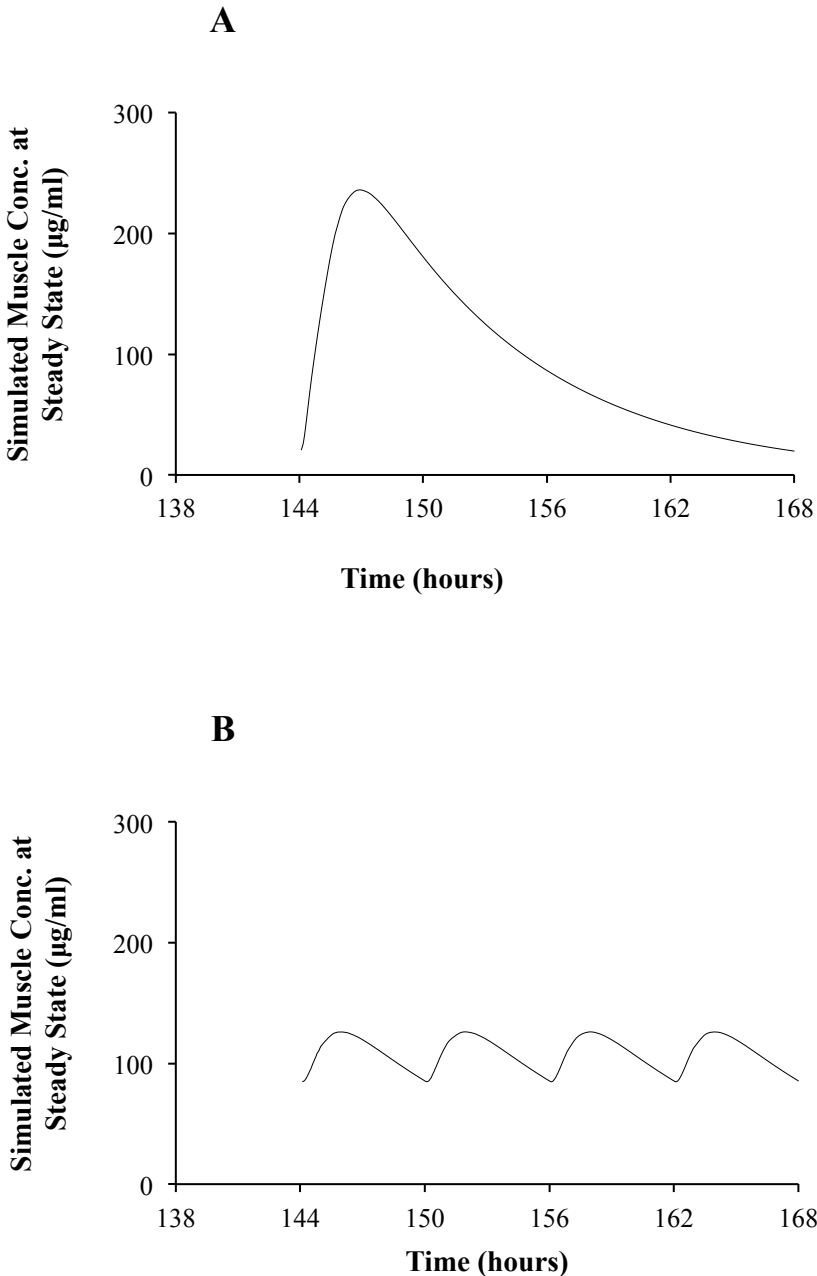


Table 16. The area under the curve at steady state (AUC_{ss}) during 24 hours for plasma, brain, and muscles concentration-time curves following administration of oral CM 20 g/day or 4 x 5 g per day.

	AUC_{ss} ($\mu\text{g}\cdot\text{h}/\text{ml}$) during 24 hours (20 g Once Daily)	AUC_{ss} ($\mu\text{g}\cdot\text{h}/\text{ml}$) During 24 hours (4 x 5 g)
Plasma	2351	2420
Brain	400	412
Muscles	2410	2428

3.2.3.4. Impact of a Sustained Release Dosage Formulation of CM on Plasma and Tissue Levels of Creatine

Since CM is usually given in large doses (i.e. > 20 g/day), those doses are likely saturating the CRT1, limiting the uptake of CM into the various tissues. Due in large part to the inefficiencies in current creatine supplement formulations, there has been growing interest in formulating newer dosage forms with improved absorption and/or distribution.

For this part, we examined the effect of administering a sustained release (SR) formulation of CM on plasma and tissue levels of creatine. In theory, the advantage of an SR dosage formulation is the slower release of creatine from its dosage form, leading to lower concentration of creatine in plasma preventing saturation of the creatine transporter and ultimately better distribution into tissues such as the skeletal muscle and brain. Figure 27 shows plasma, brain, and muscle concentration-time curves following administration of 20 g CM once daily for 7 days as an SR form. Table 17 compares AUC_{ss} and C_{ss} between SR and immediate release (IR) dosage forms of CM given at a dose of 20 g once daily for 7 days.

AUC_{ss} of plasma was slightly smaller following SR form compared to IR CM (2270 vs. 2351 $\mu\text{g}\cdot\text{h}/\text{ml}$, for SR and IR, respectively). In contrast, AUC_{ss} in brain and muscles were significantly higher following administration of the SR form compared to IR form (brain concentrations were 565 and 400 for SR and IR, respectively, and muscles concentrations were 2852 and 2410 $\mu\text{g}\cdot\text{h}/\text{ml}$, for SR and IR, respectively). These data suggest that having a slower and sustained release of creatine is likely to result in higher tissue concentrations compared to IR dosage forms.

Figure 27. (A) Plasma, (B) brain, and (C) skeletal muscle concentration-time curve following administration of 20 g once daily oral CM in SR formulation for 7 days

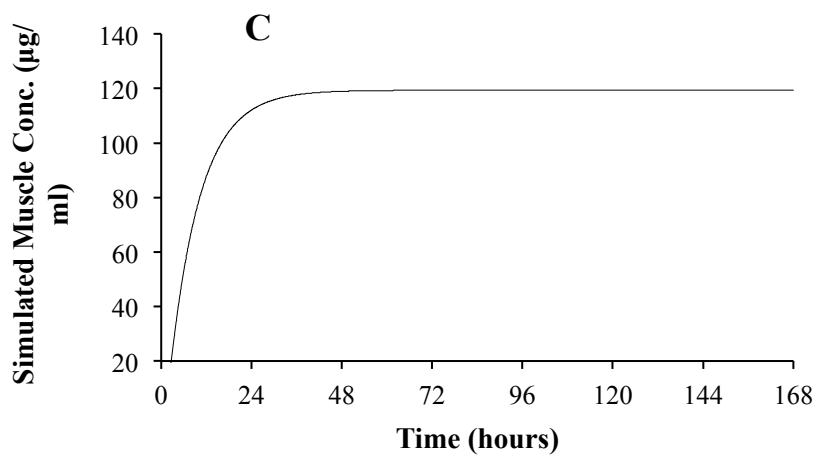
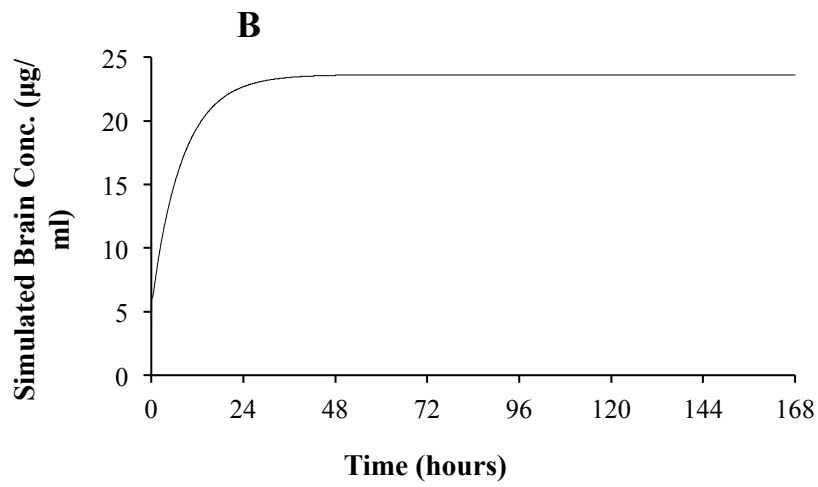
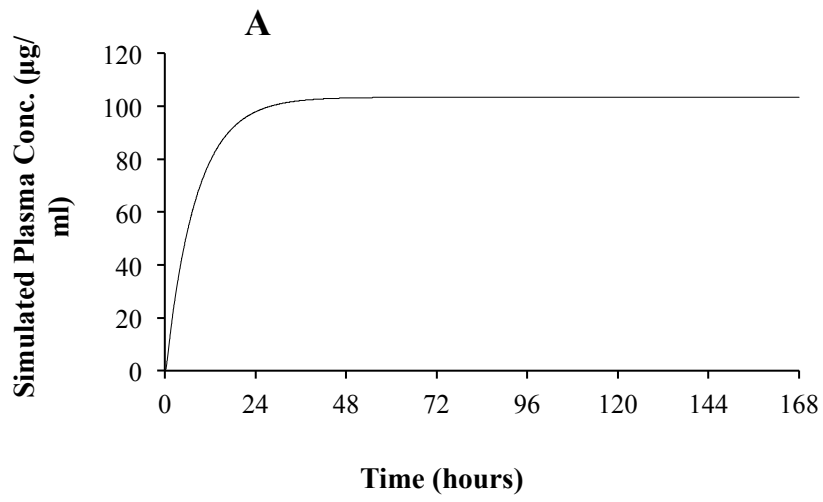


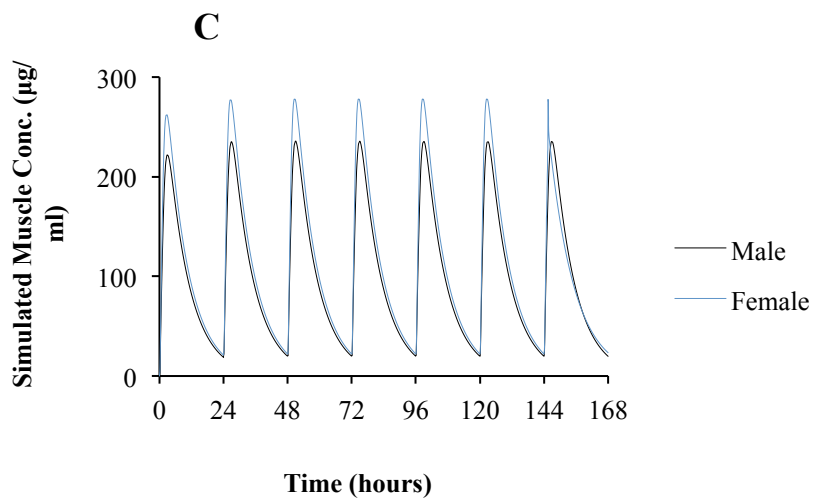
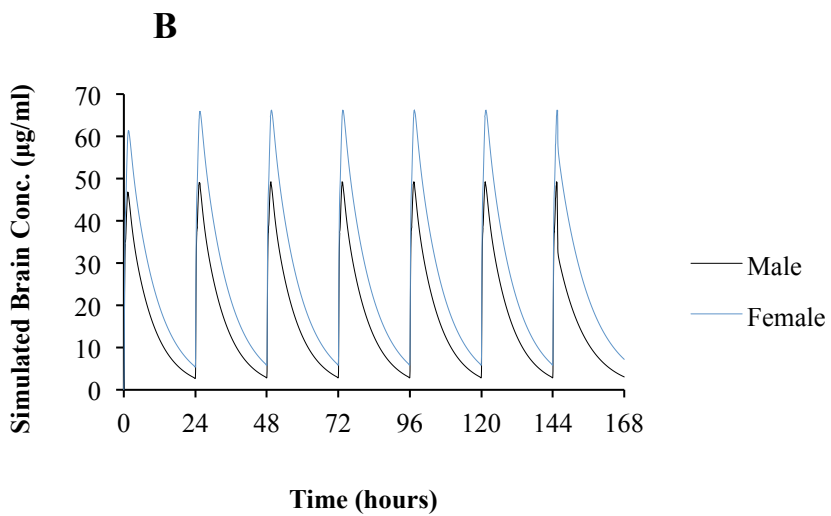
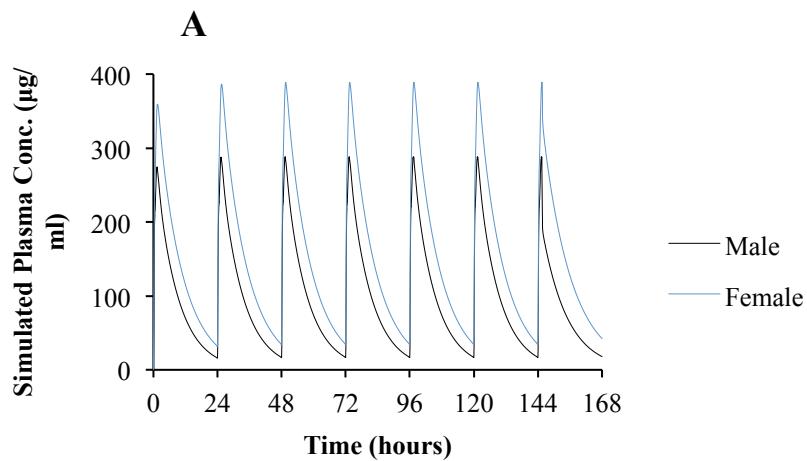
Table 17. Comparison between AUC_{ss} and C_{ss} following administration of 20 g once daily oral CM in SR or IR (suspension) dosage forms for 7 days. $CC_{ss} = AUC_{ss}/\tau$, where τ is the dosing interval (24 hours)

		AUC_{ss} ($\mu\text{g}\cdot\text{h}/\text{ml}$) during one dose interval (24 hours)	CC_{ss} ($\mu\text{g}/\text{ml}$)
SR 20 g once daily for 7 days	Plasma	2270	95
	Brain	565	24
	Muscles	2852	119
IR (suspension) 20 g once daily for 7 days	Plasma	2351	98
	Brain	400	17
	Muscles	2410	100
Relative Bioavailability SR/IR	Plasma	1	1
	Brain	1.4	1.4
	Muscle	1.2	1.2

3.2.3.5. Evaluation of Sex-dependent Differences in Plasma and Tissue Levels of Creatine

Next, we wanted to determine if there are sex-dependent differences in the uptake and tissue distribution of creatine following administration of a single-dose oral 20 g CM. To adjust for the weight differences between male and females (70 vs. 60 kg, respectively), an equivalent dose of 17.14 g was given to female compared to 20 g for male. Predicted female plasma concentrations following administration of 17.14 g CM were higher compared to the predicted male plasma concentration after administration of 20 g dose CM. The resulting C_{\max} in female model was estimated to be 389 $\mu\text{g/ml}$ compared to 288 $\mu\text{g/ml}$ in the male model simulations. Similarly, tissue (muscles and brain) creatine concentrations were higher in female compared to those predicted for male, Figure 28.

Figure 28. PBPK model simulations of (A) Plasma, (B) brain, and (C) muscles concentration-time curves following administration of 20 g once daily oral CM in male (black line) or female (blue line) for 7 days.



3.2.3.6. Physiologically Based Pharmacokinetic Modeling of CHCl, CrC, and CrPyr Following Administration of Single-Dose in Humans

The PBPK model was also used to predict the impact of other creatine salt forms on plasma and tissue levels of creatine. For these simulations, CM was compared to CHCl, CrC and CrPyr, which are newer salt forms of creatine with higher aqueous solubility (708, 52, and 107 mg/ml, respectively). Figure 29A shows simulated plasma concentration-time curves following administration of a 5 g oral dose of CM, CrC, CrPyr, or CHCl dissolved in 450 ml (i.e. 15 ounces). Under these conditions, all the doses administered for the four different creatine forms are in solution. Figure 29B and Figure 29C show the simulated brain and muscle concentration-time curves for the various creatine salts following administration of the same oral dose.

Once the model for a 5 g creatine dose was established, a 20 g oral dose dissolved in 450 ml water of CM and creatine salts was simulated. Under these conditions, CM and CrC are given in suspension form, while CrPyr and CHCl are in solution. Simulated plasma, brain, and muscle concentration-time curves are shown in Figures 30A, 30B, and 30C, respectively.

With a small single oral dose (i.e. 5 g), there was no significant difference between CM and the three salt forms in terms of predicted C_{\max} and $AUC_{0-\infty}$ in plasma and the tissue examined (Figure 29). On the other hand, with a large 20 g dose, Figure 30, C_{\max} in plasma increased by 11.3, 22.3, and 25.0% and $AUC_{0-\infty}$ by 5.0, 25.5, and 26.3% for CrC, CrPyr, and CHCl, respectively, compared to CM, Table 18. In the brain, C_{\max} was increased by 11.2, 22.6, and 25.01% and $AUC_{0-\infty}$ by 5.0, 24.1, and 25.0%, for CrC, CrPyr, and CHCl, respectively. Lastly, in the

muscles, C_{\max} was increased by 6.2, 20.0, and 22.1% and $AUC_{0-\infty}$ by 1.1, 32.0, and 32.3%, for CrC, CrPyr, and CHCl, respectively, Figure 30C.

Figure 29. Simulated (A) plasma, (B) brain, and (C) muscles concentrations-time curve following administration of a 5 g oral single dose of CM, CrC, CrPyr, or CHCl.

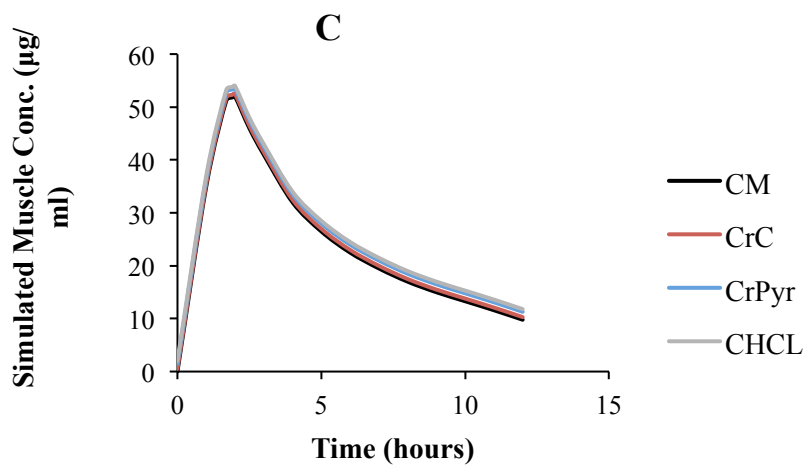
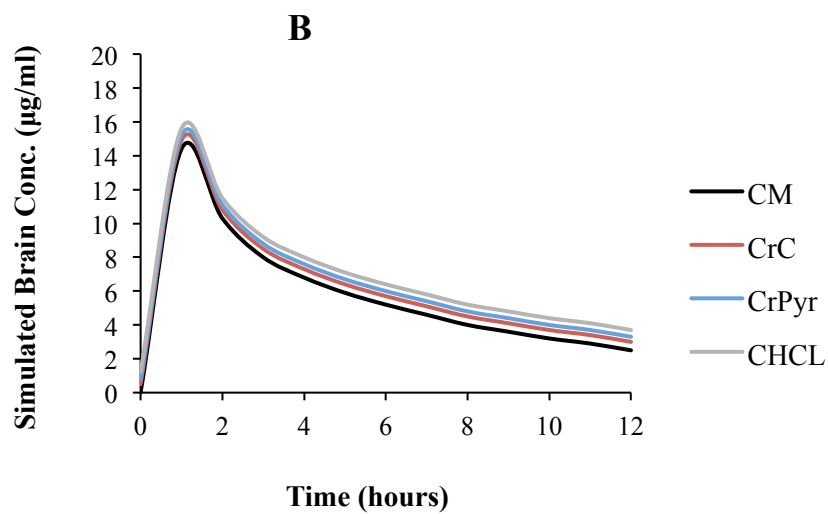
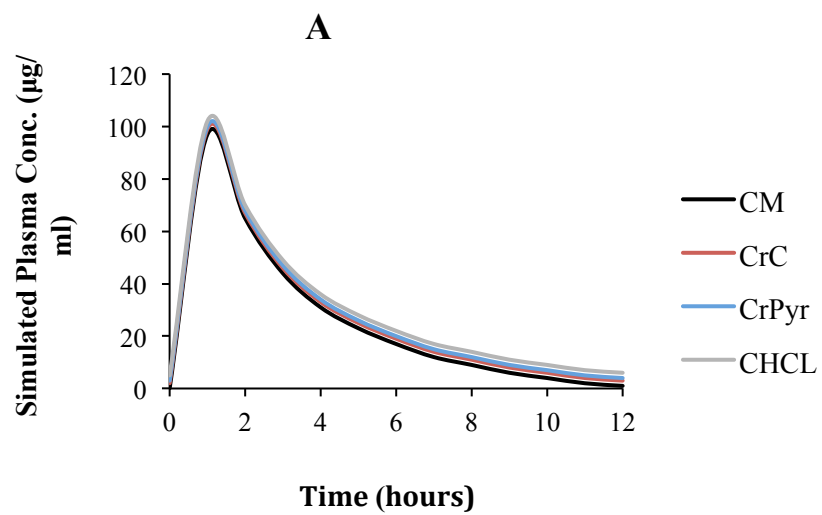


Figure 30. Simulated (A) plasma, (B) brain, and (C) muscles concentrations-time curve following administration of a 20 g oral single dose of CM, CrC, CrPyr, or CHCl.

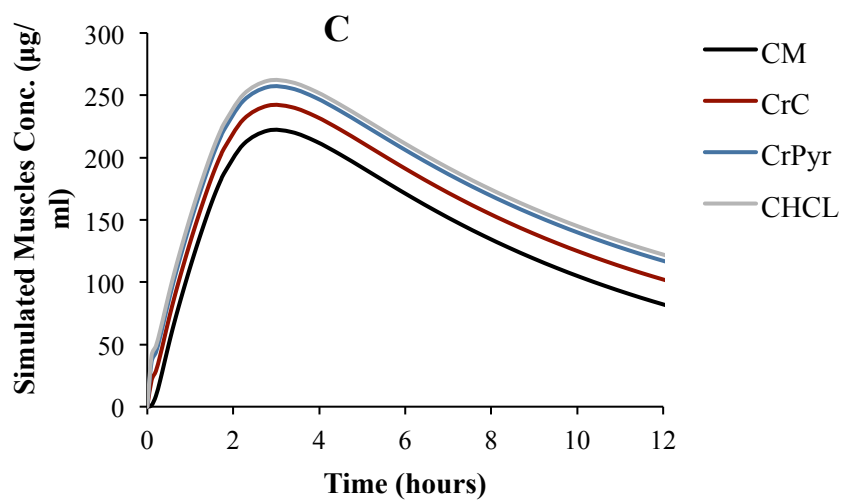
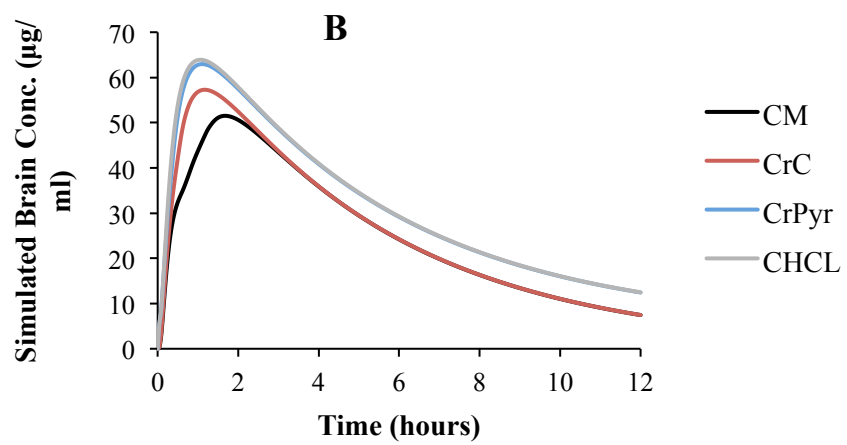
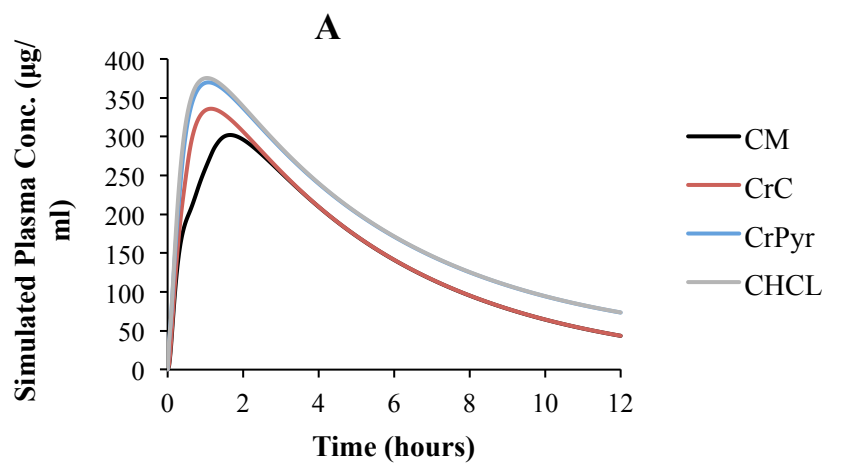


Table 18. C_{\max} and $AUC_{0-\infty}$ following administration of 20 g oral dose of CM, CrC, CrPyr, or CHCl in plasma, brain, and muscle.

		CM	CrC	CrPyr	CHCl
Plasma	C_{\max} ($\mu\text{g}/\text{ml}$)	302	336	369	376
	% Increase compared to CM		11	22	25
	$AUC_{0-\infty}$ ($\mu\text{g}\cdot\text{h}/\text{ml}$)	1761	1849	2211	2224
	% Increase compared to CM		5	26	27
Brain	C_{\max} ($\mu\text{g}/\text{ml}$)	52	57	63	64
	% Increase compared to CM		10	21	23
	$AUC_{0-\infty}$ ($\mu\text{g}\cdot\text{h}/\text{ml}$)	303	317	375	378
	% Increase compared to CM		5	24	25
Muscle	C_{\max} ($\mu\text{g}/\text{ml}$)	222	242	257	262
	% Increase compared to		9	16	18

	CM				
	AUC _{0-∞} (µg.h/ml)	1781	2026	2230	2272
	% Increase compared to CM		14	25	28

3.2.3.7. Physiologically Based Pharmacokinetic Modeling of CHCl, CrC, and CrPyr Following Administration of Multiple-Dose in Humans

The PBPK model was also used to predict the impact of the various creatine salt forms on plasma and tissue levels of creatine following administration of multiple doses (4 x 5 g or 20 g once daily for 7 days). In the case of 4 x 5 g dosing, all compounds are in solution. In contrast, with the 20 g daily dose, CM and CrC are provided as suspensions, while CrPyr and CHCl were in solution form. Figure 31 shows the plasma, brain, and muscle concentrations following administration of 4 x 5 g CM, CrC, CrPyr, or CHCl. Figure 32, shows the plasma, brain, and muscle concentrations of creatine at steady state during one dose interval (i.e. 6 hours).

In contrast, following administration of a large dose once daily (20 g/day), there was significant difference between the different salts forms in creatine levels in plasma, muscle, and brain, Figure 33 and Figure 34. As shown in Table 19, C_{max} in plasma increased by 9.4, 20.1, and 22.2% and AUC_{0-∞} by 24.4, 52.1, and 56.3% for CrC, CrPyr, and CHCl, respectively, compared to CM. In the brain, C_{max} was

increased by 12.1, 21.0, and 26.1% and $AUC_{0-\infty}$ by 31.0, 55.1, and 70.1%, for CrC, CrPyr, and CHCl, respectively. Lastly, in the muscles, C_{max} was increased by 9.1, 15.0, and 17.4% and $AUC_{0-\infty}$ by 20.1, 35.1, and 40.1%, for CrC, CrPyr, and CHCl, respectively, Table 19.

Figure 31. Simulated (A) plasma, (B) brain, and (C) muscle concentration-time curves following administration of a 4 x 5 g oral of CM, CrC, CrPyr, or CHCl for 7 days.

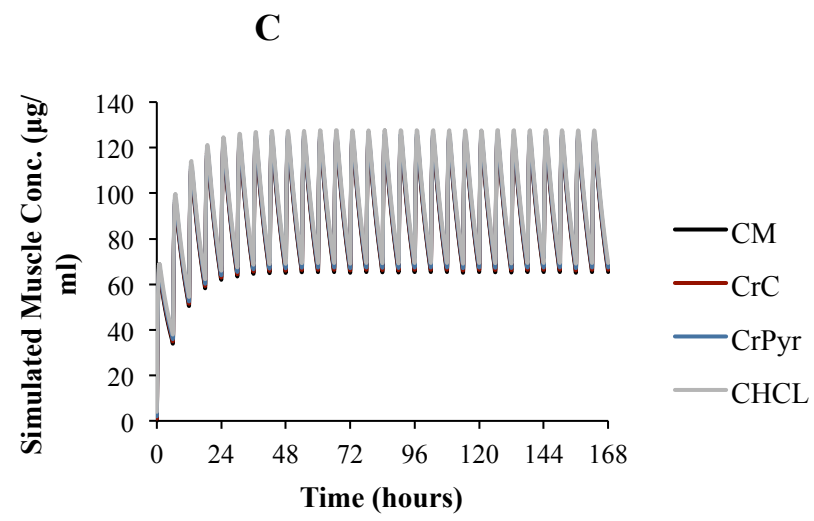
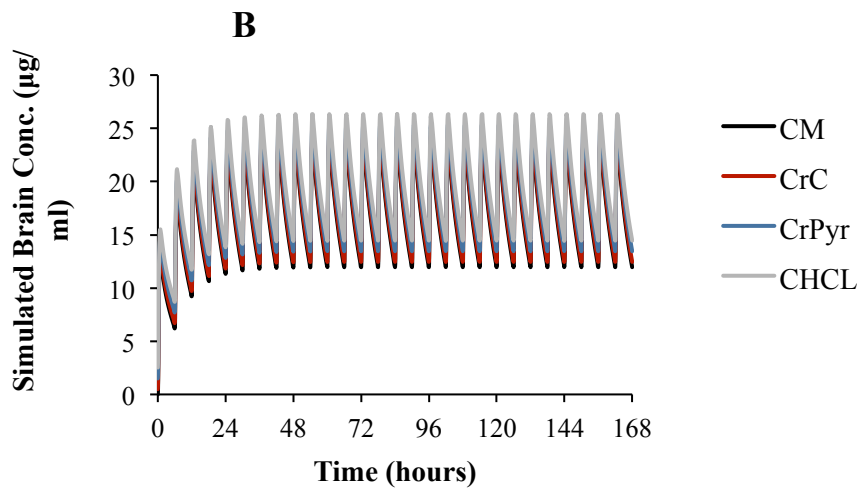
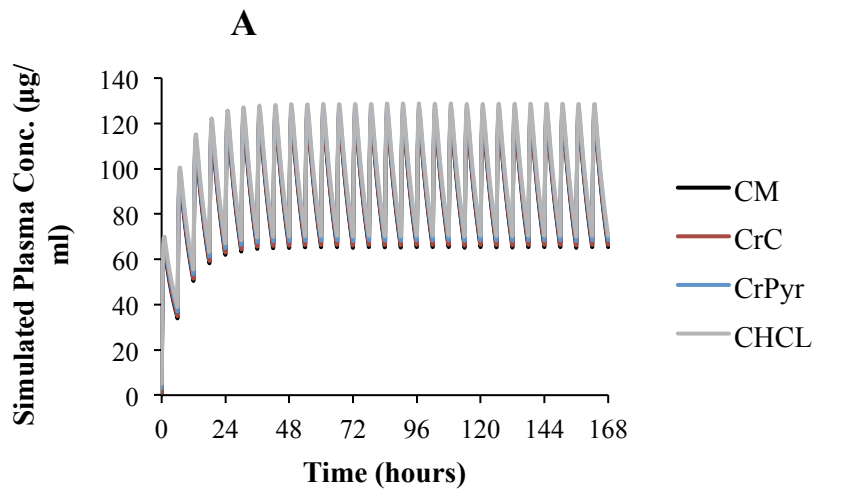


Figure 32. Simulated (A) plasma, (B) brain, and (C) muscle concentrations-time curves at steady state during one dosing interval (6 hours) following administration of a 4 x 5 g oral CM, CrC, CrPyr, or CHCl.

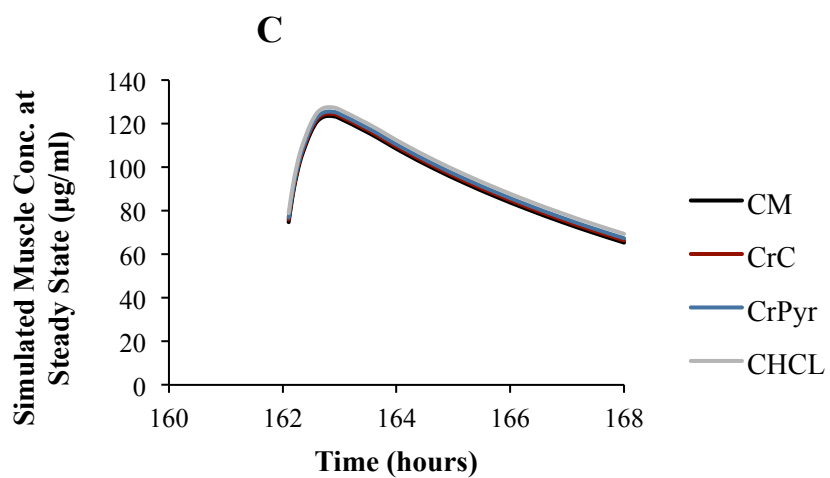
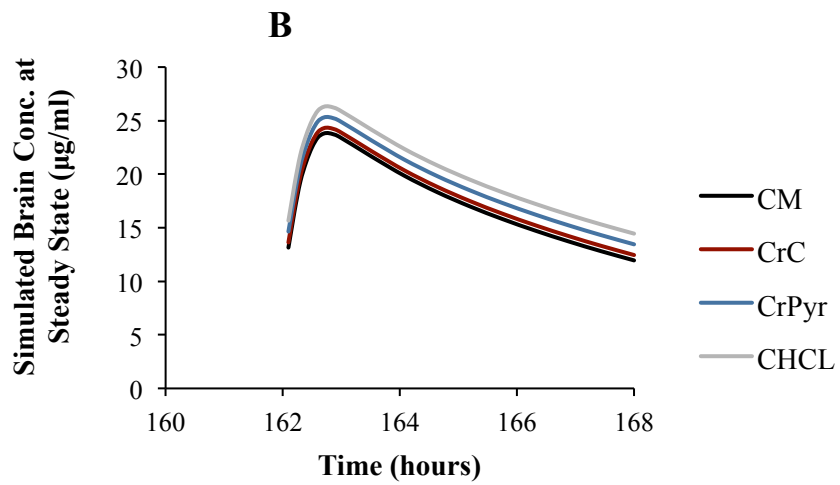
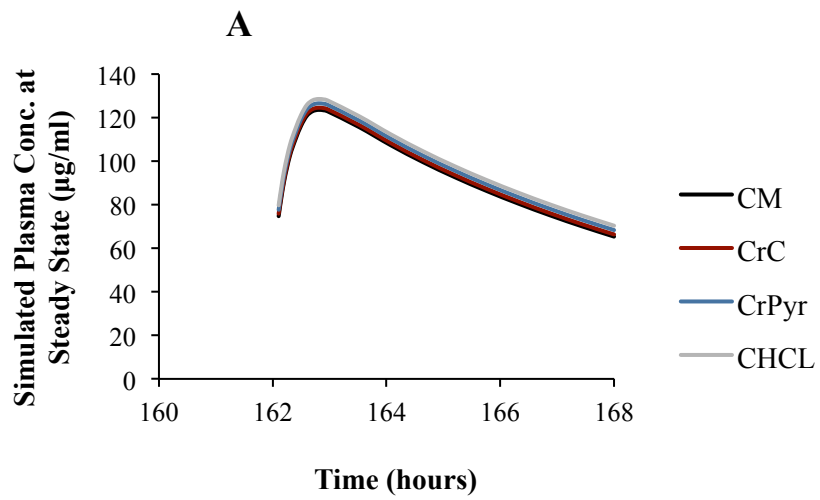


Figure 33. Simulated (A) plasma, (B) brain, and (C) muscle concentration-time curves following administration of a 20 g once daily oral CM, CrC, CrPyr, or CHCl for 7 days.

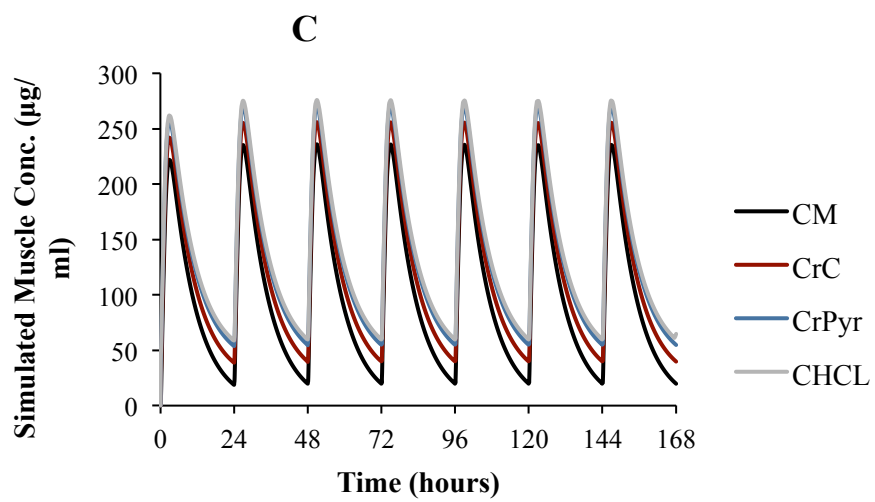
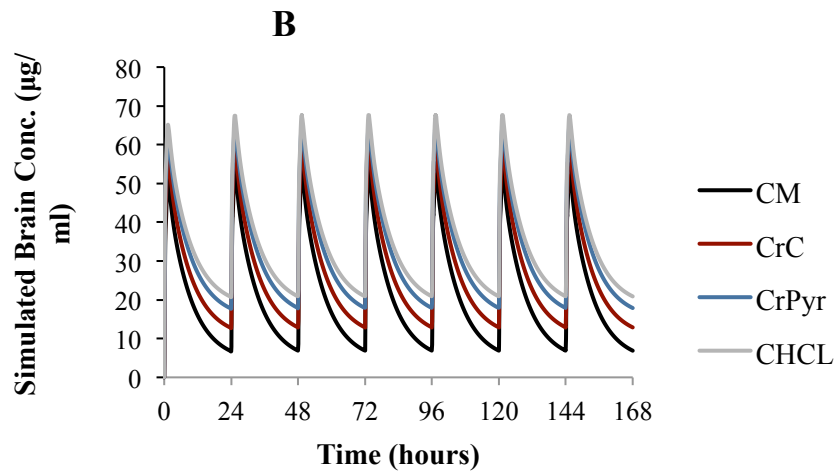
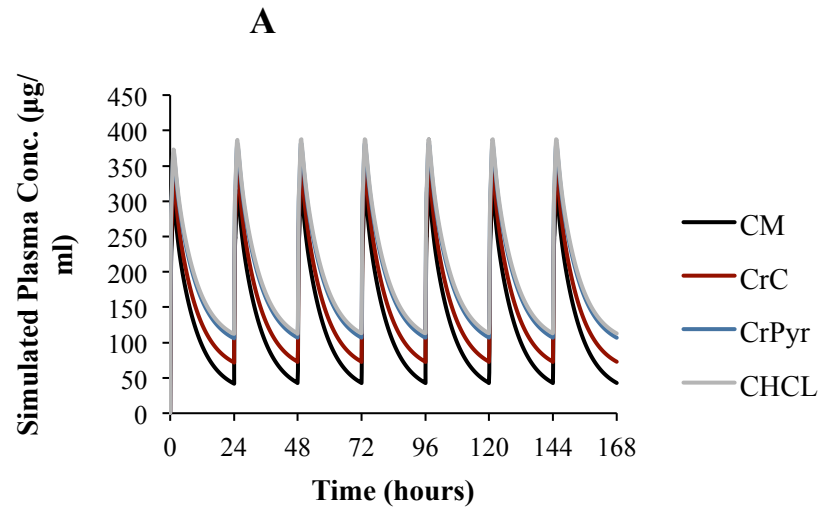


Figure 34. Simulated (A) plasma, (B) brain, and (C) muscle concentration-time curves at steady state during one dosing interval (24 hours) following administration of a 20 g once daily oral CM, CrC, CrPyr, or CHCl.

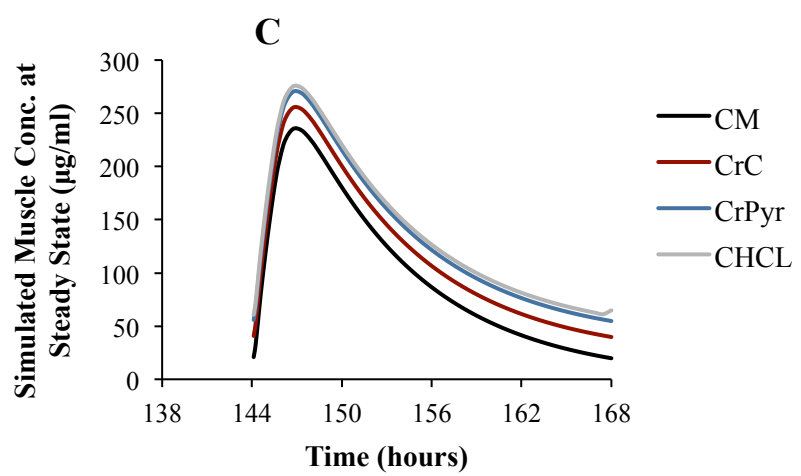
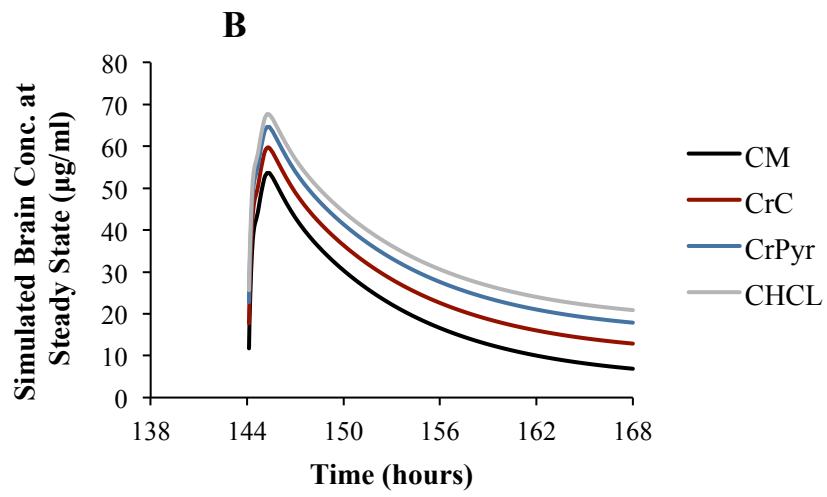
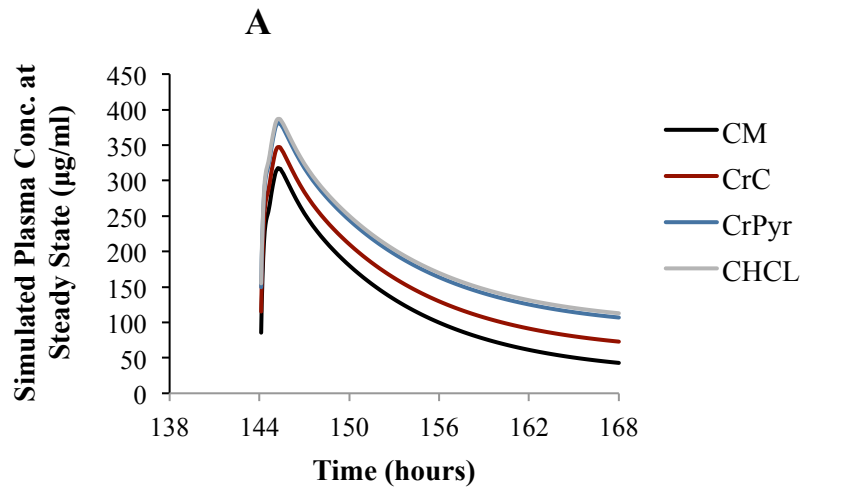


Table 19. C_{max} and AUC_{ss} at steady state during one dosing interval following administration of 20 g oral dose once daily for 7 days of CM, CrC, CrPyr, or CHCl in plasma, brain, and muscle.

	CM	CrC	CrPyr	CHCl
Plasma				
C_{max} ($\mu\text{g}/\text{ml}$)	317	347	381	387
AUC_{ss} ($\mu\text{g}\cdot\text{h}/\text{ml}$)	2351	2915	3550	3668
Brain				
C_{max} ($\mu\text{g}/\text{ml}$)	54	60	65	68
AUC_{ss} ($\mu\text{g}\cdot\text{h}/\text{ml}$)	400	520	620	680
<i>Relative Brain Bioavailability</i>	<i>100</i>	<i>130</i>	<i>155</i>	<i>170</i>
Muscle				
C_{max} ($\mu\text{g}/\text{ml}$)	235	255	270	276
AUC_{ss} ($\mu\text{g}\cdot\text{h}/\text{ml}$)	2410	2892	3253	3374
<i>Relative Muscle Bioavailability</i>	<i>100</i>	<i>120</i>	<i>135</i>	<i>140</i>

3.3. CEE PK Study in Rats

In addition to creatine salt forms, there are newer ester creatine analogs that have improved aqueous solubility and octanol partitioning coefficients compared to CM. For instance, CEE has an aqueous solubility of 970 ± 14.3 mg/ml and partition coefficient of 0.21 ± 0.13 compared to 0.1 ± 0.02 for CM as indicated in previous *in-vitro* permeability studies in Caco-2 model. (147) Based on these findings, studies examining the PK profile and oral bioavailability of CEE in rats were performed.

As CEE is not stable in neutral and basic pH environments and is subject to rapid degradation to CRN, (147) the pH of the prepared CEE solution was adjusted to 4 before administering the compounds to the rats in an attempt to slow the hydrolysis of CEE. For this reason, in the present study, the concentrations of CEE, creatine, and CRN were measured and the levels of all three were combined to provide a more accurate estimation of CEE absorption into the systemic blood compartment.

The plasma concentration-time curve for CEE-¹³C following an iv bolus injection is shown in Figure 35. Figure 36A and Figure 36B show the plasma concentration–time curves for oral high dose (70 mg/kg) and low dose (10 mg/kg) CEE-¹³C. In the plasma, following administration of iv or oral CEE-¹³C, only low concentrations of CEE-¹³C or CRN-¹³C were detected. The levels of creatine-¹³C were below the detection limit.

In contrast, in the muscle and brain, the levels of creatine-¹³C were surprisingly elevated above baseline levels following iv and oral administration of CEE-¹³C, Figure 37. Muscle and brain concentrations of creatine-¹³C were around 15-20 µg/ml and 3-5 µg/ml, respectively (Figures 37A and 37B), which is close to

the levels obtained following administration of iv or oral CM-¹³C. Small amounts of CRN¹³C were found in the muscles samples, Figure 38; however, the levels were below the limit of detection in samples from the brain. The levels of CEE¹³C were below the limit of detection in all the tissue samples examined. The results of this PK study indicate that although CEE was rapidly degraded to CRN, the levels of creatine found in the muscle and brain were comparable to the levels seen after administration of CM. This supports a rapid uptake of CEE from the blood compartment into the various tissues examined.

Figure 35. Plasma CEE-¹³C and CRN-¹³C concentration-time curve following iv administration of CEE-¹³C in adult male rats. Values represent the mean ± SEM. *n* = 4 rats.

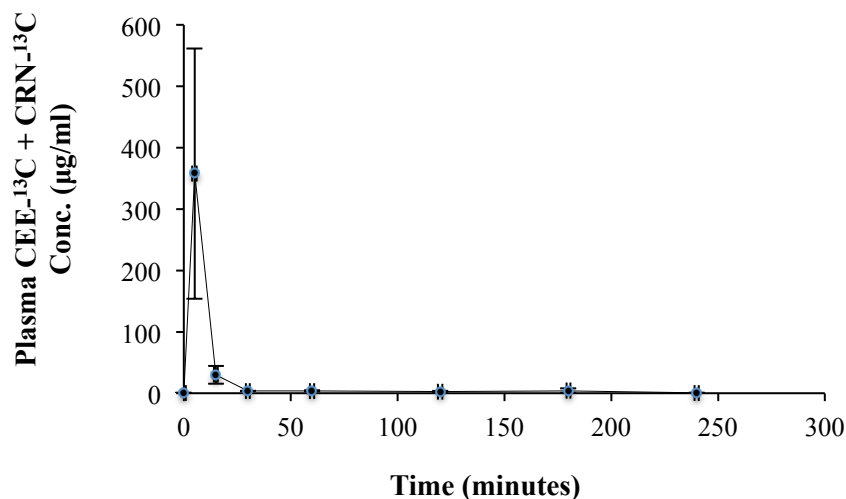


Figure 36. Plasma concentration–time curves following administration of (A) high dose (70 mg/kg) or (B) low dose (10 mg/kg) oral CEE-¹³C. Values represent the mean ± SEM. *n* = 4 rats

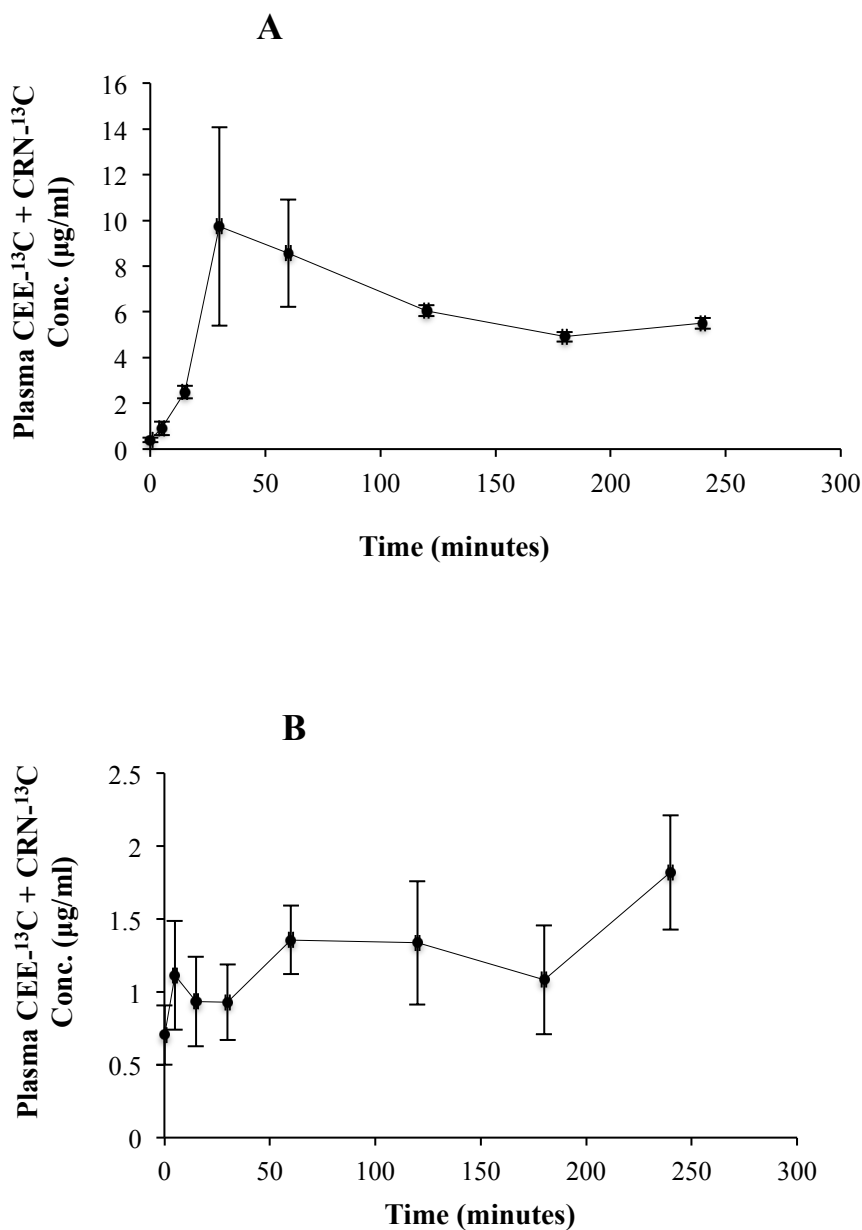


Figure 37. (A) Muscle and (B) Brain concentrations of Creatine-¹³C 4 h after administration of iv or oral dose of CEE-¹³C. Values represent the mean ± SEM. *n* = 4 rats. Creatine-¹³C content in muscle and brain samples from non-treated rats was below detection limits (0.5 µg/g tissue). ns= non significant, * *p* < 0.05, ** *p* < 0.01, *** *p* < 0.001, **** *p* < 0.0001 compared to levels in non-treated group (one-way ANOVA). BDL = below detection limit

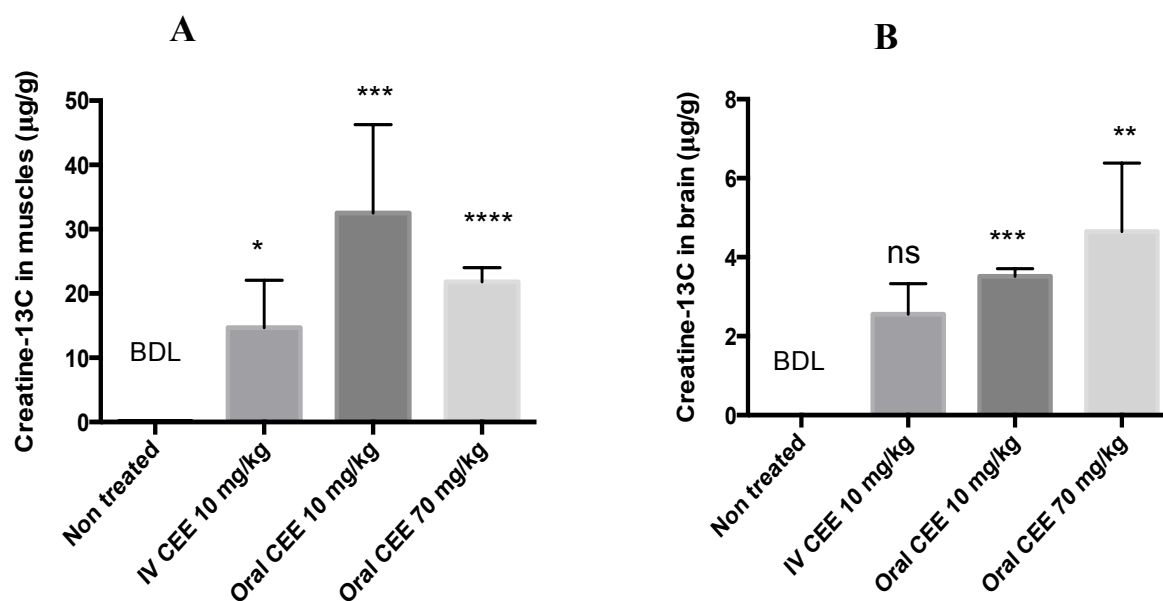
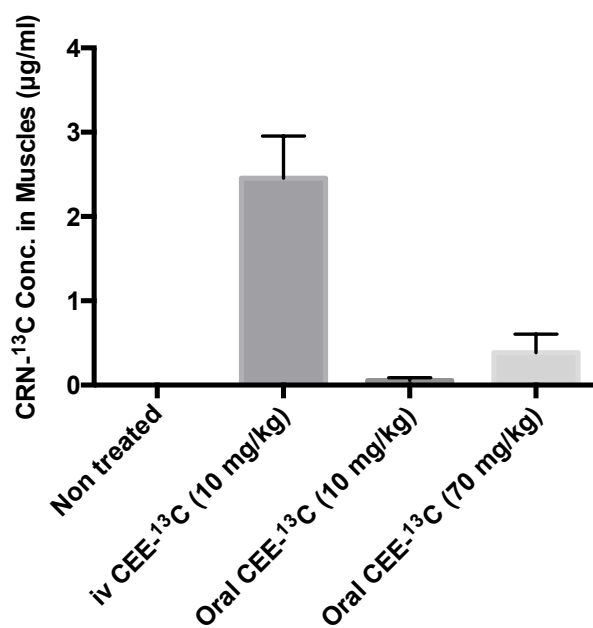


Figure 38. Muscle concentrations of CRN-¹³C 4 h after administration of iv or oral CEE-¹³C. Values represent the mean ± SEM. CRN-¹³C content in muscle samples from non-treated rats was below detection limits (0.5 µg/g tissue). *n* = 4 rats.



Chapter 4. Discussion

Creatine, mostly in the form of CM, has been used widely by athletes and bodybuilders as an ergogenic aid to improve performance and muscle mass. (9) Creatine supplementation has been reported to increase muscle creatine by approximately 5-30%. (61) While there has been much research predominately devoted to understanding the uptake of CM into muscle cells and to explore the effects of CM on exercise and performance, there have been few studies investigating the PK profile and oral bioavailability of CM supplements.

Initial evidence reported by Chanutin (172) and later confirmed by Deldicque, (167) indicates that intestinal absorption of exogenously administered CM is nearly complete. However, in these studies, CM was administered orally in low doses (2 g) to healthy volunteers, and the increases in tissue levels of creatine combined with the increases in CRN elimination in the urine were used to provide an assessment of the oral bioavailability of CM. (167, 172) Both studies claimed complete absorption of orally administered CM based on increased creatine in blood and tissue and the absence of creatine or CRN observed in fecal samples. However, there are three major limitations in these studies. First, the use of urinary CRN levels as an index of the amount of CM absorbed from the GIT assumes that all urinary CRN is a result of the conversion of creatine in the various tissues to CRN, which is then readily excreted into the urine. However, this approach is not accurate and it neglects to account for potential creatine utilization by the intestinal epithelial cells and the bacterial flora in the GIT. (14, 141, 173, 174) This ability to acquire and metabolically process creatine within the intestine provides a potential source of CRN in the GIT. Thus the conversion of creatine to CRN within the lumen of the GIT, and its subsequent absorption into the bloodstream would result in a potential overestimate of the amount of creatine that has been systemically

absorbed. Secondly, potential issues such as gastric degradation, site-dependent intestinal absorption and incomplete dissolution of creatine solid dosage forms, outlined by McCall and Persky, (175) are all likely to result in less than complete absorption of creatine. The final consideration regarding the early studies by Chanutin and Deldicque (167, 172) is the lack of CM iv arm, which is required to accurately determine oral bioavailability.

Given the physicochemical properties of CM, we hypothesized that the oral bioavailability of CM is low. In the present study, CM-¹³C was given as either oral or bolus iv dose. In our study, iv administration of CM-¹³C resulted in a rapid distribution phase, in which creatine-¹³C was distributed out of the central (blood) compartment into the different tissues and this was followed by a slower terminal elimination phase. This finding is consistent with the known distribution kinetics of creatine into the muscles, brain, and other tissues. (14) There was a slight increase in plasma creatine-¹³C observed at the last time point sampled following iv administration of CM-¹³C. Multiple peaking PK can occur due to a variety of both formulation and physiological factors. (176) For the iv administration route, the most likely contributor to multiple peaking phenomena would be enterohepatic recycling. (176) As the physicochemical properties and metabolic pathway for creatine are not supportive of biliary secretion, (13) it is unlikely that enterohepatic recycling of creatine is occurring in the present study. Given the rapid distribution of creatine into skeletal muscle and relatively the large depot site it represents, the plasma creatine levels observed likely reflect the slow and sustained release of creatine from these deep tissue sites.

Oral administration of CM-¹³C resulted in dose-dependent increases in plasma creatine concentrations. C_{max} of creatine-¹³C in the plasma increased 10 to 25-fold from baseline levels (<0.5 µg/mL). The plasma creatine-¹³C profile observed in the present study was similar to those previously reported. (166, 167, 169) Despite the

substantial increase in plasma creatine-¹³C, there was no detectable increase in CRN-¹³C in the present study. There are conflicting reports regarding the increase in CRN following oral administration of CM. While Schedel and colleagues reported increases in plasma CRN following oral CM administration, (169) others have reported no change in blood CRN. (166) It should be noted that those studies reporting increases in plasma CRN following oral CM administration were using either large doses (20 g) of creatine (169) or extended multi-day exposure. (167) Even under these conditions the increases in plasma CRN were small in comparison to the increases in plasma creatine; thus the conversion of creatine to CRN was not considered to play a significant role in creatine elimination.

In the present study, dose-dependent effects on oral bioavailability of CM were examined by administering oral CM-¹³C at both low (10 mg/kg) and high (70 mg/kg) dose. As CM has relatively low aqueous solubility (around 17 mg/ml), the conditions selected for the high dose reported here were designed to more closely represent the standard dosing used in therapeutic applications in which large daily doses (≥ 20 g) of CM are more likely administered in suspension form. For the high dose used in this study, which was administered in suspension form, the oral bioavailability of CM-¹³C was around 15%. As the high dose used in this study is equivalent to approximately 1 g dose in humans, the oral bioavailability of the high doses of CM used in humans (10-30 g) could be even lower. On the other hand, the oral bioavailability of low doses CM-¹³C, which was administered as a solution, was 48%. The data reported in the present study represent a significant departure from the relatively complete oral absorption of CM claimed in earlier reports and suggest that oral bioavailability of CM is low and far from complete. (167, 172)

While suggested in various human studies, (171, 177) this study was the first to assess dose-dependent changes in oral bioavailability of CM. The difference in oral bioavailability of high and low dose CM-¹³C could be due to two reasons. The

first consideration is the saturation of the CRT1 transporter with high dose CM. Given the known CRT1 kinetics, (178) it is likely that concentrations of creatine in the GIT would be well above those required for saturation of CRT1 at even the lowest doses of CM administered. The second consideration regarding oral administration of high doses of CM is the incomplete dissolution of CM dosage form under most dosing conditions, and this might explain the dose-dependent CM oral bioavailability. Given the low aqueous solubility of CM, which is around 17 mg/mL, (128) and the high doses required for CM supplementation (i.e., around 20+ g/day), a suspension is the likely form of CM being administered. In the present study, the 70 mg/kg dose was administered as a suspension. Under these conditions, oral bioavailability was even less than observed with the 10 mg/kg dose, which was administered in solution form.

Tissue concentrations of creatine-¹³C following administration of oral CM-¹³C were also assessed in the present study. The tissues examined in the present study were muscles, brain, and blood cells. The highest levels of creatine were found in the muscles followed by the brain and the blood cells. The distribution profile of CM-¹³C and the fact that creatine-¹³C accumulated in high concentrations in the muscles followed by the brain is consistent with previous studies. (13) The concentration of creatine¹³C in the muscles was similar (around 15 µg/g) following administration of iv or oral (either high or low dose) CM-¹³C. This finding could be explained by the saturation of CRT1 found in the muscles by high levels of creatine preventing further uptake of creatine-¹³C into the muscles.

The results from our *in-vivo* PK study of CM in rats suggest that the oral bioavailability of CM was far from complete. Given the fact that low doses of CM were used in the current study (the high dose given is equivalent to around 1 g dose in humans) and as most therapeutic indications require rather large doses (>150 mg/kg), the actual bioavailability of such doses might be even lower and may be

limited by either physiological and/or formulation factors. These studies suggest that newer forms of creatine with improved physicochemical properties and/or improved dosage formulations of creatine might be superior to CM.

The *in-vitro* permeability of CM in Caco-2 and MDCK-*MDR1* cell lines was also assessed in the present study. Caco-2 and MDCK-*MDR1* are two of the most commonly used cell lines for *in-vitro* permeability testing of compounds. (165) Permeability in both cell lines is well documented to correlate with human intestinal absorption and both cell lines are equally suited and commonly used in Biopharmaceutics Classification System (BCS) intestinal permeability ranking in pharmaceuticals industry. (165) Cell line models for *in-vitro* permeability testing have the advantage of being less time- and cost- intensive, and are easier to establish and maintain compared to primary cell cultures. (179)

Caco-2 cells are epithelial cells isolated from human colorectal carcinoma and is considered to be the *in-vitro* gold standard for assessing the intestinal permeability of drug candidates. (165, 180, 181) Under normal conditions of cell culture, Caco-2 cells spontaneously differentiate to mature cells to form tight monolayers. (182) Although Caco-2 cells originated from the human colon carcinoma, they acquire many features of absorptive intestinal cells during culture, such as microvillous structure, hydrolysis and cytochrome P450 (CYP) enzymes and carrier mediated transport systems (e.g. P-glycoprotein (P-gp) encoded by MRD1 and multidrug resistance-associated protein 2 (MRP2)). (183) In addition, adjacent cells adhere through tight-junctions formed at the apical side of the monolayer, which can discriminate the transcellular and paracellular transport of drugs across the epithelial layer. (183) The resemblance of Caco-2 cell monolayers to intestinal cells yielded a high expectation of good *in-vitro–in-vivo* correlation. (183)

MDCK-*MDR1* cells are canine kidney epithelial cells that have been transfected with human P-gp (MDR1). (184) When grown in culture, MDCK cells differentiate into columnar epithelium and form tight junctions in a shorter period of time than Caco-2 cells (3 days vs. 21 days). (184) In addition to the use of MDCK-*MDR1* cells as an *in-vitro* model to study intestinal permeability, these cells are also commonly used to screen for BBB permeability. (185) Although MDCK-*MDR1* cells are not derived from human endothelial brain cells, this cell line is unique in that it expresses high levels of human P-gp and has high trans-epithelial electrical resistance, making it a standard *in-vitro* model for assessing brain penetration and BBB permeability. (186) In the present study, the permeability of CM was examined in both cell lines, Caco-2 and MDCK-*MDR1* to provide an initial assessment of intestinal and BBB permeability of the creatine compounds.

For the permeability studies, three fluorescent markers were used as permeability standards to assess the integrity of the monolayers, identify any differences in baseline permeability in the cell culture models, and to ensure that the monolayers were not altered by the creatine compounds at the concentrations examined. Fluorescein is a low molecular weight, hydrophilic molecule, with low permeability values in Caco-2 assay, and was chosen as a low permeability standard to assess passive diffusion across the monolayers. On the other hand, rhodamine 800 is a low molecular weight, lipophilic molecule that is a reported transport substrate for the P-glycoprotein drug efflux transporter expressed in Caco-2 and MDCK-*MDR1* cell culture models. (187) The final fluorescent probe, IR dye 800 CW PEG, is a large molecular weight compound (approximately 35K molecular weight) and is used as a paracellular diffusion permeability marker. Results from these studies indicate that monolayers from Caco-2 and MDCK-

MDR1 cell lines were confluent and intact and exposure to the creatine compounds did not alter the integrity of the monolayers.

In the present study, the permeability of CM was low in Caco-2 cells and was dose-dependent, with the lower concentrations (10 μM) having higher permeability compared to high concentrations of CM (100 and 1000 μM). The result of this study is the first evidence of dose-dependent permeability of CM in Caco-2 cell line. The concentration dependency observed with CM suggests transporter uptake of CM through Caco-2 cells as opposed to passive diffusion. The observed dose-dependent effects could be attributed to saturation of CRT1 with high concentrations of CM preventing further uptake of CM across the cells. The fact that lower concentrations of CM have improved permeability compared to high concentrations is consistent with our CM *in-vivo* PK study, in which a lower dose of CM has higher oral bioavailability compared to a higher dose, which might also be explained by the saturation of CRT1 by high concentrations of CM.

The low CM permeability in Caco-2 cells in the present study is also in agreement with the relatively low permeability of radiolabeled CM in Caco-2 monolayers reported previously by Dash and colleagues, (146) and to the low permeability of CM and the various creatine salts forms (CHCl, CrC, and CrPyr) in the same *in-vitro* model. (128, 147) Of note, the present study focused on the absorptive transport/permeability of creatine compounds. However, the previous studies by Dash and colleagues, examined the permeability of radiolabeled CM in both apical to basolateral (a-b) and basolateral to apical directions (b-a) were examined. Whereas the permeability of CM was low in both directions, the b-a transfer of the compound was significantly greater than the a-b transfer. In this study, the potential involvement of drug efflux transporters, such as P-gp, was excluded, suggesting the possibility of the interaction of CM with other transport systems or the presence of CRT1 in the basolateral side. (146)

Permeability of CM in MDCK-*MDR1* monolayers was also low but did not show a strong dose-dependency effect as in the case with Caco-2 cells. The permeability of all the three CM concentrations examined was in the same range. However, the permeability coefficients vs concentration data suggest there is a decrease in permeability but only at the highest concentration of CM (1000 μ M). The reason for the lack of concentration dependency in MDCK-*MDR1* compared to Caco-2 cells is unknown but it might be due to the presence of more CRT1 at the BBB as compared to the intestinal epithelial cells. An alternative possibility is that the Caco-2 have reduced paracellular diffusion than the MDCK-*MDR1* model as indicated by the difference in permeability to both small and large hydrophilic permeability markers in the two culture models.

Additional creatine compounds were examined for permeability in the Caco-2 and MDCK-*MDR1* in-vitro models. In this regard, the permeability of CC, a creatine analogue that has been used in various therapeutic applications to augment creatine content in tissues was lower in both the Caco-2 and MDCK-*MDR1* models compared to the permeability of CM. Based on these initial permeability studies CC would not be expected to provide improved bioavailability compared to CM.

Based on the preclinical data obtained from *in-vivo* and *in-vitro* experiments, simulation of rat and human PK profiles of CM were performed via PBPK modeling. The basic inputs required to run the simulation such as the physicochemical properties of the compound were obtained from previously published studies (e.g. solubility and LogP) or by using the built-in GastroPlus ADMET predictor. The permeability coefficient used in the current simulations is obtained from our *in-vitro* permeability experiments, and is the permeability coefficient for the 10 μ M CM concentrations in Caco-2 cells, which was the highest permeability in the Caco-2 model. Using the permeability coefficient for

10 μM CM resulted in better prediction accuracy and better fitting between simulated and observed data in comparison with the lower permeability coefficients of the higher concentrations of CM (100 or 1000 μM). Ideally, reliable experimental data for all physicochemical parameters values, including an estimate of effective intestinal permeability in the species simulated should be available. However, in drug discovery and early development this is rarely the case. Because experiments to measure effective permeability (P_{eff}) are time consuming and expensive, actual P_{eff} values in human or animals are rarely available. Data from Caco-2 or MDCK cell cultures, or artificial membranes are most often available prior to “first in man” experiments, and such data can be used, provided a valid correlation is developed between P_{eff} in human (or other species to be simulated) and the experimental model.

Using GastroPlus software, we were able to model the plasma concentration-time profile for CM in rats with good agreement to the observed values. In addition, the PBPK model was also able to predict concentrations of creatine in various tissue compartments. PBPK modeling is a tool that can be used to predict absorption and distribution of compounds and the tissue concentration-time profiles for the various compartments in the model. PBPK models provide a quantitative means of extrapolating absorption, distribution, metabolism, and excretion (ADME) properties across species by having the ability to substitute species-specific physiological and biochemical parameters into the model. (188) Based on the established PBPK model for CM and its similarities to the observed values from the oral bioavailability studies performed in the rat, extrapolation of the model to examine the impact of different creatine formulations and dosage strategies on creatine plasma and tissues concentration in humans was performed (188) The main advantages of PBPK modeling in comparison with classical PK models is the ability to predict simultaneous time-concentration curves for a

compound in any organ or tissue and the incorporation of anatomical and physiologic information as well as chemical specific *in-vitro* derived parameters (i.e. K_m or V_{max} of transporter). (188)

The PBPK model was initially optimized and validated in rats by using the obtained preclinical data. For the present study, the reliability of the model was tested by simulating bolus iv (10 mg/kg) injection and oral (70 mg/kg) CM in rats. The resultant PK parameters were compared to the observed values. While our model predictions will require additional validation, there was reasonable agreement of the PBPK model of CM in plasma to the observed iv and oral CM (R^2 of 0.99 and 0.84, respectively). According to the literature [31, 34], less than a twofold error was considered to be an accurate prediction using PBPK modeling. All the simulated PK parameters were within 1.6-fold of the observed values for iv and oral CM in rats, indicating that the current PBPK model provided high prediction accuracy.

There is increasing interest in different salt forms of creatine with improved solubility parameters over CM. (128, 145) One of the newer salt forms of creatine, CHCl, has an aqueous solubility of around 700 mg/mL. The markedly enhanced solubility of CHCl to that of CM suggests that improved oral absorption and more efficient dosing formulations should be possible. Indeed, based on the PBPK model simulations in rats, substantial increases in blood and tissue levels of creatine are likely following oral supplementation with CHCl compared to CM. However, more investigation regarding the use of different salt forms of creatine in humans should be performed.

Given the agreement of the established PBPK model with observed PK values for CM in rats, our model was further extrapolated to humans. A literature review was conducted to collect *in-vivo* creatine concentrations in plasma or tissue

following administration of oral single- or multiple-dose CM in humans. The muscle and brain tissue were chosen for our simulations, as these two tissues are the targets for creatine supplementation estimates and predictions of creatine content in the muscle and brain were of interest. The effects of CM supplementation on muscle creatine levels and exercise performance in young adults have been extensively studied and reviewed. (189-191) As with muscle creatine, increasing brain creatine may confer benefits to athletes, non-athletes, older adults, and in certain brain pathologies and disorders. (192-194) Relative to skeletal muscle, only a small percentage of total body creatine is in the brain (i.e. <5%). However, the brain is highly metabolically active, responsible for 20% of basal metabolism, and, as in skeletal muscle, brain creatine is essential for energy production.

It is commonly accepted that a loading phase of 20 g/day (4 x 5 g) for 5 days followed by a maintenance dose of 5 g/day should increase muscle total creatine concentrations by approximately 20– 30%. However, the dosing strategy required to optimally increase brain creatine levels has yet to be established, and this is largely due to limited data that directly measures the concentration of creatine in the brain following exogenous creatine administration. While direct measurement of muscle creatine can be accomplished through analysis of tissue obtained from muscle biopsies, assessment of brain creatine is more difficult. (195) Direct measurement of brain creatine pre- and post-creatine supplementation can be accomplished in animals, but species differences in creatine uptake reveal the complications of generalizing data from this experimental model to humans. (196, 197) Brain creatine can be assessed using proton or phosphorous nuclear magnetic resonance spectroscopy (^1H -NMR and ^{31}P -NMR, respectively), but this is costly and not widely available. These complications may have contributed to the fact that only a small number of human studies are available in which changes in brain

creatine levels were assessed pre- and post-creatine supplementation. In addition, brain creatine content seems to be highly site-specific, (170, 195, 198) which renders it difficult to directly compare studies measuring creatine in different brain areas.

Available published data on creatine supplementation in humans were limited to either plasma or skeletal muscle concentration of creatine following administration of single and multiple dose of CM in humans and to the change of total creatine, PCr, or free creatine in the brain following exogenous administration of CM by using magnetic resonance spectroscopy (MRS) analysis. However, little to no data were found regarding the actual concentration of free creatine in the brain following exogenous supplementations of CM in rodents or humans. Our predicted plasma concentration-time curves and PK values following single- and multiple-dose CM were compared to previously published data. All the fold errors of the predicted and observed PK parameters in plasma and muscles were less than 1.6, which indicated that the human model extrapolated from rats was successful and the model was able to accurately simulate the plasma and muscle concentration-time profile of CM.

CM is usually consumed in very large doses. Manufacturer's instructions and athletes' use of CM follows a dosing regimen of a "loading" phase of 20 g/day (4 x 5 g) for 5 days followed by a maintenance dose of 3 to 5 g/day. On the other hand, therapeutic applications of CM often require doses that are larger than 20 g/day. Given the aqueous solubility of CM, a dose of 20 g should be dissolved in more than 1000 ml of fluid to ensure the dose is completely solubilized. As a result of this, most CM products are taken as suspension and would be incompletely absorbed in the GIT. In most of the published clinical trials, CM was given as a single large daily dose (20 g/day) in an attempt to increase brain levels of creatine

to achieve beneficial effects.

In the present study, CM profile was simulated using two different dosing strategies, 20 g/day given as a large dose in suspension form once daily, or 20 g/day divided in 4 equal doses (5 g each dose four times daily) given in solution form. Steady state levels of creatine in plasma and tissue (muscle and brain) under these dosing strategies were compared. A large 20 g dose of CM resulted in higher C_{\max} in the plasma and the tissue compared to smaller 5 g doses. When the AUCs for the plasma and the tissue were compared the total exposure to creatine was slightly lower in plasma and tissue with the large dose compared to the small divided doses. Given the known PK of creatine and the known creatine transporter kinetics, dividing the dose of CM into 4 smaller doses would be expected to increase the levels of creatine in the tissue more efficiently than taking 20 g CM as a whole, as the smaller doses would keep the levels of creatine in the plasma at steady state at lower concentrations that would prevent the saturation of the creatine transporter allowing further uptake of creatine into the tissue.

Various strategies have been widely investigated to enhance the bioavailability and tissue distribution of drugs with poor oral bioavailability. In the case of CM, in which absorption and bioavailability is limited by both formulational and physicochemical properties, two strategies can be undertaken to improve oral absorption and tissue uptake of creatine, using different dosage formulations (i.e. sustained release dosage forms) or finding alternative forms of creatine with improved physicochemical properties.

The importance of the formulation and its impact on oral absorption is often under appreciated. In the ideal case, a drug or dietary supplement would be applied *in-vivo* at exactly the therapeutic concentration and would precisely target the desired tissues and cells. However, drug delivery is not easily controlled. Drug

release rates, cell- and tissue-specific targeting, and drug stability are difficult to predict. (199) To address these limitations, drug delivery systems (DDS) have been designed using a wide array of materials and chemical strategies. DDS are defined as technologies that are designed to improve the specificity of therapeutics by stabilizing them in vivo, controlling their release, and localizing their effect. (199) One important class of DDS is controlled release (CR) or SR systems. SR formulations have special coatings or ingredients that control how fast the drug is released from the pill into the body. (134) The main advantage of the SR formulations is its ability to release the compound or drug at a predetermined rate in order to maintain a constant drug or compound concentration for a specific period of time as opposed to immediate release dosage forms, which result in greater peaks and troughs in plasma concentrations. (134) Additional advantages of SR formulations include improving adherence by reducing the total number of required doses. However, SR dosage formulations engineering is challenging and costly compared to IR dosage forms. Furthermore, use of SR formulations for dietary supplements is complicated by the amount of active compound required.

In the case of CM, which is consumed in large doses, high plasma concentrations would likely saturate the transporters limiting the uptake of creatine into the various tissues. The use of a SR formulation of CM is likely to keep the plasma concentrations of creatine low or near baseline and to extend the release of creatine over 24 hours, allowing more creatine to be distributed to the tissue, especially the brain. Our PBPK simulations of a 20 g SR formulation of CM given once daily for 7 days, show that although the C_{\max} in the plasma were lower compared to IR form, the release of creatine from the SR formulation was slower and sustained at a steady level allowing more creatine to be taken up by the muscles and the brain and this is reflected by the larger $AUC_{0-\infty}$, which increased by 4, 41, and 18 %, for plasma, brain, and muscles, respectively, with SR form

compared to IR dosage form. A possible explanation for the higher change in the concentration of creatine in the brain following supplementation of SR CM compared to the muscles and plasma could be the role of CRT1 at the BBB. As the brain creatine content depends on exogenously administered creatine, which should be transported by the CRT1, and plays a significant role in transporting creatine to the brain. Keeping creatine levels near the baseline in the plasma ensures that more creatine would go into the brain preventing saturation of the CRT1.

Another approach that can be taken to improve oral bioavailability of creatine supplements is to use different creatine forms with improved physicochemical properties. Due in large part to the inefficiencies in current creatine supplement formulations there has been growing interest in new and improved forms of creatine. In the present study, we were interested in three newer forms of creatine, CrC, CrPyr, and CHCl, which have improved solubility parameters over CM. Indeed, based on the PBPK model simulations in rats, substantial increases in blood and tissue levels of creatine are likely following oral supplementation with CHCl compared to CM. When simulations of the different salt forms of creatine were performed in humans, similar increases of creatine in plasma and tissue were found with the newer salt forms.

Prediction of creatine levels in plasma and tissue was performed following administration of single- or multiple- dose of the various creatine salt forms. For single dose simulations, a 5 g low dose and a 20 g high dose were chosen. With the 5 g dose, the various creatine forms simulated were given in solution form (assuming that the doses are dissolved in 450 ml water). Under this condition, no significant differences were found in plasma or tissue creatine concentrations. However, with 20 g dose, CM was given in suspension form due to its low

solubility (20 g CM require more than 1 liter to be dissolved), while CrC, CrPyr and CHCl were given in solution. Under these conditions, increases of creatine in the plasma and tissue were found with the newer salts forms. CHCl led to the highest increase in plasma and tissue of creatine as it has the highest aqueous solubility between all the other forms. These results suggest that giving the newer salts forms, which has improved aqueous solubility compared to CM, as a single large dose leads to the biggest increase in creatine in the brain and the muscles as opposed to smaller doses in which the aqueous solubility is of no importance.

The same trend was found when multiple-dose simulations were performed. The large increase in creatine plasma and tissue was found when given a large single dose (20 g) as opposed to dividing the dose to four equal smaller doses. Our model predicted the highest increase with CHCl in plasma, muscle, and tissue creatine when given as a single large dose. It should also be noted that our predictions of improved oral absorption and PK properties with more soluble creatine salt forms are consistent with previous studies comparing creatine citrate and creatine pyruvate salts. In these studies, Jager et al. compared the oral bioavailability of creatine citrate and creatine pyruvate to that of CM. They found that creatine pyruvate, which has around eight-fold higher aqueous solubility than CM, had a significant (approximately 25%) increase in oral bioavailability compared to the latter. In addition to providing further evidence of less than complete oral bioavailability for CM, such findings suggest that creatine salts with improved aqueous solubility and oral absorption characteristics could provide improvements over CM in therapeutic applications requiring high doses of creatine.

Another approach for improved creatine formulations is to use newer ester creatine analogs. In addition to having improved aqueous solubility, they have

improved water octanol partition coefficient compared to CM. Of interest for this project is CEE. CEE has an aqueous solubility of around 900 mg/ml and a 2-fold partition coefficient value compared to CM. We performed a PK study of CEE in rats to compare its PK profile to that of CM. The fact that CEE is not stable in basic media was challenging, as samples of CEE were pH adjusted to 5 to keep the compound stable as long as possible. Based on the results of our PK study, CEE levels were very low in the plasma. However, surprisingly, the levels of creatine in the brain and muscles were comparable to those obtained following administration of CM. This finding is in agreement with a previously published study in which CEE rapidly degraded to CRN in the aqueous medium when incubated with *in-vitro* brain slices, however, it remained in solution long enough to cause a significant increase in tissue content of creatine. (200) This suggests that although CEE rapidly hydrolyses in the plasma to CRN, there are increases in creatine in the tissues indicative of rapid entry of CEE into tissue sites. As there was no detectable CEE in the tissue, it appears that CEE was taken up by tissue and then converted to creatine in the tissue.

In the present study, sex-dependent differences in creatine concentrations were also assessed. A number of differences in the storage and utilization of creatine have been identified between healthy males and females. (201) When assessing creatine synthesis rates, females produced amounts of endogenous creatine that were consistently 70–80 % lower than males. Dietary intake of creatine of adult females aged 20–39 was also reported to be lower than their male counterparts. This lowered rate of synthesis and consumption of creatine is the likely driver behind the reduced mean excretion rate of creatinine in females, which is ~80 % of the rate of excretion in males. (201) As skeletal muscle is the major storage compartment of creatine in the human body variation in the physical make up of

men and women may be a major determinant of the difference of creatine homeostasis between the sexes. Males have significantly more skeletal muscle, both in terms of total mass (33 kg for men and 21 kg for women) and percentage body composition (38.4 % mens and 30.6 % for womens). Interestingly, in a study where biopsies of the vastus lateralis muscle were assessed for creatine content, females appeared to store about 10 % more creatine compared to males.

In our simulation of 20 g/day CM for 7 days, females had higher levels of creatine in the plasma and tissue (muscles and brain) compared to males. Previous reports indicate that sex hormones, particularly estrogen is associated with increased CK activity. This had led to suggestions that creatine might be more beneficial in treating depression in females over males. (200) It was shown that increasing dietary intake of creatine to 4% in rats for 5 weeks prior to assessment significantly improved performance on tests such as the forced swim test known to identify depressive like behaviors in females but not in male rats. (201)

A limitation for our predictions using GastroPlus, is the lack of data concerning the concentrations of free creatine that are required in the brain to produce the beneficial responses observed in rodents or humans. However, in a study of creatine supplementation in an animal model of HD where they showed neuroprotective effects of 2% creatine in the diet, they reported around 48% increase in total creatine in the brain following supplementation. (94) If we can increase creatine in the brain with the newer creatine salts forms by 25-70% then the desired concentration reported in the HD animal study should be achievable. Another limitation is the lack of clinical data regarding sustained release formulation of CM or the PK profile of the various creatine salts to verify and refine our model. Based on our simulations, a 20 g dose of SR CM resulted in higher tissue levels of CM compared to IR CM. however, as it is not feasible to

formulate such a large dose as a SR formulation. It is possible to formulate smaller doses of CM (e.g. 5 g) to be given 3-4 times daily, which would result in comparable plasma and tissue levels of CM to a single large dose (20 g) SR-CM.

In conclusion, our results suggest that the oral bioavailability of CM is less than complete and is dose-dependent. As most therapeutic indications require rather large doses (>150 mg/kg), the actual bioavailability of such doses may be limited by either physiological and/or formulation factors. However, examination of the PK of CM at therapeutically relevant doses (i.e. > 5 g) is warranted. These studies also suggest that newer forms and dosage formulations of creatine might be superior to CM, but further studies comparing newer formulations to CM will be required. The issue with CM is that large doses are required to produce therapeutic effects. Given the physicochemical properties of CM and the known kinetics of the creatine transporter, a sustained release dosage form could potentially improve the delivery of large doses of creatine to the various tissues.

References

1. Hall M, Trojian TH. Creatine supplementation. *Curr Sports Med Rep*. 2013;12(4):240-4.
2. Kreider RB. Effects of creatine supplementation on performance and training adaptations. *Molecular and cellular biochemistry*. 2003;244(1-2):89-94.
3. Clarke H, Kim D, Meza C, A., Ormsbee M, J., Hickner R, C. The Evolving Applications of Creatine Supplementation: Could Creatine Improve Vascular Health? *Nutrients*. 2020;12(2834).
4. Williams MH, Branch JD. Creatine supplementation and exercise performance: an update. *J Am Coll Nutr*. 1998;17(3):216-34.
5. Balsom PD, Ekblom B, Soderlund K, Sjodin B, Hultman E. Creatine supplementation and dynamic high-intensity intermittent exercise. *Scand J Med Sci Sports*. 1993;3:143-9.
6. Browne SE, Yang L, DiMauro JP, Fuller SW, Licata SC, Beal MF. Bioenergetic abnormalities in discrete cerebral motor pathways presage spinal cord pathology in the G93A SOD1 mouse model of ALS. *Neurobiol Dis*. 2006;22(3):599-610.
7. Hackett DA, Johnson NA, Chow CM. Training practices and ergogenic aids used by male bodybuilders. *Journal of strength and conditioning research*. 2013;27(6):1609-17.
8. Evans MW, Jr., Ndetan H, Perko M, Williams R, Walker C. Dietary supplement use by children and adolescents in the United States to enhance sport performance: results of the National Health Interview Survey. *The journal of primary prevention*. 2012;33(1):3-12.
9. Butts J, Jacobs B, Silvis M. Creatine Use in Sports. *Sports Health*. 2017;10(1):31-4.
10. Jager R, Purpura M, Shao A, Inoue T, Kreider RB. Analysis of the efficacy, safety, and regulatory status of novel forms of creatine. *Amino Acids*. 2011;40(5):1369-83.
11. Walker JB. Creatine: biosynthesis, regulation, and function. *Adv Enzymol Relat Areas Mol Biol*. 1979;50:177-242.
12. Brosnan JT, Brosnan ME. Creatine: endogenous metabolite, dietary, and therapeutic supplement. *Annu Rev Nutr*. 2007;27:241-61.
13. Persky AM, Brazeau GA. Clinical pharmacology of the dietary supplement creatine monohydrate. *Pharmacol Rev*. 2001;53(2):161-76.
14. Wyss M, Kaddurah-Daouk R. Creatine and creatinine metabolism. *Physiol Rev*. 2000;80(3):1107-213.
15. Wang L, Chen D, Yang L, Huang S, Zhang Y, Zhang H. Expression patterns of the creatine metabolism-related molecules AGAT, GAMT and CT1 in adult zebrafish *Danio rerio*. *Journal of fish biology*. 2010;76(5):1212-9.
16. Goldman R, Moss JX. Creatine synthesis after creatinine loading and after nephrectomy. *Proceedings of the Society for Experimental Biology and Medicine Society for Experimental Biology and Medicine*. 1960;105:450-3.
17. Pisano J, Abraham D, Udenfriend S. Biosynthesis and disposition of γ -guanidinobutyric acid in mammalian tissues. *Archives of Biochemistry and Biophysics*. 1963;100(2):323-9.

18. Beard E, Braissant O. Synthesis and transport of creatine in the CNS: importance for cerebral functions. *J Neurochem.* 2010;115(2):297-313.
19. Braissant O, Henry H, Loup M, Eilers B, Bachmann C. Endogenous synthesis and transport of creatine in the rat brain: an in situ hybridization study. *Brain Res Mol Brain Res.* 2001;86(1-2):193-201.
20. Nakashima T, Tomi M, Tachikawa M, Watanabe M, Terasaki T, Hosoya K. Evidence for creatine biosynthesis in Muller glia. *Glia.* 2005;52(1):47-52.
21. Tachikawa M, Fukaya M, Terasaki T, Ohtsuki S, Watanabe M. Distinct cellular expressions of creatine synthetic enzyme GAMT and creatine kinases uCK-Mi and CK-B suggest a novel neuron-glia relationship for brain energy homeostasis. *The European journal of neuroscience.* 2004;20(1):144-60.
22. Wallimann T, Wyss M, Brdiczka D, Nicolay K, Eppenberger HM. Intracellular compartmentation, structure and function of creatine kinase isoenzymes in tissues with high and fluctuating energy demands: the 'phosphocreatine circuit' for cellular energy homeostasis. *Biochem J.* 1992;281 (Pt 1):21-40.
23. Wallimann T, Dolder M, Schlattner U, Eder M, Hornemann T, O'Gorman E, et al. Some new aspects of creatine kinase (CK): compartmentation, structure, function and regulation for cellular and mitochondrial bioenergetics and physiology. *Biofactors.* 1998;8(3-4):229-34.
24. Andres RH, Ducray AD, Schlattner U, Wallimann T, Widmer HR. Functions and effects of creatine in the central nervous system. *Brain Res Bull.* 2008;76(4):329-43.
25. Saks VA, Rosenshtaukh LV, Smirnov VN, Chazov EI. Role of creatine phosphokinase in cellular function and metabolism. *Can J Physiol Pharmacol.* 1978;56(5):691-706.
26. Bessman SP, Carpenter CL. The creatine-creatine phosphate energy shuttle. *Annual review of biochemistry.* 1985;54:831-62.
27. Howald H, Poortmans JR. Metabolic Adaptation to Prolonged Physical Exercise. *Proceedings of Second International Symposium on Biochemistry of Exercise.* Birkhauser, Basel. 1975.
28. Trask RV, Strauss AW, Billadello JJ. Developmental Regulation and Tissue-specific Expression of the Human Muscle Creatine Kinase Gene. *The Journal of Biological Chemistry.* 1988;263(32):17142-9.
29. Schlattner U, Tokarska-Schlattner M, Wallimann T. Mitochondrial Creatine Kinase in Human Health and Disease. Elsevier Inc. 2006;1762(2):164-80.
30. Wallimann T, Dolder M, Schlattner U, Eder M, Hornemann T, Kraft T, et al. Creatine kinase: an enzyme with a central role in cellular energy metabolism. *MAGMA.* 1998;6(2-3):116-9.
31. Bernardi P, Di Lisa F. The mitochondrial permeability transition pore: molecular nature and role as a target in cardioprotection. *J Mol Cell Cardiol.* 2015;78:100-6.
32. Perasso L, Spallarossa P, Gandolfo C, Ruggeri P, Balestrino M. Therapeutic use of creatine in brain or heart ischemia: available data and future perspectives. *Medicinal research reviews.* 2013;33(2):336-63.
33. Sullivan PG, Geiger JD, Mattson MP, Scheff SW. Dietary supplement creatine protects against traumatic brain injury. *Annals of neurology.* 2000;48(5):723-9.
34. Sestili P, Martinelli C, Bravi G, Piccoli G, Curci R, Battistelli M, et al. Creatine supplementation affords cytoprotection in oxidatively injured cultured mammalian cells via direct antioxidant activity. *Free radical biology & medicine.* 2006;40(5):837-49.

35. Santos RV, Bassit RA, Caperuto EC, Costa Rosa LF. The effect of creatine supplementation upon inflammatory and muscle soreness markers after a 30km race. *Life Sci.* 2004;75(16):1917-24.
36. Bassit RA, Curi R, Costa Rosa LF. Creatine supplementation reduces plasma levels of pro-inflammatory cytokines and PGE2 after a half-ironman competition. *Amino Acids.* 2008;35(2):425-31.
37. Deminice R, Rosa FT, Franco GS, Jordao AA, de Freitas EC. Effects of creatine supplementation on oxidative stress and inflammatory markers after repeated-sprint exercise in humans. *Nutrition.* 2013;29(9):1127-32.
38. AlRaddadi EA, Winter T, Aukema HM, Miller DW. Effects of various dietary supplements on inflammatory processes in primary canine chondrocytes as a model of osteoarthritis. *Can J Vet Res.* 2019;83(3):206-17.
39. Leland KM, McDonald TL, Drescher KM. Effect of creatine, creatinine, and creatine ethyl ester on TLR expression in macrophages. *Int Immunopharmacol.* 2011;11(9):1341-7.
40. Nomura A, Zhang M, Sakamoto T, Ishii Y, Morishima Y, Mochizuki M, et al. Anti-inflammatory activity of creatine supplementation in endothelial cells in vitro. *Br J Pharmacol.* 2003;139(4):715-20.
41. Broer S, Gether U. The solute carrier 6 family of transporters. *Br J Pharmacol.* 2012;167(2):256-78.
42. Derave W, Eijnde BO, Hespel P. Creatine supplementation in health and disease: what is the evidence for long-term efficacy? *Molecular and cellular biochemistry.* 2003;244(1-2):49-55.
43. Nash SR, Giros B, Kingsmore SF, Rochelle JM, Suter ST, Gregor P, et al. Cloning, pharmacological characterization, and genomic localization of the human creatine transporter. *Receptors & channels.* 1994;2(2):165-74.
44. Sora I, Richman J, Santoro G, Wei H, Wang Y, Vanderah T, et al. The cloning and expression of a human creatine transporter. *Biochem Biophys Res Commun.* 1994;204(1):419-27.
45. Salomons GS, van Dooren SJ, Verhoeven NM, Cecil KM, Ball WS, Degrauw TJ, et al. X-linked creatine-transporter gene (SLC6A8) defect: a new creatine-deficiency syndrome. *American journal of human genetics.* 2001;68(6):1497-500.
46. Iyer GS, Krahe R, Goodwin LA, Doggett NA, Siciliano MJ, Funanage VL, et al. Identification of a testis-expressed creatine transporter gene at 16p11.2 and confirmation of the X-linked locus to Xq28. *Genomics.* 1996;34(1):143-6.
47. Salomons GS, Wyss M. Creatine and Creatine Kinase in Health and Disease: From Cell Deconstruction to System Reconstruction. *Subcellular Biochemistry.* 2007(46):99-113.
48. Marescau B, Deshmukh D, R., Kockx M, Possemiers I, Qureshi I, A., Wiechert P, et al. Guanidino compounds in serum, urine, liver, kidney, and brain of man and some ureotelic animals. *Metabolism.* 1992;41(5):526-32.
49. Ohtsuki S, Tachikawa M, Takanaga H, Shimizu H, Watanabe M, Hosoya K, et al. The blood-brain barrier creatine transporter is a major pathway for supplying creatine to the brain. *J Cereb Blood Flow Metab.* 2002;22(11):1327-35.
50. Mak CS, Waldvogel HJ, Dodd JR, Gilbert RT, Lowe MT, Birch NP, et al. Immunohistochemical localisation of the creatine transporter in the rat brain. *Neuroscience.* 2009;163(2):571-85.

51. Lunardi G, Parodi A, Perasso L, Pohvozcheva AV, Scarrone S, Adriano E, et al. The creatine transporter mediates the uptake of creatine by brain tissue, but not the uptake of two creatine-derived compounds. *Neuroscience*. 2006;142(4):991-7.
52. Allen PJ. Creatine metabolism and psychiatric disorders: Does creatine supplementation have therapeutic value? *Neurosci Biobehav Rev*. 2012;36(5):1442-62.
53. Stockler S, Isbrandt D, Hanefeld F, Schmidt B, von Figura K. Guanidinoacetate methyltransferase deficiency: the first inborn error of creatine metabolism in man. *American journal of human genetics*. 1996;58(5):914-22.
54. Ganesan V, Johnson A, Connelly A, Eckhardt S, Surtees RA. Guanidinoacetate methyltransferase deficiency: new clinical features. *Pediatric neurology*. 1997;17(2):155-7.
55. Schulze A, Mayatepek E, Bachert P, Marescau B, De Deyn PP, Rating D. Therapeutic trial of arginine restriction in creatine deficiency syndrome. *European journal of pediatrics*. 1998;157(7):606-7.
56. Balestrino M, Adriano E. Beyond sports: Efficacy and safety of creatine supplementation in pathological or parapsychological conditions of brain and muscle. *Medicinal research reviews*. 2019;39(6):2427-59.
57. Kreider RB, Ferreira M, Wilson M, Grindstaff P, Plisk S, Reinardy J, et al. Effects of creatine supplementation on body composition, strength, and sprint performance. *Medicine and science in sports and exercise*. 1998;30(1):73-82.
58. Balsom PD, Soderlund K, Ekblom B. Creatine in humans with special reference to creatine supplementation. *Sports Med*. 1994;18(4):268-80.
59. Volek JS, Kraemer WJ, Bush JA, Boetes M, Incledon T, Clark KL, et al. Creatine supplementation enhances muscular performance during high-intensity resistance exercise. *Journal of the American Dietetic Association*. 1997;97(7):765-70.
60. Bagchi D, Nair S, Sen C. *Nutrition and Enhanced Sports Performance. Muscle Building, Endurance, and Strength*. 2nd Edition. Elsevier Inc. 2018.
61. Harris RC, Soderlund K, Hultman E. Elevation of creatine in resting and exercised muscle of normal subjects by creatine supplementation. *Clin Sci (Lond)*. 1992;83(3):367-74.
62. Greenhaff PL, Bodin K, Soderlund K, Hultman E. Effect of oral creatine supplementation on skeletal muscle phosphocreatine resynthesis. *Am J Physiol*. 1994;266(5 Pt 1):E725-30.
63. Hultman E, Soderlund K, Timmons JA, Cederblad G, Greenhaff PL. Muscle creatine loading in men. *J Appl Physiol (1985)*. 1996;81(1):232-7.
64. Steenge GR, Lambourne J, Casey A, Macdonald IA, Greenhaff PL. Stimulatory effect of insulin on creatine accumulation in human skeletal muscle. *Am J Physiol*. 1998;275(6 Pt 1):E974-9.
65. Gordon A, Hultman E, Kaijser L, Kristjansson S, Rolf CJ, Nyquist O, et al. Creatine supplementation in chronic heart failure increases skeletal muscle creatine phosphate and muscle performance. *Cardiovascular research*. 1995;30(3):413-8.
66. Casey A, Constantin-Teodosiu D, Howell S, Hultman E, Greenhaff PL. Creatine ingestion favorably affects performance and muscle metabolism during maximal exercise in humans. *Am J Physiol*. 1996;271(1 Pt 1):E31-7.
67. Earnest CP, Snell PG, Rodriguez R, Almada AL, Mitchell TL. The effect of creatine monohydrate ingestion on anaerobic power indices, muscular strength and body composition. *Acta Physiol Scand*. 1995;153(2):207-9.

68. Vandenberghe K, Goris M, Van Hecke P, Van Leemputte M, Vangerven L, Hespel P. Long-term creatine intake is beneficial to muscle performance during resistance training. *J Appl Physiol* (1985). 1997;83(6):2055-63.
69. Hespel P, Op't Eijnde B, Van Leemputte M, Urso B, Greenhaff PL, Labarque V, et al. Oral creatine supplementation facilitates the rehabilitation of disuse atrophy and alters the expression of muscle myogenic factors in humans. *J Physiol*. 2001;536(Pt 2):625-33.
70. Op 't Eijnde B, Urso B, Richter EA, Greenhaff PL, Hespel P. Effect of oral creatine supplementation on human muscle GLUT4 protein content after immobilization. *Diabetes*. 2001;50(1):18-23.
71. Rahimi R. Creatine supplementation decreases oxidative DNA damage and lipid peroxidation induced by a single bout of resistance exercise. *Journal of strength and conditioning research / National Strength & Conditioning Association*. 2011;25(12):3448-55.
72. Alraddadi EA, Miller, D.W. Evaluation of anti-inflammatory effects of different creatine supplements in a canine chondrocytes model. Abstract presented at: Canadian Society of Pharmacology and Therapeutics (CSPT). June, 2015; Toronto, Ca. Abstract 36.
73. Kley RA, Tarnopolsky MA, Vorgerd M. Creatine for treating muscle disorders. *The Cochrane database of systematic reviews*. 2013(6):CD004760.
74. Beal MF. Neuroprotective effects of creatine. *Amino Acids*. 2011;40(5):1305-13.
75. Ferrante RJ, Andreassen OA, Jenkins BG, Dedeoglu A, Kuemmerle S, Kubilus JK, et al. Neuroprotective effects of creatine in a transgenic mouse model of Huntington's disease. *J Neurosci*. 2000;20(12):4389-97.
76. Brewer GJ, Wallimann TW. Protective effect of the energy precursor creatine against toxicity of glutamate and beta-amyloid in rat hippocampal neurons. *J Neurochem*. 2000;74(5):1968-78.
77. Klivenyi P, Ferrante RJ, Matthews RT, Bogdanov MB, Klein AM, Andreassen OA, et al. Neuroprotective effects of creatine in a transgenic animal model of amyotrophic lateral sclerosis. *Nature medicine*. 1999;5(3):347-50.
78. Matthews RT, Ferrante RJ, Klivenyi P, Yang L, Klein AM, Mueller G, et al. Creatine and cyclocreatine attenuate MPTP neurotoxicity. *Exp Neurol*. 1999;157(1):142-9.
79. Beal MF, Ferrante RJ. Experimental therapeutics in transgenic mouse models of Huntington's disease. *Nature reviews Neuroscience*. 2004;5(5):373-84.
80. Andres RH, Ducray AD, Huber AW, Perez-Bouza A, Krebs SH, Schlattner U, et al. Effects of creatine treatment on survival and differentiation of GABA-ergic neurons in cultured striatal tissue. *J Neurochem*. 2005;95(1):33-45.
81. Rikani AA, Choudhry Z, Choudhry AM, Rizvi N, Ikram H, Mobassarah NJ, et al. The mechanism of degeneration of striatal neuronal subtypes in Huntington disease. *Annals of neurosciences*. 2014;21(3):112-4.
82. Djousse L, Knowlton B, Cupples LA, Marder K, Shoulson I, Myers RH. Weight loss in early stage of Huntington's disease. *Neurology*. 2002;59(9):1325-30.
83. Kuhl DE, Phelps ME, Markham CH, Metter EJ, Riege WH, Winter J. Cerebral metabolism and atrophy in Huntington's disease determined by 18FDG and computed tomographic scan. *Annals of neurology*. 1982;12(5):425-34.
84. Mazziotta JC, Phelps ME, Pahl JJ, Huang SC, Baxter LR, Riege WH, et al. Reduced cerebral glucose metabolism in asymptomatic subjects at risk for Huntington's disease. *N Engl J Med*. 1987;316(7):357-62.

85. Koroshetz WJ, Jenkins BG, Rosen BR, Beal MF. Energy metabolism defects in Huntington's disease and effects of coenzyme Q10. *Annals of neurology*. 1997;41(2):160-5.
86. Jenkins BG, Koroshetz WJ, Beal MF, Rosen BR. Evidence for impairment of energy metabolism in vivo in Huntington's disease using localized ¹H NMR spectroscopy. *Neurology*. 1993;43(12):2689-95.
87. Harms L, Meierkord H, Timm G, Pfeiffer L, Ludolph AC. Decreased N-acetyl-aspartate/choline ratio and increased lactate in the frontal lobe of patients with Huntington's disease: a proton magnetic resonance spectroscopy study. *Journal of neurology, neurosurgery, and psychiatry*. 1997;62(1):27-30.
88. Parker WD, Jr., Boyson SJ, Luder AS, Parks JK. Evidence for a defect in NADH: ubiquinone oxidoreductase (complex I) in Huntington's disease. *Neurology*. 1990;40(8):1231-4.
89. Brouillet E, Hantraye P, Ferrante RJ, Dolan R, Leroy-Willig A, Kowall NW, et al. Chronic mitochondrial energy impairment produces selective striatal degeneration and abnormal choreiform movements in primates. *Proceedings of the National Academy of Sciences of the United States of America*. 1995;92(15):7105-9.
90. Gu M, Gash MT, Mann VM, Javoy-Agid F, Cooper JM, Schapira AH. Mitochondrial defect in Huntington's disease caudate nucleus. *Annals of neurology*. 1996;39(3):385-9.
91. Browne SE, Bowling AC, MacGarvey U, Baik MJ, Berger SC, Muqit MM, et al. Oxidative damage and metabolic dysfunction in Huntington's disease: selective vulnerability of the basal ganglia. *Annals of neurology*. 1997;41(5):646-53.
92. Matthews RT, Yang L, Jenkins BG, Ferrante RJ, Rosen BR, Kaddurah-Daouk R, et al. Neuroprotective effects of creatine and cyclocreatine in animal models of Huntington's disease. *J Neurosci*. 1998;18(1):156-63.
93. Shear DA, Haik KL, Dunbar GL. Creatine reduces 3-nitropropionic-acid-induced cognitive and motor abnormalities in rats. *Neuroreport*. 2000;11(9):1833-7.
94. Dedeoglu A, Kubilus JK, Yang L, Ferrante KL, Hersch SM, Beal MF, et al. Creatine therapy provides neuroprotection after onset of clinical symptoms in Huntington's disease transgenic mice. *J Neurochem*. 2003;85(6):1359-67.
95. Verbessem P, Lemiere J, Eijnde BO, Swinnen S, Vanhees L, Van Leemputte M, et al. Creatine supplementation in Huntington's disease: a placebo-controlled pilot trial. *Neurology*. 2003;61(7):925-30.
96. Tabrizi SJ, Blamire AM, Manners DN, Rajagopalan B, Styles P, Schapira AH, et al. Creatine therapy for Huntington's disease: clinical and MRS findings in a 1-year pilot study. *Neurology*. 2003;61(1):141-2.
97. Rosas HD, Doros G, Gevorkian S, Malarick K, Reuter M, Coutu JP, et al. PRECREST: a phase II prevention and biomarker trial of creatine in at-risk Huntington disease. *Neurology*. 2014;82(10):850-7.
98. Hersch SM, Schifitto G, Oakes D, Bredlau AL, Meyers CM, Nahin R, et al. The CREST-E study of creatine for Huntington disease: A randomized controlled trial. *Neurology*. 2017;89(6):594-601.
99. Adhietty PJ, Beal MF. Creatine and its potential therapeutic value for targeting cellular energy impairment in neurodegenerative diseases. *Neuromolecular medicine*. 2008;10(4):275-90.
100. Serrano-Pozo A, Frosch MP, Masliah E, Hyman BT. Neuropathological alterations in Alzheimer disease. *Cold Spring Harbor perspectives in medicine*. 2011;1(1):a006189.

101. Duara R, Grady C, Haxby J, Sundaram M, Cutler NR, Heston L, et al. Positron emission tomography in Alzheimer's disease. *Neurology*. 1986;36(7):879-87.
102. Parker WD, Jr. Cytochrome oxidase deficiency in Alzheimer's disease. *Annals of the New York Academy of Sciences*. 1991;640:59-64.
103. Maurer I, Zierz S, Moller HJ. A selective defect of cytochrome c oxidase is present in brain of Alzheimer disease patients. *Neurobiology of aging*. 2000;21(3):455-62.
104. Haxby JV, Grady CL, Friedland RP, Rapoport SI. Neocortical metabolic abnormalities precede nonmemory cognitive impairments in early dementia of the Alzheimer type: longitudinal confirmation. *Journal of neural transmission Supplementum*. 1987;24:49-53.
105. Markesbery WR. Oxidative stress hypothesis in Alzheimer's disease. *Free radical biology & medicine*. 1997;23(1):134-47.
106. Butterfield DA, Lauderback CM. Lipid peroxidation and protein oxidation in Alzheimer's disease brain: potential causes and consequences involving amyloid beta-peptide-associated free radical oxidative stress. *Free radical biology & medicine*. 2002;32(11):1050-60.
107. Alimohammadi-Kamalabadi M, Eshraghian M, Zarindast MR, Aliaghaei A, Pishva H. Effect of creatine supplementation on cognitive performance and apoptosis in a rat model of amyloid-beta-induced Alzheimer's disease. *Iran J Basic Med Sci*. 2016;19(11):1159-65.
108. AliMohammadi M, Eshraghian M, Zarindast MR, Aliaghaei A, Pishva H. Effects of creatine supplementation on learning, memory retrieval, and apoptosis in an experimental animal model of Alzheimer disease. *Medical journal of the Islamic Republic of Iran*. 2015;29:273.
109. Kones R. Parkinson's disease: mitochondrial molecular pathology, inflammation, statins, and therapeutic neuroprotective nutrition. *Nutrition in clinical practice : official publication of the American Society for Parenteral and Enteral Nutrition*. 2010;25(4):371-89.
110. Wakabayashi K, Tanji K, Mori F, Takahashi H. The Lewy body in Parkinson's disease: molecules implicated in the formation and degradation of alpha-synuclein aggregates. *Neuropathology : official journal of the Japanese Society of Neuropathology*. 2007;27(5):494-506.
111. Beal MF. Aging, energy, and oxidative stress in neurodegenerative diseases. *Annals of neurology*. 1995;38(3):357-66.
112. Bindoff LA, Birch-Machin M, Cartlidge NE, Parker WD, Jr., Turnbull DM. Mitochondrial function in Parkinson's disease. *Lancet*. 1989;2(8653):49.
113. Parker WD, Jr., Boyson SJ, Parks JK. Abnormalities of the electron transport chain in idiopathic Parkinson's disease. *Annals of neurology*. 1989;26(6):719-23.
114. Chan P, DeLanney LE, Irwin I, Langston JW, Di Monte D. Rapid ATP loss caused by 1-methyl-4-phenyl-1,2,3,6-tetrahydropyridine in mouse brain. *J Neurochem*. 1991;57(1):348-51.
115. Yang L, Calingasan NY, Wille EJ, Cormier K, Smith K, Ferrante RJ, et al. Combination therapy with coenzyme Q10 and creatine produces additive neuroprotective effects in models of Parkinson's and Huntington's diseases. *J Neurochem*. 2009;109(5):1427-39.
116. Investigators NN-P. A randomized, double-blind, futility clinical trial of creatine and minocycline in early Parkinson disease. *Neurology*. 2006;66(5):664-71.
117. Hervias I, Beal MF, Manfredi G. Mitochondrial dysfunction and amyotrophic lateral sclerosis. *Muscle & nerve*. 2006;33(5):598-608.

118. Dupuis L, Oudart H, Rene F, Gonzalez de Aguilar JL, Loeffler JP. Evidence for defective energy homeostasis in amyotrophic lateral sclerosis: benefit of a high-energy diet in a transgenic mouse model. *Proceedings of the National Academy of Sciences of the United States of America*. 2004;101(30):11159-64.
119. Browne SE, Bowling AC, Baik MJ, Gurney M, Brown RH, Jr., Beal MF. Metabolic dysfunction in familial, but not sporadic, amyotrophic lateral sclerosis. *J Neurochem*. 1998;71(1):281-7.
120. Borthwick GM, Johnson MA, Ince PG, Shaw PJ, Turnbull DM. Mitochondrial enzyme activity in amyotrophic lateral sclerosis: implications for the role of mitochondria in neuronal cell death. *Annals of neurology*. 1999;46(5):787-90.
121. Shefner JM, Cudkowicz ME, Schoenfeld D, Conrad T, Taft J, Chilton M, et al. A clinical trial of creatine in ALS. *Neurology*. 2004;63(9):1656-61.
122. Groeneveld GJ, Veldink JH, van der Tweel I, Kalmijn S, Beijer C, de Visser M, et al. A randomized sequential trial of creatine in amyotrophic lateral sclerosis. *Annals of neurology*. 2003;53(4):437-45.
123. Rosenfeld J, King RM, Jackson CE, Bedlack RS, Barohn RJ, Dick A, et al. Creatine monohydrate in ALS: effects on strength, fatigue, respiratory status and ALSFRS. *Amyotroph Lateral Scler*. 2008;9(5):266-72.
124. Juhn MS, Tarnopolsky M. Oral creatine supplementation and athletic performance: a critical review. *Clin J Sport Med*. 1998;8(4):286-97.
125. Volek JS, Duncan ND, Mazzetti SA, Staron RS, Putukian M, Gomez AL, et al. Performance and muscle fiber adaptations to creatine supplementation and heavy resistance training. *Medicine and science in sports and exercise*. 1999;31(8):1147-56.
126. de Salles Painelli V, Alves VT, Ugrinowitsch C, Benatti FB, Artioli GG, Lancha AH, Jr., et al. Creatine supplementation prevents acute strength loss induced by concurrent exercise. *Eur J Appl Physiol*. 2014;114(8):1749-55.
127. Kerksick CM, Wilborn CD, Campbell WI, Harvey TM, Marcello BM, Roberts MD, et al. The effects of creatine monohydrate supplementation with and without D-pinitol on resistance training adaptations. *Journal of strength and conditioning research*. 2009;23(9):2673-82.
128. Gufford BT, Sriraghavan K, Miller NJ, Miller DW, Gu X, Vennerstrom JL, et al. Physicochemical characterization of creatine N-methylguanidinium salts. *J Diet Suppl*. 2010;7(3):240-52.
129. Bender A, Koch W, Elstner M, Schombacher Y, Bender J, Moeschl M, et al. Creatine supplementation in Parkinson disease: a placebo-controlled randomized pilot trial. *Neurology*. 2006;67(7):1262-4.
130. Writing Group for the NETiPDI, Kieburtz K, Tilley BC, Elm JJ, Babcock D, Hauser R, et al. Effect of creatine monohydrate on clinical progression in patients with Parkinson disease: a randomized clinical trial. *JAMA*. 2015;313(6):584-93.
131. Greenwood-Van Meerveld B, Johnson AC, Grundy D. *Gastrointestinal Physiology and Function. Handbook of experimental pharmacology*. 2017;239:1-16.
132. Kiela PR, Ghishan FK. *Physiology of Intestinal Absorption and Secretion. Best practice & research Clinical gastroenterology*. 2016;30(2):145-59.
133. Gropper S, S., Smith J, L., Groff J, L. *Advanced Nutrition and Human Metabolism. Fifth Edition. USA: Wadsworth/Cengage Learning*. 2009.

134. Harvey R, A., Clark MA, Finkel R, Rey J, A., Whalen K. Lippincott's Illustrated Reviews: Pharmacology. Lippincott Williams & Wilkins. 2012.
135. Dahan A, Miller JM. The solubility-permeability interplay and its implications in formulation design and development for poorly soluble drugs. *The AAPS journal*. 2012;14(2):244-51.
136. Andrews CW, Bennett L, Yu LX. Predicting human oral bioavailability of a compound: development of a novel quantitative structure-bioavailability relationship. *Pharmaceutical research*. 2000;17(6):639-44.
137. Artursson P, Ungell AL, Lofroth JE. Selective paracellular permeability in two models of intestinal absorption: cultured monolayers of human intestinal epithelial cells and rat intestinal segments. *Pharmaceutical research*. 1993;10(8):1123-9.
138. Fihn BM, Jodal M. Permeability of the proximal and distal rat colon crypt and surface epithelium to hydrophilic molecules. *Pflugers Archiv : European journal of physiology*. 2001;441(5):656-62.
139. Hediger MA, Kanai Y, You G, Nussberger S. Mammalian ion-coupled solute transporters. *The Journal of physiology*. 1995;482:7S-17S.
140. Alraddadi EA, Augustine S, Robinson DH, Vennerstrom JL, Wagner JC, Miller DW. Oral Bioavailability of Creatine Supplements: Insights into Mechanism and Implications for Improved Absorption. In Bagchi, D.; Nair, S.; and Sen, C., *Nutrition and Enhanced Sports Performance*. Elsevier Inc. 2018.
141. Garcia-Miranda P, Garcia-Delgado M, Peral MJ, Calonge ML, Ilundain AA. Ontogeny regulates creatine metabolism in rat small and large intestine. *J Physiol Pharmacol*. 2009;60(3):127-33.
142. Peral MJ, Garcia-Delgado M, Calonge ML, Duran JM, De La Horra MC, Wallimann T, et al. Human, rat and chicken small intestinal Na⁺ - Cl⁻ -creatine transporter: functional, molecular characterization and localization. *The Journal of physiology*. 2002;545(1):133-44.
143. Tosco M, Faelli A, Sironi C, Gastaldi G, Orsenigo MN. A creatine transporter is operative at the brush border level of the rat jejunal enterocyte. *The Journal of membrane biology*. 2004;202(2):85-95.
144. Orsenigo MN, Faelli A, De Biasi S, Sironi C, Laforenza U, Paulmichl M, et al. Jejunal creatine absorption: what is the role of the basolateral membrane? *The Journal of membrane biology*. 2005;207(3):183-95.
145. Jager R, Harris RC, Purpura M, Francaux M. Comparison of new forms of creatine in raising plasma creatine levels. *J Int Soc Sports Nutr*. 2007;4:17.
146. Dash AK, Miller DW, Huai-Yan H, Carnazzo J, Stout JR. Evaluation of creatine transport using Caco-2 monolayers as an in vitro model for intestinal absorption. *J Pharm Sci*. 2001;90(10):1593-8.
147. Gufford BT, Ezell EL, Robinson DH, Miller DW, Miller NJ, Gu X, et al. pH-dependent stability of creatine ethyl ester: relevance to oral absorption. *J Diet Suppl*. 2013;10(3):241-51.
148. Hidalgo IJ, Raub TJ, Borchardt RT. Characterization of the human colon carcinoma cell line (Caco-2) as a model system for intestinal epithelial permeability. *Gastroenterology*. 1989;96(3):736-49.

149. Landowski CP, Anderle P, Sun D, Sadee W, Amidon GL. Transporter and ion channel gene expression after Caco-2 cell differentiation using 2 different microarray technologies. *The AAPS journal*. 2004;6(3):e21.
150. Chow SC. Bioavailability and Bioequivalence in Drug Development. Wiley interdisciplinary reviews Computational statistics. 2014;6(4):304-12.
151. Miller DW, Vennerstrom JL, Faulkner MC. Creatine Oral Supplementation Using Creatine Hydrochloride Salt. US Patent Publication Patent No 760864. 2011.
152. Spillane M, Schoch R, Cooke M, Harvey T, Greenwood M, Kreider R, et al. The effects of creatine ethyl ester supplementation combined with heavy resistance training on body composition, muscle performance, and serum and muscle creatine levels. *J Int Soc Sports Nutr*. 2009;6:6.
153. Adriano E, Gulino M, Arkel M, Salis A, Damonte G, Liessi N, et al. Di-acetyl creatine ethyl ester, a new creatine derivative for the possible treatment of creatine transporter deficiency. *Neurosci Lett*. 2018;665:217-23.
154. Hoang K. Physiologically based pharmacokinetic models: mathematical fundamentals and simulation implementations. *Toxicology letters*. 1995;79(1-3):99-106.
155. Grass GM, Sinko PJ. Physiologically-based pharmacokinetic simulation modelling. *Advanced drug delivery reviews*. 2002;54(3):433-51.
156. Lin L, Wong H. Predicting Oral Drug Absorption: Mini Review on Physiologically-Based Pharmacokinetic Models. *Pharmaceutics*. 2017;9(4).
157. Zhuang X, Lu C. PBPK modeling and simulation in drug research and development. *Acta pharmaceutica Sinica B*. 2016;6(5):430-40.
158. Yu LX, Lipka E, Crison JR, Amidon GL. Transport approaches to the biopharmaceutical design of oral drug delivery systems: prediction of intestinal absorption. *Advanced drug delivery reviews*. 1996;19(3):359-76.
159. Agoram B, Woltoz WS, Bolger MB. Predicting the impact of physiological and biochemical processes on oral drug bioavailability. *Advanced drug delivery reviews*. 2001;50 Suppl 1:S41-67.
160. Parrott N, Lukacova V, Fraczkiwicz G, Bolger MB. Predicting pharmacokinetics of drugs using physiologically based modeling--application to food effects. *The AAPS journal*. 2009;11(1):45-53.
161. Upton RN, Foster DJ, Abuhelwa AY. An introduction to physiologically-based pharmacokinetic models. *Paediatric anaesthesia*. 2016;26(11):1036-46.
162. Ashutosh K. *Essentials of Biopharmaceutics and Pharmacokinetics*. 1st Edition. Elsevier Inc. 2010.
163. Boenzi S, Rizzo C, Di Ciommo VM, Martinelli D, Goffredo BM, la Marca G, et al. Simultaneous determination of creatine and guanidinoacetate in plasma by liquid chromatography-tandem mass spectrometry (LC-MS/MS). *J Pharm Biomed Anal*. 2011;56(4):792-8.
164. Carling RS, Hogg SL, Wood TC, Calvin J. Simultaneous determination of guanidinoacetate, creatine and creatinine in urine and plasma by un-derivatized liquid chromatography-tandem mass spectrometry. *Annals of clinical biochemistry*. 2008;45(Pt 6):575-84.
165. Thiel-Demby VE, Humphreys JE, St John Williams LA, Ellens HM, Shah N, Ayrton AD, et al. Biopharmaceutics classification system: validation and learnings of an in vitro permeability assay. *Mol Pharm*. 2009;6(1):11-8.

166. Harris RC, Nevill M, Harris DB, Fallowfield JL, Bogdanis GC, Wise JA. Absorption of creatine supplied as a drink, in meat or in solid form. *J Sports Sci.* 2002;20(2):147-51.
167. Deldicque L, Decombaz J, Zbinden Foncea H, Vuichoud J, Poortmans JR, Francaux M. Kinetics of creatine ingested as a food ingredient. *Eur J Appl Physiol.* 2008;102(2):133-43.
168. Persky AM, Muller M, Derendorf H, Grant M, Brazeau GA, Hochhaus G. Single- and multiple-dose pharmacokinetics of oral creatine. *J Clin Pharmacol.* 2003;43(1):29-37.
169. Schedel JM, Tanaka H, Kiyonaga A, Shindo M, Schutz Y. Acute creatine ingestion in human: consequences on serum creatine and creatinine concentrations. *Life Sci.* 1999;65(23):2463-70.
170. Dechent P, Pouwels PJ, Wilken B, Hanefeld F, Frahm J. Increase of total creatine in human brain after oral supplementation of creatine-monohydrate. *Am J Physiol.* 1999;277(3 Pt 2):R698-704.
171. Atassi N, Ratai EM, Greenblatt DJ, Pulley D, Zhao Y, Bombardier J, et al. A phase I, pharmacokinetic, dosage escalation study of creatine monohydrate in subjects with amyotrophic lateral sclerosis. *Amyotroph Lateral Scler.* 2010;11(6):508-13.
172. Chanutin A. The fate of creatine when administered to man. *JBC.* 1925.
173. ten Krooden E, Owens CW. Creatinine metabolism by *Clostridium welchii* isolated from human faeces. *Experientia.* 1975;31(11):1270.
174. Twort FW, Mellanby E. On creatin-destroying bacilli in the intestine, and their isolation. *The Journal of physiology.* 1912;44(1-2):43-9.
175. McCall W, Persky AM. Pharmacokinetics of creatine. *Sub-cellular biochemistry.* 2007;46:261-73.
176. Davies NM, Takemoto JK, Brocks DR, Yanez JA. Multiple peaking phenomena in pharmacokinetic disposition. *Clin Pharmacokinet.* 2010;49(6):351-77.
177. Sale C, Harris RC, Florance J, Kumps A, Sanvura R, Poortmans JR. Urinary creatine and methylamine excretion following 4 x 5 g x day⁻¹ or 20 x 1 g x day⁻¹ of creatine monohydrate for 5 days. *J Sports Sci.* 2009;27(7):759-66.
178. Snow RJ, Murphy RM. Creatine and the creatine transporter: a review. *Molecular and cellular biochemistry.* 2001;224(1-2):169-81.
179. Bittermann K, Goss KU. Predicting apparent passive permeability of Caco-2 and MDCK cell-monolayers: A mechanistic model. *PloS one.* 2017;12(12):e0190319.
180. Alsenz J, Haenel E. Development of a 7-day, 96-well Caco-2 permeability assay with high-throughput direct UV compound analysis. *Pharmaceutical research.* 2003;20(12):1961-9.
181. Artursson P, Palm K, Luthman K. Caco-2 monolayers in experimental and theoretical predictions of drug transport. *Advanced drug delivery reviews.* 2001;46(1-3):27-43.
182. Lee KJ, Johnson N, Castelo J, Sinko PJ, Grass G, Holme K, et al. Effect of experimental pH on the in vitro permeability in intact rabbit intestines and Caco-2 monolayer. *European journal of pharmaceutical sciences : official journal of the European Federation for Pharmaceutical Sciences.* 2005;25(2-3):193-200.
183. Yamashita S, Furubayashi T, Kataoka M, Sakane T, Sezaki H, Tokuda H. Optimized conditions for prediction of intestinal drug permeability using Caco-2 cells. *European journal of pharmaceutical sciences : official journal of the European Federation for Pharmaceutical Sciences.* 2000;10(3):195-204.

184. Tang F, Horie K, Borchardt RT. Are MDCK cells transfected with the human MDR1 gene a good model of the human intestinal mucosa? *Pharmaceutical research*. 2002;19(6):765-72.
185. Garberg P. In vitro models of the blood-brain barrier. *Alternatives to laboratory animals : ATLA*. 1998;26(6):821-47.
186. Wang Q, Rager JD, Weinstein K, Kardos PS, Dobson GL, Li J, et al. Evaluation of the MDR-MDCK cell line as a permeability screen for the blood-brain barrier. *International journal of pharmaceutics*. 2005;288(2):349-59.
187. ON NH, Chen F, Hinton M, Miller DW. Assessment of P-glycoprotein Activity in the Blood-Brain Barrier (BBB) Using Near Infrared Fluorescence (NIRF) Imaging Techniques. *Pharmaceutical research*. 2011;28(11):2505-15.
188. Campbell A. Development of PBPK model of molinate and molinate sulfoxide in rats and humans. *Regulatory toxicology and pharmacology : RTP*. 2009;53(3):195-204.
189. Branch JD. Effect of creatine supplementation on body composition and performance: a meta-analysis. *International journal of sport nutrition and exercise metabolism*. 2003;13(2):198-226.
190. Rawson ES, Volek JS. Effects of creatine supplementation and resistance training on muscle strength and weightlifting performance. *Journal of strength and conditioning research*. 2003;17(4):822-31.
191. Rawson ES, Miles MP, Larson-Meyer DE. Dietary Supplements for Health, Adaptation, and Recovery in Athletes. *International journal of sport nutrition and exercise metabolism*. 2018;28(2):188-99.
192. Gualano B, Roschel H, Lancha AH, Jr., Brightbill CE, Rawson ES. In sickness and in health: the widespread application of creatine supplementation. *Amino Acids*. 2012;43(2):519-29.
193. Gualano B, Rawson ES, Candow DG, Chilibeck PD. Creatine supplementation in the aging population: effects on skeletal muscle, bone and brain. *Amino Acids*. 2016;48(8):1793-805.
194. Rae CD, Broer S. Creatine as a booster for human brain function. How might it work? *Neurochem Int*. 2015;89:249-59.
195. Dolan E, Gualano B, Rawson ES. Beyond muscle: the effects of creatine supplementation on brain creatine, cognitive processing, and traumatic brain injury. *European journal of sport science*. 2019;19(1):1-14.
196. Kreider RB. Species-specific responses to creatine supplementation. *American journal of physiology Regulatory, integrative and comparative physiology*. 2003;285(4):R725-6.
197. Ipsiroglu OS, Stromberger C, Ilas J, Hoger H, Muhl A, Stockler-Ipsiroglu S. Changes of tissue creatine concentrations upon oral supplementation of creatine-monohydrate in various animal species. *Life Sci*. 2001;69(15):1805-15.
198. Rawson ES, Venezia AC. Use of creatine in the elderly and evidence for effects on cognitive function in young and old. *Amino Acids*. 2011;40(5):1349-62.
199. Tibbitt MW, Dahlman JE, Langer R. Emerging Frontiers in Drug Delivery. *Journal of the American Chemical Society*. 2016;138(3):704-17.
200. Adriano E, Garbati P, Damonte G, Salis A, Armirotti A, Balestrino M. Searching for a therapy of creatine transporter deficiency: some effects of creatine ethyl ester in brain slices in vitro. *Neuroscience*. 2011;199:386-93.

201. Ellery SJ, Walker DW, Dickinson H. Creatine for women: a review of the relationship between creatine and the reproductive cycle and female-specific benefits of creatine therapy. *Amino Acids*. 2016;48(8):1807-17.